FRIEDRICH-SCHILLER-
UNIVERSITÄT
JENA

On a vacuum state redefinition in QED corrections to energy shifts of heavy highly charged ions

DISSERTATION

submitted to the council of the
PHYSIKALISCH-ASTONOMISCHEN FAKULTÄT
of
FRIEDRICH-SCHILLER UNIVERSITÄT JENA, GERMANY

for the degree of
doctor rerum naturalium
(Dr. rer. nat)

Put forward by

M. Sc. Romain N. Soguel

born on 2nd June 1994 in Morges, Switzerland

Examiners:

1. Prof. Dr. Vladimir A. Yerokhin, Max-Planck-Institut für Kernphysik Heidelberg

2. Prof. Dr. Paul Indelicato, Sorbonne Universtié Paris

3. Prof. Dr. Stephan Fritzsche, Friedrich-Schiller-Universität Jena

Day of the defense: 04.07.2023

Pour Beuhn.
Repose en paix poto.

"Celle-là c'est pour mon étoile, celle qui brille plus que les autres"
- Tekilla

Abstract

Every interesting quantity to be investigated in the realm of bound-state quantum electrodynamics (BSQED), such as, for example, the Lamb shift, the (hyper)fine-splitting or the g-factor, is closely or remotely connected to the energy levels of the considered system. Therefore, as a prerequisite, it is mandatory to have the ability to accurately assess energy levels of increasingly sophisticated electronic configurations of atoms or ions. BSQED predictive powers are nowadays limited to either simple light systems, where an αZ expansion is justified, or heavy few-electron highly-charged ions, where specialized all-order methods in αZ are required, to reliably capture interelectronic interactions. The redefined vacuum state approach, which is frequently employed in the many-body perturbation theory, proved to be a powerful tool allowing analytical insights.

This thesis elaborates on this approach within BSQED perturbation theory, based on the two-time Green's function method. In addition to a rather formal formulation, the particular example of a single-particle (electron or hole) excitation with respect to the redefined vacuum state is considered. Starting with simple one-particle Feynman diagrams, characterized by radiative corrections to identical single incoming and single outgoing state, first- and second-order many-electron contributions are derived, namely screened self-energy, screened vacuum-polarization, one-photon-exchange, and two-photon-exchange. The redefined vacuum state approach provides a straightforward and streamlined derivation facilitating its application to any electronic configuration. Moreover, based on the gauge invariance of the one-particle diagrams, various gauge-invariant subsets within analyzed many-electron QED contributions are identified.

Building on the gathered expertise, the framework is extended to account for valence-hole excitation from the redefined vacuum state. Full first-order corrections in α are inferred, as a validation of the established formalism, and gauge-invariant subsets are highlighted. To showcase on the strength offered by the use of a vacuum state redefinition, a partial third-order interelectronic calculation is worked out, relying on the extension of the direct two-photon-exchange gauge invariant subset. The resulting formulas are cross-checked with an independent perturbative derivation, and the cancellation of infrared divergences is demonstrated explicitly. The identification of gauge-invariant subsets in the framework of the proposed approach opens a way to tackle more complex diagrams, where the decomposition into simpler subsets is crucial for a successful calculation.

Zusammenfassung

Jede interessante Größe, die im Bereich der Quantenelektrodynamik mit gebundenen Zuständen (BSQED) untersucht werden soll, wie z. B. die Lamb-Verschiebung, die (Hyper-)Feinaufspaltung oder der g-Faktor, steht in engem oder entferntem Zusammenhang mit den Energieniveaus des betrachteten Systems. Daher ist es zwingend erforderlich, dass man in der Lage ist, die Energieniveaus von immer komplizierteren elektronischen Konfigurationen von Atomen oder Ionen genau zu bestimmen. Die Vorhersagekraft der BSQED ist heutzutage entweder auf einfache leichte Systeme beschränkt, bei denen eine αZ-Entwicklung gerechtfertigt ist, oder auf schwere, hochgeladene Ionen mit wenigen Elektronen, bei denen spezialisierte Methoden erforderlich sind, die Beiträge aller Ordnungen in αZ berücksichtigen, um interelektronische Wechselwirkungen zuverlässig zu erfassen. Der neu definierte Vakuumansatz, der häufig in der Vielteilchen-Störungstheorie verwendet wird, erwies sich als ein leistungsfähiges Werkzeug, das analytische Einblicke ermöglicht.

In dieser Arbeit wird dieser Ansatz im Rahmen der BSQED-Störungstheorie auf Grundlage der Green'schen-Funktions-Methode weiterentwickelt. Zusätzlich zu einer eher formalen Formulierung wird das spezielle Beispiel einer Ein-Teilchen-Anregung (Elektron oder Loch) in Bezug auf den neu definierten Vakuumzustand betrachtet. Ausgehend von einfachen Ein-Teilchen-Feynman-Diagrammen, die durch Strahlungskorrekturen eines einzigen eintretenden und austretenden Zustand gekennzeichnet sind, werden Beiträge erster und zweiter Ordnung für viele Elektronen abgeleitet, nämlich abgeschirmte Selbstenergie, abgeschirmte Vakuumpolarisation, Ein-Photonen-Austausch und Zwei-Photonen-Austausch. Der neu definierte Vakuumzustandsansatz bietet eine unkomplizierte und rationalisierte Herleitung, die die Anwendung auf jede elektronische Konfiguration erleichtert. Darüber hinaus werden, basierend auf der Eichinvarianz der Ein-Teilchen-Diagramme, verschiedene eichinvariante Untergruppen innerhalb der analysierten Vielelektronen-QED-Beiträge identifiziert.

Aufbauend auf dem gesammelten Fachwissen wird der Rahmen erweitert, um die Valenzlochanregung aus dem neu definierten Vakuumzustand zu berücksichtigen. Als Bestätigung des etablierten Formalismus werden vollständige Korrekturen erster Ordnung in α hergeleitet und eichinvariante Teilmengen werden hervorgehoben. Um die Stärke der Neudefinition des Vakuumzustands zu demonstrieren, wird eine partielle interelektronische Berechnung dritter Ordnung durchgeführt, die sich auf die Erweiterung der eichinvarianten Untermenge des direkten Zwei-Photonen-Austauschs stützt. Die sich ergebenden Formeln werden mit einer unabhängigen perturbativen Herleitung überprüft, und die Aufhebung von Infrarot-Divergenzen wird explizit demonstriert. Die Identifizierung eichinvarianter Teilmengen im Rahmen des

vorgeschlagenen Ansatzes eröffnet einen Weg, komplexere Diagramme anzugehen, bei denen die Zerlegung in einfachere Teilmengen entscheidend für eine erfolgreiche Berechnung ist.

Publications

Within the framework of this thesis, the following papers have been published in peer-reviewed journals:

- *Redefined vacuum approach and gauge-invariant subsets in two-photon-exchange diagrams for a closed-shell system with a valence electron*
  R. N. Soguel, A. V. Volotka, E. V. Tryapitsyna, D. A. Glazov and S. Fritzsche
  Phys. Rev. A **103**, 042818 (2021)

- *Many-electron QED with redefined vacuum approach*
  R. N. Soguel, A. V. Volotka, D. A. Glazov and S. Fritzsche
  Symmetry **13(6)**, 1014 (2021)

- *QED approach to valence-hole excitation in closed-shell systems*
  R. N. Soguel, A. V. Volotka and S. Fritzsche
  Phys. Rev. A **106**, 012802 (2022)

The following article is submitted to Physical Review A:

- *A prospective insight toward third-order interelectronic corrections of Li-like ions*
  R. N. Soguel and S. Fritzsche

The following article is in preparations:

- *Screened self-energy corrections to the g-factor and hyperfine splitting in Li-like ions: Gauge invariant subsets*
  E. V. Tryapitsyna, A. V. Volotka, R. N. Soguel and D. A. Glazov

Acknowledgements

This whole PhD thesis would not have been possible without the help and support of Prof. Dr. Andrey V. Volotka, who introduced me to bound-state QED. I thank you Andrey for the interesting, but not so easy to schedule and complicate to keep up with the pace, discussions we had on the different projects and for the insights you brought me in understanding the theory. I am grateful to Prof. Dr. Stephan Fritzsche for the freedom given to conduct research on the topics of my interest during my PhD time.

I warmly thank Prof. Dr. Vladimir A. Yerokhin, Prof. Dr Andrzej Czarnecki and Prof. Dr Paul Indelicato for their acceptance to be examiners of my work. A special thanks, and my gratitude, to Dr. Felix Karbstein, Dr. Anna V. Maiorova, Prof. Dr. Dmitry D. Glazov, Jean-Marc Badan and Roxane Kreuter for their help in proof-reading the manuscript and improving its quality and its understandability.

Ich danke meinen Kollegen Darvin Wanisch, mit dem ich das Büro geteilt habe, Björn Minneker und Baghdasar Baghdasaryan. Unsere Freundschaft half mir dabei, die Corona Krise, und auch die Promotion zu überstehen. Ich bin dankbar euch kennengelernt zu haben und schätze die Zeit, die wir zusammen erlebt haben.

I am especially grateful to Prof. Dr. Riccardo Rattazzi, who gave me the opportunity to enter the field of high energy physics during my studies at the EPFL, and accepted me as a master student in the Theoretical Particle Physics Laboratory. Thank you for showing faith in me. Un grand merci à mon voisin (Prof. honoraire) Claude-Alain Roulet pour nos discussions nombreuses et fournies, à l'ombre d'une bouteille de Chasselas, au fur et à mesure des années ainsi que pour l'intérêt qu'il a fait grandir en moi pour la physique et pour avoir forgé mon esprit critique (ne pas confondre la carte avec le territoire, on ne sera pas d'accord à ce sujet).

À mes potes physiciens, Jonas, Thibault, Antonin et Roberto, avec qui on s'est bien marré dans ce bureau pendant le master, un grand merci, aussi pour ces noces mémorables. Un merci à mon cousin Christophe pour nos nombreuses conversations.

À mes gars sûrs, Xavier et Kevin, merci pour votre amitié fidèle et sincère depuis toutes ces années. Big up au trou noir béant; mes divas de l'EMS.

Une attention toute particulière pour ma copine, le sourire dans ma vie, ma lanterne dans les moments difficiles; merci de tout coeur de ton soutien, de ton support et de ta patience. Sans toi je n'en serai pas là.

Que serait ces remerciements sans y inclure mes parents, Catherine et Cédric, ma belle-mère, Muriel, ainsi que mon frère, Benoît, envers qui j'ai une gratitude infinie, et qui m'ont toujours soutenu dans mes projets et mes choix. Merci d'être toujours présent pour moi, dans les bons comme dans les mauvais moments.

"The saddest aspect of life right now is that science gathers knowledge faster than society gathers wisdom. "

— Isaac Asimov, 1920–1992

CONTENTS

1. INTRODUCTION **1**
   1.1. Structure of the thesis 4
   1.2. Notation and conventions 6

2. BOUND-STATE QUANTUM ELECTRODYNAMICS **7**
   2.1. Gauge invariance in Dirac Theory: from free electron theory to QED 7
   2.2. Furry Picture 11
   2.3. Vacuum state redefinition's approach 17
      2.3.1. Redefined vacuum state and implications 19
      2.3.2. Extraction of interelectronic interactions with core electrons 21
   2.4. Perturbation Theory 22

3. TWO-TIME GREEN'S FUNCTION **23**
   3.1. Shabaev's two-time Green's function method 26
      3.1.1. Electron states 30
      3.1.2. Hole states 34
   3.2. Single-valence electron over closed shells 37
      3.2.1. One-photon-exchange corrections 38
      3.2.2. Two-photon-exchange corrections 40
      3.2.3. Numerical evaluation for Lithium-like ions 54
   3.3. Single-hole (electronic vacancy) in closed shells 57
      3.3.1. One- and two-photon-exchange corrections 58
      3.3.2. Screened-radiative corrections 58
   3.4. Discussion 63

4. VALENCE-HOLE EXCITATION IN CLOSED-SHELL SYSTEMS **65**
   4.1. Devise the valence-hole two-time Green's function 65
   4.2. First-order shift to valence-hole binding energy 70
      4.2.1. One-particle contributions 71
      4.2.2. Two-particle contributions 74
      4.2.3. Standard vacuum description 75
   4.3. Discussion 77

5. THREE-PHOTON-EXCHANGE CORRECTIONS FOR SINGLE-VALENCE ELECTRON OVER CLOSED SHELLS **79**
5.1. Redefined vacuum state approach 79
5.2. Perturbation theory approach 88
5.3. Regularization of infrared divergences 90
5.4. Comparison 94

6. CONCLUSION AND OUTLOOKS **97**

A. APPENDICES **101**
A.1. Renormalization of the free-electron self-energy and vertex operators 101
A.2. Convergence plots for the principal values contributions in the truncated κ expansion 103
A.3. Two-photon-exchange gauge-invariant subsets in extended Furry picture . . . 105
A.4. Two-photon-exchange corrections: matching between QED and RMBPT . . . 107
A.5. Valence-hole zeroth-order Green function 109
A.6. Third-order interelectronic corrections derived by a perturbative treatment . . 111
A.6.1. Four-electron subset 111
A.6.2. Three-electron subset 115
A.7. Symmetry argument for vanishing ladder reducible 2 terms 120

BIBLIOGRAPHY **121**

CHAPTER 1.

INTRODUCTION

Quantum electrodynamics (QED) is the cornerstone of modern physics. Its development led to massive progresses in the understanding of Nature and the Universe, resulting in the Standard Model of particle physics, the pinnacle of human knowledge pertaining three of the four fundamental interactions. The genesis of quantum mechanics started almost simultaneously, with Heisenberg and his non-commutative matrix mechanics [1], and with Schrödinger and his famous partial differential equation [2]. Born introduced the probabilistic interpretation of Schrödinger's wave equation later in the same year [3, 4]. Dirac, being puzzled by the absence of Lorentz covariance in Schrödinger's framework, devised his solution to the problem, namely Dirac's one-electron space-time equation [5, 6]. A very intriguing feature of the solution to his equation is the negative-energy states, the Dirac sea, also sometimes referred to as hole theory. It took him a year or two to properly understand their roles. The (real) development of QED started with the measurement conducted in 1947 by Lamb and Retherford on the transition energy between the $2s_{1/2}$ and $2p_{1/2}$ states in hydrogen atom [7], which is now referred to as the Lamb shift. According to Dirac's prediction, both states should have been degenerated, which turned out to be inaccurate. Another striking discovery enhanced the spark to ignite extensive developments in the field, the anomalous magnetic moment of the electron, nowadays called g-factor. Owing to Dirac's prediction, its value was supposedly equal to two, but the one measured by Kusch and Foley [8] revealed a slightly greater magnetic moment. These enigmatic discrepancies lead to seminal works from Bethe [9], Feynman [10, 11], Schwinger [12–15] and many others. It gave birth to a common framework to describe the electromagnetic interaction, compatible with special relativity and quantum mechanics. The first[1] Lorentz-covariant wave equation for two interacting particles was proposed by Bethe and Salpeter [19]. Sucher extended Salpeter's work [20] and made a decisive step forward, the S-matrix [21], applying the QED formalism to calculate a two-electron system in an external Coulomb field, in his case the helium atom [22]. Later, Logunov and Tavkhelidze [23], and Faustov [24] dealt with a quasi-potential method to circumvent the many-body problem.

In principle, QED can be applied to any many-electron atoms. However, the computations are so far limited to selected, relatively simple systems not only due to the complexity of

[1] Nambu wrote down this expression at the end of a paper without explanation a year before [16]. Schwinger formulated it too [17], as well a Gell-Mann and Low [18], in the same year as Bethe and Salpeter.

numerical calculations but also because of difficulties in deriving tractable formal expressions. In this regard, highly-charged ions became a field of interest both from the theoretical and experimental sides. From the former perspective, it has the advantage that QED corrections enter on the same footing as the correlation effects. In the latter point of view, the transition energies in many-electron ions, which spread from soft x-ray to ultraviolet, and therefore, are accessible by laser spectroscopy techniques over a wide range of Z values [25], with Z the nuclear charge or *effective* charge in the case of the outer electrons. Furthermore, highly-charged ions are currently considered as one of the best available natural laboratories to access strong-field effects [26]. They allow to probe QED corrections up to second-order in α [27, 28], the fine-structure constant, although being a demanding task. This requires to go beyond the perturbative regime since for high Z, the αZ expansion parameter is comparable to one (for uranium, $\alpha Z \approx 0.67$). Hence, calculations to all orders in αZ are sought, which require special methods of bound-state QED (BSQED) to be developed within the corresponding framework, known as the Furry picture [29]. The evaluation of the dynamical properties and the structure of highly relativistic, tightly bound electrons in highly-charged ions with utmost accuracy represents one of the most important and demanding problems in modern theoretical atomic physics. As a consequence, *ab initio* calculations are the holy grail in the quest for many-electron atoms in the frame of BSQED. Moreover, pushing QED, in the presence of the binding nuclear field, to its limits is a great way to earn in-depth knowledge about the theory and to probe potential new physics [30].

QED is most deeply developed for hydrogen [31] and hydrogen-like ions [32], where the accuracy of the calculations has reached a remarkably high level. In the case of highly-charged ions, the comparison of the experimental value of the $1s$ Lamb shift, 460.2 ± 4.6 eV [33], allows one to test the first-order QED effects on a level of 1.7% [26]. However, the probe of the second-order QED effects, which contribute $-1.26(33)$ eV [34], are limited by the experimental accuracy, where improvements represent a rather challenging task [35]. Nevertheless, the increasing experimental precision pushes theoretical predictions to their limits and enforces an accurate description of complex electrons dynamics. In this view, the treatment of the interelectronic interaction is a fundament for accurate theoretical predictions of the energy levels in many-electron atoms or ions. Several approximate methods, such as the relativistic many-body perturbation theory (RMBPT), the relativistic configuration-interaction (RCI) method, or the multi-configuration Dirac-Fock (MCDF) method, usually treat the electron-electron interaction within the Breit approximation on the basis of the so-called *no-pair* Hamiltonian [24, 36]. However, the use of this approximation allows one to evaluate energy levels accurately only up to the order $(\alpha Z)^2$, having nonetheless access to higher-order corrections. In order to account for higher-order effects, one has to employ the

BSQED formalism. The QED treatment of the interelectronic interaction yields additional corrections of the order $(\alpha Z)^3$ and higher, which in many cases become comparable with the experimental uncertainty and the accuracy reached for correlation effects.

Highly-charged ions are such systems. As a consequence, the $(\alpha Z)^3$ corrections beyond the no-pair Hamiltonian should be taken into account by theory in order to achieve an agreement with the numerous dedicated high-precision experimental investigations carried over the years in a variety of system, ranging from H-like [33, 35, 37], He-like [38–42], Li-like [43, 44] and Be-like [45, 46], to B-like [47–50] and F-like [51–53] ions. Other examples of many-electron ions where the correlation energies can be grasped rather accurately, from a theoretical point of view, are F-like [54–56], Na-like [57], Mg-like [58], Al-like [59] and Co-like [60] ions. Within BSQED, the interelectronic interaction is usually treated perturbatively as an expansion over the number of exchanged photons. While the first-order contribution, which corresponds to the one-photon-exchange, is relatively simple to deal with, most of the attention is paid to the next order, namely, the two-photon-exchange. The two-photon-exchange diagrams were first calculated in the milestone paper by Blundell *et al.* [61] for the ground state of He-like ions. Later, the results were confirmed by several groups and the calculations were extended to their excited states [62–70]. Presently, the two-photon-exchange has been also evaluated for Li-like [65, 66, 71–76], Be-like [77–79], B-like [80–82], and Na-like [83] ions. The current experimental and theoretical developments recently reviewed by Indelicato [26] suggest the necessity to extend these computations also to other systems with more complicated electronic structures.

In this context, the question following arises: can we perform *ab initio* QED calculations for many-electron systems? An essential step towards this goal is to derive the explicit formulas for the corresponding diagrams. All the derivations performed so far used a zeroth-order many-electron wave function constructed as a Slater determinant (or sum of Slater determinants) with all electrons involved [61, 83, 84]. Such a derivation becomes increasingly difficult for many-electron systems. The vacuum state redefinition approach in QED, which is extensively used in RMBPT to describe the states with many electrons involved, is proposed in this thesis as a path towards an extension of the calculations of QED corrections to the energy shifts of other ions and atoms. The redefined vacuum state formalism is implemented within the two-time Green's function (TTGF) method introduced by Shabaev [85]. In this respect, the effectiveness of the vacuum state redefinition approach is demonstrated for closed-shells systems with the following extra configurations: (i) a single-valence electron, (ii) an electronic vacancy (single-hole state), and (iii) a valence-hole excitation. The advantages of the method are as follows. First, the effective one-particle frame makes formulas valid for any system with respect to configurations (i) and (ii). An analogous statement holds true for the effective two-particle case with regard

to configuration (iii). Second, the transposition of the one-particle many-loop gauge-invariant (GI) subsets into the generic many-electron system allows to identify simple GI subsets. The identification of GI subsets offers the possibility to verify the consistency of the results piece by piece, as cross-checks along the way, rather than solely the final expressions. Third, instead of the all-particle states, one deals with few-particle states, which amounts to a much smaller Hilbert space. Moreover, the redefinition of the vacuum state allows to focus on the particles distinguishing between the different electronic configurations investigated. Overall, it opens a way to apprehend high-order corrections by providing cross-checks and benchmarks on the way, namely via the identification of GI subsets.

1.1. Structure of the thesis

The thesis is organized as follows. Chapter 2 starts with the Dirac equation and derives the QED Lagrangian relying on the gauge invariance of the theory. A small digression on the renormalization of the Lagrangian is conducted after the gauge fixing of the photon propagator is discussed. Afterwards, the Furry picture of QED is introduced, accounting for the presence of a classical external field. The framework of BSQED is based on the resummation of all Feynman diagrams involving the interaction of the (free) electron with the classical field of the nucleus. Such a procedure, applied by Weinberg [86], leads to the bound-state electron propagator. The procedure presented thereafter is different but closely related. The eigen-energies of the Dirac equation for the point-like nucleus case are discussed briefly. The attention is then focused on the vacuum state of the theory and the derivation of the electron propagator, in the non-interacting field approximation, as well as an explicit expression for the photon propagator. Later on, the redefinition of the vacuum state and its effects are addressed. Moreover, it is discussed how the interelectronic interactions are retrieved as a difference of the two vacua, or equivalently as the difference of a contour integral over two different integration paths. The interaction Hamiltonian is introduced, and the philosophy of perturbation theory in the BSQED realm is sketched at the end of the chapter.

The two-time Green's function method applied in this work to handle perturbation theory in the Furry picture, is discussed in Chapter 3. Following Shabaev, the spectral representation of the two-time Green's function is derived, but from the perspective of the redefined vacuum state. In line with that, the positron term, that corresponds to electronic vacancies (or hole states) in the filled electronic shells, is investigated as well. Cornerstone integral expressions are derived for the energy shift of an N-particle state, involving either only electrons or only holes. An odd-parity symmetry, with respect to the redefined Fermi level, in the expressions of the energy

shifts between valence and holes states is demonstrated. The single-valence electron state and the single-hole state QED corrections to the energy shifts are worked out in details up second order in the fine-structure constant. The gauge invariance of many-electron subsets, based on the effective one-particle picture applied in the derivation, is demonstrated analytically and numerically for the single-electron state. In the single-hole state case the reduction to RMBPT formulas is carried out, for the two-photon-exchange corrections, to cross-check and validate the derivation with previously derived expressions.

Having at the disposal the necessary ingredients to describe a valence-hole state, the associated two-time Green's function is lacking. Upon discussion of the spectral representation of the two-time Green's function, it has been observed that no neutrally charged states were allowed. The framework suited to achieve a valence-hole excitation in closed shells system is devised in Chapter 4. The derivation is based on a different initial equal-time choice (compared to Shabaev's one) to infer the appropriate two-time Green's function. Its spectral representation is worked out, which allows to see that its poles are located at the valence-hole excitation energies. The cornerstone expression to calculate the energy shift is derived as a contour integral, and expanded to the first order. There, the different Feynman diagrams are investigated and the first-order energy correction is calculated by applying the formalism of the redefinition of the vacuum state. The results are mapped to the standard vacuum case, where the one-photon-exchange expression is reduced to the RMBPT case for verification.

Chapter 5 is the most ambitious and challenging part of this work. Relying on the redefined vacuum state approach, partial third-order interelectronic corrections are investigated, based on one-particle three-loop Feynman diagrams. The idea is to begin with simple one-particle GI subsets and keep track of them in the many-electron frame, which is a strong asset of the formalism. In order to minimize the occurrence of mistakes, an independent derivation is undertaken with the help of perturbation theory. This two-method scheme helps to resolve how the different terms are distributed among three- and four-electron contributions. Furthermore, it provides a tool to overcome the difficulties related to the derivation of reducible terms, which are tricky to deal with. The out-coming formulas contain infrared (IR) divergences. They are investigated and regularized by the introduction of a photon mass term. It is shown that the IR divergent terms are compensated by contributions belonging to the same GI subsets proposed.

In the end, Chapter 6 wraps up the developments found along the different analyses conducted throughout the thesis. A concluding discussion provides an outlook for future research works.

1.2. Notation and conventions

Throughout the thesis natural units are used ($\hbar = \mathrm{c} = \mathrm{m}_e = 1$) as well as the Heaviside-Lorentz convention for the charge, hence the fine-structure constant is $\alpha = \mathrm{e}^2/4\pi$ and $\mathrm{e} < 0$. Whenever it may be convenient the electron mass m_e is restored in some expressions. The contravariant four-vector is $x^\mu = (\mathrm{x}^0, \boldsymbol{x}) \equiv (\mathrm{t}, \boldsymbol{x})$ and the covariant four-vector reads $x_\mu = \eta_{\mu\nu} x^\nu$. The metric tensor is

$$\eta_{\mu\nu} = \eta^{\mu\nu} = \begin{pmatrix} 1 & 0 & 0 & 0 \\ 0 & -1 & 0 & 0 \\ 0 & 0 & -1 & 0 \\ 0 & 0 & 0 & -1 \end{pmatrix}.$$

The Einstein convention is applied, where repeated indices are summed over. The four-vector scalar product is defined as $kx = k^\mu x_\mu = \mathrm{k}^0\mathrm{x}^0 - \boldsymbol{k}\cdot\boldsymbol{x}$. Greek indices run from 0 to 3, or equivalently over t, x, y, z, and Roman indices only over spatial coordinates. Boldface type indicates three-vectors, whereas four-vectors are denoted by italic type and scalars as Roman style. The 4-by-4 Dirac matrices $\alpha^\mu = \gamma^0\gamma^\mu$ are represented via their "standard representation" for γ matrices, namely the Dirac basis.

$$\gamma^0 \equiv \beta = \begin{pmatrix} \mathbb{1}_2 & 0 \\ 0 & -\mathbb{1}_2 \end{pmatrix}, \quad \boldsymbol{\gamma} = \begin{pmatrix} 0 & \boldsymbol{\sigma} \\ -\boldsymbol{\sigma} & 0 \end{pmatrix}, \text{hence } \alpha^0 = \begin{pmatrix} \mathbb{1}_2 & 0 \\ 0 & \mathbb{1}_2 \end{pmatrix}, \quad \boldsymbol{\alpha} = \begin{pmatrix} 0 & \boldsymbol{\sigma} \\ \boldsymbol{\sigma} & 0 \end{pmatrix},$$

and the Pauli matrices are 2-by-2 matrices

$$\sigma^1 = \begin{pmatrix} 0 & 1 \\ 1 & 0 \end{pmatrix}, \quad \sigma^2 = \begin{pmatrix} 0 & -i \\ i & 0 \end{pmatrix}, \quad \sigma^3 = \begin{pmatrix} 1 & 0 \\ 0 & -1 \end{pmatrix}.$$

$\mathbb{1}_d$ is a $d \times d$ unitary matrix, which dimension is indicated by the subscript d. Unless explicitly stated all integrals are meant to be on the interval $]-\infty, +\infty[$.

CHAPTER 2.

BOUND-STATE QUANTUM ELECTRODYNAMICS

Symmetries, either intact or broken, have proved to be at the heart of how matter interacts. The prototype gauge theory is QED, the quantum relativistic description of the interaction between the electron-positron field with the electromagnetic field. QED is a local Abelian $U(1)$ theory. In the following, it is shown how such local symmetry can be used to generate dynamics, or gauge interactions, starting from the Dirac Lagrangian, according to the derivation presented in Ref. [87]. Then, the BSQED framework is introduced with the description of the (extended) Furry picture. Later, the redefinition of the vacuum state, a commonly used principle in relativistic many-body perturbation theory, is brought in to facilitate the derivation of tractable formal expressions. The difference between the vacuum states allows to retrieve the interelectronic interactions with previously hidden core electrons. Perturbation theory is briefly introduced at the very end of the chapter.

2.1. Gauge invariance in Dirac Theory: from free electron theory to QED

If fields at different space-time points transform in the same manner under a symmetry transformation, the symmetry is said to be a global one; the parameter describing the symmetry transformation is space-time independent. *A contrario*, if the symmetry transformation is space-time dependent, the symmetry is said to be a local one or a gauge symmetry; the parameter describing the transformation is space-time dependent.

To illustrate the difference, let us take the Lagrangian describing a free electron-positron field (spin-1/2 particle) in the Heisenberg representation, denoted by the subscript $_H$,

$$\mathcal{L}_{\text{Dirac}} = \bar{\psi}_H(x)\left(i\gamma^\mu\partial_\mu - \mathrm{m}_e\right)\psi_H(x)\,, \tag{2.1}$$

where $\bar{\psi}_H(x) = \psi_H^\dagger(x)\gamma^0$, and see how QED arises from the requirement of gauge invariance. This Lagrangian is invariant under a global $U(1)$ symmetry, namely a change in the phase of the field $\psi(x)$

$$\psi_H(x) \to \psi'_H(x) = e^{-i\alpha}\psi_H(x)\,, \quad \bar{\psi}_H(x) \to \bar{\psi}'_H = e^{i\alpha}\bar{\psi}_H(x)\,. \tag{2.2}$$

The global symmetry is turned into a gauge symmetry when α is promoted to $\alpha(x)$. The transformation reads now

$$\psi_H(x) \to \psi'_H(x) = e^{-i\alpha(x)}\psi_H(x)\,. \tag{2.3}$$

The transformation for $\bar{\psi}_H(x)$ is given by the Hermitian conjugate of the previous equation. The derivative term transforms in a more complicated manner

$$\bar{\psi}_H(x)\partial_\mu\psi_H(x) \to \bar{\psi}'_H(x)\partial_\mu\psi'_H(x) = \bar{\psi}_H(x)\partial_\mu\psi_H(x) - i\bar{\psi}_H(x)\partial_\mu\alpha(x)\psi_H(x)\,. \tag{2.4}$$

The second term spoils the invariance. To remove the extra term coming from the derivative and keep the form of the transformation unchanged, one has to come up with a *gauge covariant derivative* D_μ to replace ∂_μ such that

$$D_\mu\psi_H(x) \to \Big[D_\mu\psi_H(x)\Big]' = e^{-i\alpha(x)}D_\mu\psi_H(x)\,, \tag{2.5}$$

in order for $\bar{\psi}_H(x)D_\mu\psi_H(x)$ to be invariant under the local symmetry. A new vector field $A_\mu(x)$, the *gauge field*, extends the theory to form the gauge covariant derivative

$$D_\mu = \partial_\mu + ieA_\mu(x)\,, \tag{2.6}$$

where e is a free parameter, identified with the electric charge. For Eq. (2.5) to be fulfilled, $A_\mu(x)$ has to transform as

$$A_\mu(x) \to A'_\mu(x) = A_\mu(x) + \frac{1}{e}\partial_\mu\alpha(x)\,. \tag{2.7}$$

So far the gauge field is not a true dynamical variable since no term involving its derivatives is present. To achieve this purpose, one introduces the simplest gauge-invariant four dimensional entity

$$\mathcal{L}_{\text{Maxwell}} = -\frac{1}{4}F_{\mu\nu}(x)F^{\mu\nu}(x)\,, \text{ where } F_{\mu\nu}(x) = \partial_\mu A_\nu(x) - \partial_\nu A_\mu(x)\,. \tag{2.8}$$

In fact, the electromagnetic field tensor $F_{\mu\nu}(x)$ is already gauge invariant by itself, nevertheless it can be written in term of covariant derivative

$$[D_\mu, D_\nu] = i\mathrm{e}F_{\mu\nu}\,. \tag{2.9}$$

Collecting together the gauge field dynamics describing its interactions (2.8) and the initial Lagrangian (2.1) in term of gauge covariant derivative (2.6), the obtained Lagrangian provides the description of interactions between light and matter (of the first lepton generation)

$$\begin{aligned}\mathcal{L}_{\mathrm{QED}} &= \bar{\psi}_H(x)\left(i\gamma^\mu\partial_\mu - \mathrm{m}_e\right)\psi_H(x) - \frac{1}{4}F_{\mu\nu}(x)F^{\mu\nu}(x) - \mathrm{e}\bar{\psi}_H(x)\gamma^\mu\psi_H(x)A_\mu(x)\\ &= \mathcal{L}_{\mathrm{Dirac}} + \mathcal{L}_{\mathrm{Maxwell}} + \mathcal{L}_{\mathrm{int}}\,.\end{aligned} \tag{2.10}$$

Hence, starting from the free electron-positron field Lagrangian and requiring gauge-invariance under the $U(1)$ group, the QED Lagrangian has been derived. An important point to make is that the gauge-field is massless, the term $A_\mu(x)A^\mu(x)$ is not gauge invariant. One shall now proceed to derive the gauge field propagator $\tilde{D}^{\mu\nu}_{\mathcal{F}}(k)$. A detailed treatment based on the functional method in path integral language can be found in Ref. [88]. Recall that the propagator is found as the inverse of the quadratic term in the field of interest in the Lagrangian [see Eq. (3.4)]. One notices that the matrix equation associated to the quadratic term in $A_\mu(x)$ is twofold singular; in momentum space it reads

$$\left(-k^2\eta_{\mu\nu} + k_\mu k_\nu\right)\tilde{D}^{\nu\rho}(k) = i\delta^\rho_\mu\,. \tag{2.11}$$

A first singularity occurs due to the $1/k^2$ behaviour in the photon propagator $\tilde{D}^{\nu\rho}(k)$. When the momentum goes to zero, the result is ill-defined. This issue is cured by the adjunction of a small imaginary part, the $i\varepsilon$ prescription, to the denominator, arising from causality considerations. The second singularity is related to the fact that the inverse matrix is not uniquely determined, the transverse part is defined up to a constant. The introduction of a term called *gauge fixing term* solves the second issue,

$$\mathcal{L}_{\mathrm{G.F}} = -\frac{1}{2\xi}[\partial^\mu A_\mu(x)]^2\,. \tag{2.12}$$

The matrix can now be inverted, and the resulting gauge field propagator is

$$\tilde{D}^{\mu\nu}_{\mathcal{F}}(k) = \frac{-i}{k^2 + i\varepsilon}\left(\eta^{\mu\nu} - (1-\xi)\frac{k^\mu k^\mu}{k^2}\right)\,. \tag{2.13}$$

The subscript $\mathcal{F}$ means Feynman propagator in the sense of the *Feynman $i\varepsilon$ prescription*, not the propagator in the Feynman gauge. In practical calculation the value of the ξ parameter is usually chosen to a fixed one. Common choices are $\xi = (0, 1, 3)$, which corresponds respectively to Landau gauge, Feynman gauge and Fried-Yennie gauge. The latter one is used mainly in BSQED, where such a choice produces cancellations that are difficult to obtained otherwise [89]. Although this thesis deals with BSQED, the Feynman gauge is the considered covariant gauge. Later on, in the presence of the external classical field coming from the nucleus, the photon propagator in the Coulomb gauge $(\partial_i A^i(x) = 0)$ is going to be introduced [see Eq. (2.39)].

The Lagrangian (2.10) discussed so far is well suited for tree-level considerations. However, starting from the one-loop level (UV) divergences are encountered in the loop integrals. Those infinities should be cancelled in some way. The procedure developed to cure theses badly divergent behaviours, which inevitable arise in the loops calculations based on the "naive" Lagrangian (2.10), is called renormalization. It necessitates the introduction of so-called *counterterms*. In that respect, the electron mass m_e and the electric charge e are to be formally understood as *bare* quantities: the bare electron mass $\mathrm{m}_{e,0}$ and the bare electric charge e_0. Therefore, the derivations should be understood on a formal level. It is only after carrying out the renormalization procedure that one can speak of the physical mass m_e and the physical electric charge e. A detailed discussion of the renormalization procedure in free QED can be found in Ref. [88]. In a nutshell, each field is rescaled by a constant Z, i.e. $\psi = Z_2^{1/2}\psi_r$ and $A^\mu = Z_3^{1/2}A_r^\mu$. Z_2 is the electron field-strength renormalization constant and Z_3 is the photon field-strength renormalization constant. Interestingly, the interaction term is now $\mathrm{e}_0 Z_2 Z_3^{1/2}\bar{\psi}_r\gamma^\mu\psi_r A_{r\mu}$. The physical electric charge is introduced by defining a scaling factor Z_1, such that

$$\mathrm{e}_0 Z_2 Z_3^{1/2} = \mathrm{e}Z_1\,. \tag{2.14}$$

Z_1 is the vertex renormalization constant. As a side comment, the Ward-Takahashi identity ensures $Z_1 = Z_2$ at all orders in perturbation theory, hence $\mathrm{e} = \sqrt{Z_3}\mathrm{e}_0$, at one-loop level. The renormalized Lagrangian is then split into two pieces, and reads [88]

$$\begin{aligned}\mathcal{L}_{\mathrm{QED}} \;=\; & -\frac{1}{4}\left(F_r^{\mu\nu}\right)^2 + \bar{\psi}_r\left(i\partial\!\!\!/ - \mathrm{m}_e\right)\psi_r - \mathrm{e}\bar{\psi}_r\gamma^\mu\psi_r A_{r,\mu} \\ & -\frac{1}{4}\delta_3\left(F_r^{\mu\nu}\right)^2 + \bar{\psi}_r\left(i\delta_2\partial\!\!\!/ - \delta\mathrm{m}_e\right)\psi_r - \mathrm{e}\delta_1\bar{\psi}_r\gamma^\mu\psi_r A_{r,\mu}\,.\end{aligned} \tag{2.15}$$

The Feynman slash notation $\not{p} = \gamma^\mu p_\mu$ is applied and the argument of the fields are dropped out. The counterterms are given by

$$\delta_i = Z_i - 1 \ , i = 1,2,3 \ \text{and} \ \delta \mathrm{m}_e = Z_2 \mathrm{m}_{e,0} - \mathrm{m}_e \, , \tag{2.16}$$

where $\delta \mathrm{m}_e$ is the mass *counterterm* and δ_1 the charge *counterterm*. Renormalization conditions define, among others, the electron physical charge and mass. The electron physical mass is fixed by the condition that the electron self-energy Σ vanishes for on-shell momentum, whereas the physical electric charge is fixed by the requirement that the vertex function Γ^μ at zero-momentum transfer is the standard gamma matrix,

$$\Sigma(\not{p} = \mathrm{m}_e) = 0 \, , \ \text{and} \ -i\mathrm{e}\Gamma^\mu(p' - p = 0) = i\mathrm{e}\gamma^\mu \, . \tag{2.17}$$

The connection between the bare and physical electric charge is established and solely depends on the photon field-strength renormalization constant (at one-loop order). The connection between the bare and physical mass depends on the regularization scheme used and the order considered in perturbation theory.

2.2. Furry Picture

The previous discussion considered *free* QED in the sense of the absence of a binding potential, but was however an *interacting* theory due to the presence of a coupling term between electron-positron field and the photon field in $\mathcal{L}_{\text{int}}$ [see Eq. (2.10)]. This section discusses how the presence of a *classical external field* $\mathcal{A}_\mu(x)$, which describes the interaction of the electron-positron field with the (classical) nucleus, modifies the previous framework. To emphasis on the difference a superscript $^{(0)}$ is introduced to distinguish from the considerations made in the previous section. $\psi_H^{(0)}(x)$ denotes the BSQED zeroth-order term in interaction with the electromagnetic field but in the presence of the classical field of the nucleus. Let us write the vector potential associated to the classical external field as

$$\mathcal{A}_\mu(x) = \left(\frac{\mathrm{V}_{\text{nucl}}(\mathbf{x})}{\mathrm{e}}, \mathbf{0} \right) \, . \tag{2.18}$$

A few comments should be made regarding the nuclear potential introduced. The nucleus is considered to be significantly more massive than the electron, $\mathrm{M}_{\text{nucl}} \gg \mathrm{m}_e$ (m_p / $\mathrm{m}_e \approx 1836$). Therefore, recoil corrections are not accounted for in the following. Due to the infinite mass of the nucleus (in comparison to the electron one) the nuclear potential is taken to be

static, since its motion is negligible with respect to the time frame of the electronic motion, hence the time-independence of the nuclear potential. The attractive potential of the nucleus affects the matter content of the Lagrangian, as electrons are captured in its vicinity to form bound states. The parts involving the electromagnetic field are not considered in what follows. The Lagrangian of the (non-interacting) electron-positron field in the presence of the external classical field is

$$\mathcal{L}_{\text{Dirac+nucl}} = \bar{\psi}_H^{(0)}(x)\left(i\gamma^\mu\partial_\mu - \mathrm{m}_e - \mathrm{e}\gamma^\mu\mathcal{A}_\mu\right)\psi_H^{(0)}(x)\,. \tag{2.19}$$

The interaction of the electron-positron field with the external classical field of the nucleus is taken into account non-perturbatively from the beginning by solving Dirac equation in the presence of the binding potential

$$\left(i\gamma^\mu\partial_\mu - \mathrm{m}_e - \mathrm{e}\gamma^\mu\mathcal{A}_\mu\right)\psi_H^{(0)}(x) = 0\,. \tag{2.20}$$

The equation of motion of the electron-positron field $\psi_H^{(0)}(x)$ (2.20) is referred to as the Furry picture of QED [29] or BSQED. Upon a Legendre transformation, the Dirac Hamiltonian in the Furry picture is obtained

$$h_{\mathrm{D}}\phi_k(\mathbf{x}) = \left[-i\boldsymbol{\alpha}\cdot\boldsymbol{\nabla} + \beta\mathrm{m}_e + V_{\text{nucl}}(\mathbf{x})\right]\phi_k(\mathbf{x}) = \epsilon_k\phi_k(\mathbf{x})\,, \tag{2.21}$$

where $\phi_k(\mathbf{x})$ are the solutions of the stationary Dirac equation and k stands for all quantum numbers. The time-depend solution is the stationary solution $\phi_k(\mathbf{x})$ multiplied by the phase factor $\exp\left(-i\epsilon_k\mathrm{x}^0\right)$. Upon second quantization, the (non-interacting) electron-positron field can be expanded in terms of creation and annihilation operators

$$\psi_H^{(0)}(x) = \sum_{\epsilon_k > E^F} a_k\phi_k(\mathbf{x})e^{-i\epsilon_k\mathrm{x}^0} + \sum_{\epsilon_k < E^F} b_k^\dagger\phi_k(\mathbf{x})e^{-i\epsilon_k\mathrm{x}^0}\,, \tag{2.22}$$

where a_k (b_k) is the electron (positron) annihilation operator for an electron (positron) in the state k and $a_k^\dagger$ ($b_k^\dagger$) is the electron (positron) creation operator for an electron (positron) in the state k, fulfilling the usual equal-time anti-commutations relations

$$\{a_i, a_j^\dagger\} = \delta_{ij}\,, \quad \{b_i, b_j^\dagger\} = \delta_{ij}\,. \tag{2.23}$$

All other anti-commutators are trivially zero. The Fermi level E^F is set to $E^F = 0$, separating the negative-energy continuum (Dirac sea) from the rest of the spectrum. The unperturbed

normal ordered Hamiltonian is given by [90]

$$H_0 = \int d^3x : \psi_H^{(0)\dagger}(x) h_{\rm D} \psi_H^{(0)}(x) : \, . \tag{2.24}$$

The external static potential is given explicitly, under the hypothesis that the interaction is described by the electric field generated by the nucleus

$$V_{\rm nucl}(\mathbf{x}) = V_{\rm C}(\mathbf{x}) = -\frac{\alpha Z}{|\mathbf{x}|} \, . \tag{2.25}$$

One recognises the expression for the Coulomb potential of a point-like nucleus. Consequently, $\phi_k(\mathbf{x})$ are solutions to all order in αZ, in other words going beyond the perturbative regime $\alpha Z \ll 1$. The Dirac equation for the point-like nucleus is solvable analytically and the eigenvalues are given by [90]

$$\epsilon_k \equiv \epsilon_{n\kappa} = \mathrm{m}_e \left[1 + \left(\frac{\alpha Z}{n - |\kappa| + \sqrt{\kappa^2 - (\alpha Z)^2}} \right)^2 \right]^{-\frac{1}{2}} \, . \tag{2.26}$$

The eigenfunctions $\phi_k(\mathbf{x})$ are characterized by three quantum numbers $k = (n_k, \kappa_k, m_k)$. The relativistic angular momentum number κ takes non-zero integer values and is related to the total angular momentum j and the orbital angular momentum quantum number l of the Schrödinger hydrogen-like (H-like) atom by $\kappa = (-1)^{j+l+1/2}\,(j+1/2)$. For light systems, meaning small Z, the condition $\alpha Z \ll 1$ is fulfilled [91] and the energy eigenvalues can be expanded as

$$\epsilon_{n\kappa} = \mathrm{m}_e \left[1 - \frac{1}{2}\left(\frac{\alpha Z}{n}\right)^2 - \frac{1}{2}\left(\frac{\alpha Z}{n}\right)^4 \left(\frac{n}{j+\frac{1}{2}} - \frac{3}{4} \right) + \ldots \right] \, . \tag{2.27}$$

The first term in the expansion is the electron's rest mass, the second one is the non-relativistic energy level obtained by solving Schrödinger's equation for the H-like atom. The first relativistic or leading relativistic corrections enters at order $(\alpha Z)^4$, hence a $(\alpha Z)^2$ correction to the Schrödinger's energy level. Thereby, the parametrization $E_{\rm QED}(n,j,l) = \frac{\alpha}{\pi}\frac{(\alpha Z)^4}{n^3} F_{(n,j,l)}(\alpha Z)$ (in units of m_e) [26], valid in such regime. Notice that this term also depends on the total angular momentum j. Thus, the degeneracy between states with the same principal quantum number is lifted, for example between the $2p_{1/2}$ and $2p_{3/2}$ states. The splitting in the energy spectrum introduced by the presence of the total angular momentum j is usually referred to as the fine-structure splitting. It should not be confused with the Lamb shift, which arises from the interactions of the electron with (quantum) vacuum energy fluctuations. Initially, the Lamb

shift described the energy difference between the $2s_{1/2}$ and $2p_{1/2}$ states [92] but the term has a broader use nowadays. Detailed consideration of QED corrections are discussed in Chapter 3.

The extended Furry picture complements the previous treatment with the inclusion of a screening potential $U(\mathbf{x})$ in Eq. (2.25). It partially accounts for interelectronic interactions and/or correlations among electrons in many-electron system. Examples of screening potentials are core-Hartree potential [93–96] or Kohn-Sham potential [97] . In the extended Furry picture the subscript "nuclear" of the potential is dropped and one simply writes

$$V(\mathbf{x}) = V_{\mathrm{C}}(\mathbf{x}) + U(\mathbf{x})\,. \tag{2.28}$$

A *counterpotential* term is to be introduced in $\mathcal{L}_{\mathrm{int}}$ to compensate the potential added above.

The vacuum state of the theory can be addressed now. Since this thesis deals with radiative and interelectronic corrections, it implies that no real photons are present. All photon considered are virtual ones mediating the interactions among electrons and positrons. This explains why only even power are obtained as energy corrections (2.27), each vertex is proportional to e and enters twice. The vacuum state of the theory in the presence of the Coulomb field of the nucleus (2.19) is denoted as $|0\rangle$. It fulfills the usual requirement that the annihilation operators cannot decrease its occupation number in the Fock space

$$a_k|0\rangle = 0\,, \quad b_k|0\rangle = 0\,. \tag{2.29}$$

The vacuum expectation value of the time-ordered product of two electron-positron field operators defines the electron propagator. The bound state expansion in term of creation and annihilation operators of non-interacting electron-positron field (2.22) allows to write it as

$$\langle 0|T\left[\psi_H^{(0)}(x)\bar{\psi}_H^{(0)}(y)\right]|0\rangle = \frac{i}{2\pi}\int d\omega \sum_k \frac{\phi_k(\boldsymbol{x})\bar{\phi}_k(\boldsymbol{y})}{\omega - \epsilon_k(1-i\varepsilon)} e^{-i(x^0-y^0)\omega}\,, \tag{2.30}$$

where $\varepsilon > 0$ implies the limit to zero. For later use, let us define $u = 1 - i\varepsilon$. T stands for the time-ordering operator and is written explicitly in terms of the Heaviside function. The integral representation of the latter is used to get to the result (2.30)

$$\theta(x^0) = \pm\frac{1}{2\pi i}\int d\omega \frac{1}{\omega \mp i\varepsilon} e^{\pm i\omega x^0}\,. \tag{2.31}$$

Note that the propagator depends only on the time difference $x^0 - y^0$. One could Fourier transform with respect to the time variable and obtain an expression of the electron propagator

as a function of coordinates and energy

$$\frac{i}{2\pi}S(\omega,\mathbf{x},\mathbf{y}) = \frac{i}{2\pi}\sum_k \frac{\phi_k(\boldsymbol{x})\phi_k^\dagger(\boldsymbol{y})}{\omega-\epsilon_k(1-i\varepsilon)}\,. \tag{2.32}$$

The electron propagator has poles, which define the bound state energies of the electron, and branch cuts from $(-\infty,-\mathrm{m}_e]$ and $[\mathrm{m}_e,+\infty)$, see Fig. 2.1(a). The photon propagator is defined similarly to the electron propagator, being the vacuum expectation value of the time-ordered product of two electromagnetic field operators. An explicit expression in position space is calculated from expression (2.13) in the Feynman gauge

$$\langle 0|T\left[A^\mu(x)A^\nu(y)\right]|0\rangle = \int \frac{d^4k}{(2\pi)^4}\tilde{D}^{\mu\nu}_{\mathcal{F}}(k)|_{\xi=1} = -i\eta^{\mu\nu}\int \frac{d^4k}{(2\pi)^4}\frac{e^{-ik(x-y)}}{k^2+i\varepsilon}\,. \tag{2.33}$$

Fourier transforms the previous expression with respect to the time variable leads to coordinates-energy representation of the photon propagator in the Feynman gauge, denoted by the F subscript

$$D^{\mu\nu}_F(\omega,\mathbf{x}-\mathbf{y}) = -\eta^{\mu\nu}\int \frac{d^3k}{(2\pi)^3}\frac{e^{i\mathbf{k}\cdot(\mathbf{x}-\mathbf{y})}}{\omega^2-\mathbf{k}^2+i\varepsilon} = \frac{\eta^{\mu\nu}}{4\pi|\mathbf{x}-\mathbf{y}|}e^{i\sqrt{\omega^2+i\varepsilon}|\mathbf{x}-\mathbf{y}|}\,. \tag{2.34}$$

The branch of the square root is fixed by the condition $\mathrm{Im}\sqrt{\omega^2+i\varepsilon}>0$. $D^{\mu\nu}_F(\omega,\mathbf{x}-\mathbf{y})$ is an analytical function of ω in the complex ω plane with cuts beginning at the points $\omega=+i\varepsilon$ and $\omega=-i\varepsilon$, see Fig. 2.1(b) .

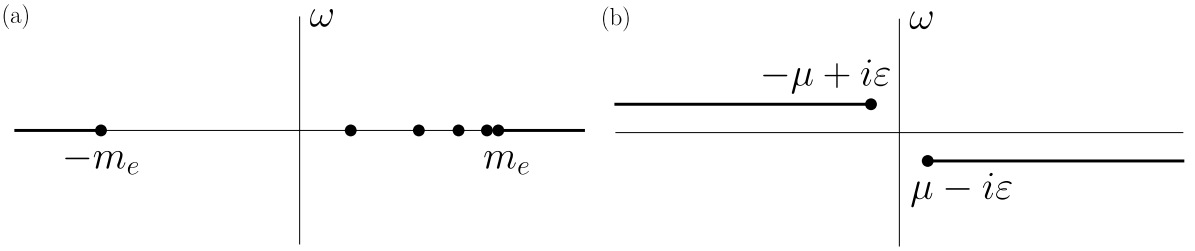

Figure 2.1.: (a) Singularities of the electron propagator in the complex ω plane. The dots denote the bound-states and the thick lines represent the branch-cuts. (b) Singularities of the photon propagator in the complex ω plane for a non-zero photon mass μ. Massless case is recovered by setting $\mu=0$.

Some notations and relevant quantities for later calculations are introduced. Here and in what follows, the RMBPT notations of Lindgren and Morisson [98] and Johnson [99] are used: v and h designate the valence electron and the hole state, respectively, $a,b,c,\ldots$ stand for

core orbitals, and i,j,k,l,p correspond to any arbitrary states. The interelectronic-interaction operator I stands for

$$I(\omega,\boldsymbol{x}-\boldsymbol{y}) = \mathrm{e}^2\alpha^\mu\alpha^\nu D_{\mu\nu}(\omega,\boldsymbol{x}-\boldsymbol{y})\,,\ \text{and}\ I'(\omega,\boldsymbol{x}-\boldsymbol{y}) \equiv \frac{dI(\omega,\boldsymbol{x}-\boldsymbol{y})}{d\omega}\,. \tag{2.35}$$

In the Feynman and Coulomb gauges, these operators fulfill the symmetry properties

$$I(\omega,\boldsymbol{x}-\boldsymbol{y}) = I(-\omega,\boldsymbol{x}-\boldsymbol{y})\,,\ I'(\omega,\boldsymbol{x}-\boldsymbol{y}) = -I'(-\omega,\boldsymbol{x}-\boldsymbol{y}) \Rightarrow I'(0,\boldsymbol{x}-\boldsymbol{y}) = 0 \tag{2.36}$$

The following shorthand notation for the matrix element will be used throughout the whole thesis

$$I_{ijkl}(\omega) = \int d^3x d^3y \phi_i^\dagger(\boldsymbol{x})\phi_j^\dagger(\boldsymbol{y}) I(\omega,\boldsymbol{x}-\boldsymbol{y})\phi_k(\boldsymbol{x})\phi_l(\boldsymbol{y})\,, \tag{2.37}$$

for which the symmetry property holds

$$I_{ijkl}(\omega) = I_{jilk}(\omega)\,. \tag{2.38}$$

The photon propagator, in the Coulomb gauge, is given by

$$\begin{aligned}
D^C_{00}(\omega,\boldsymbol{x}-\boldsymbol{y}) &= \frac{1}{4\pi|\boldsymbol{x}-\boldsymbol{y}|}\,,\\
D^C_{i0}(\omega,\boldsymbol{x}-\boldsymbol{y}) &= D^C_{0j}(\omega,\boldsymbol{x}-\boldsymbol{y}) = 0\,,\\
D^C_{ij}(\omega,\boldsymbol{x}-\boldsymbol{y}) &= -\frac{\delta_{ij}e^{i\sqrt{\omega^2+i\varepsilon}|\boldsymbol{x}-\boldsymbol{y}|}}{4\pi|\boldsymbol{x}-\boldsymbol{y}|} - \nabla_i^{(x)}\nabla_j^{(y)}\frac{1-e^{i\sqrt{\omega^2+i\varepsilon}|\boldsymbol{x}-\boldsymbol{y}|}}{4\pi\omega^2|\boldsymbol{x}-\boldsymbol{y}|}\,.
\end{aligned} \tag{2.39}$$

Thus, I^C can be expressed as

$$I^C(\omega,\boldsymbol{x}-\boldsymbol{y}) = \alpha\left(\frac{\mathbb{1}_4 - \boldsymbol{\alpha}_x\cdot\boldsymbol{\alpha}_y e^{i\sqrt{\omega^2+i\varepsilon}|\boldsymbol{x}-\boldsymbol{y}|}}{|\boldsymbol{x}-\boldsymbol{y}|} + \left[(\boldsymbol{\alpha}_x\cdot\boldsymbol{\nabla}_x),\left[(\boldsymbol{\alpha}_y\cdot\boldsymbol{\nabla}_y),\frac{e^{i\sqrt{\omega^2+i\varepsilon}|\boldsymbol{x}-\boldsymbol{y}|}-1}{\omega^2|\boldsymbol{x}-\boldsymbol{y}|}\right]\right]\right). \tag{2.40}$$

In the Feynman gauge, the operator I^F reads

$$I^F(\omega,\boldsymbol{x}-\boldsymbol{y}) = \alpha\frac{\mathbb{1}_4 - \boldsymbol{\alpha}_x\cdot\boldsymbol{\alpha}_y}{|\boldsymbol{x}-\boldsymbol{y}|}e^{i\sqrt{\omega^2+i\varepsilon}|\boldsymbol{x}-\boldsymbol{y}|}\,. \tag{2.41}$$

Matrices $\boldsymbol{\alpha}_x$ and $\boldsymbol{\alpha}_y$ act on the Dirac bispinors with the arguments $\boldsymbol{x}$ and $\boldsymbol{y}$, respectively.

In Chapter 3.2, the gauge invariance of derived expressions is going to be demonstrated. For this purpose, it is convenient to consider the difference between the matrix elements with the photon propagator in the Feynman and Coulomb gauges. This difference is given by

$$\Delta I_{ijkl}(\omega) \equiv I^F_{ijkl}(\omega) - I^C_{ijkl}(\omega) = (\omega^2 + \Delta_{ik}\Delta_{jl})\widetilde{I}_{ijkl}(\omega)\,, \tag{2.42}$$

with

$$\widetilde{I}(\boldsymbol{x}-\boldsymbol{y};\omega) = \alpha\frac{e^{i\sqrt{\omega^2+i\varepsilon}|\boldsymbol{x}-\boldsymbol{y}|}-1}{\omega^2|\boldsymbol{x}-\boldsymbol{y}|} \tag{2.43}$$

and $\Delta_{ij} = \epsilon_i - \epsilon_j$. The previous expression in terms of Δ_{ij} is obtained by noticing that $\boldsymbol{\alpha}\cdot\boldsymbol{\nabla}$ can be replaced by ih_D in the commutators, since the scalar parts of the Hamiltonian commute and cancel out. One also needs its derivative with respect to ω, which can be cast as

$$\Delta I'_{ijkl}(\omega) = 2\omega\tilde{I}_{ijkl}(\omega) + (\omega^2 + \Delta_{ik}\Delta_{jl})\widetilde{I}'_{ijkl}(\omega)\,. \tag{2.44}$$

In the case of two photon propagators, the following formula is useful to calculate the difference between the gauges,

$$I^F_{i_1j_1k_1l_1}(\omega_1)I^F_{i_2j_2k_2l_2}(\omega_2) - I^C_{i_1j_1k_1l_1}(\omega_1)I^C_{i_2j_2k_2l_2}(\omega_2) = \frac{1}{2}\left[\Delta I_{i_1j_1k_1l_1}(\omega_1)I^F_{i_2j_2k_2l_2}(\omega_2) + I^C_{i_1j_1k_1l_1}(\omega_1)\Delta I_{i_2j_2k_2l_2}(\omega_2) + F\leftrightarrow C\right]\,. \tag{2.45}$$

Note that it treats symmetrically both I operators with respect to the gauge variation. It applies as well in the case of derivative terms, replacing I_{ijkl} with I'_{ijkl}. The following rearrangement formula will be handy to demonstrate the cancellation among terms of the three-electron part,

$$\sum_m I_{i_1j_1k_1m}(\Delta_{k_1i_1})I_{mj_2k_2l_2}(\Delta_{j_2l_2}) = \sum_m I_{j_2j_1l_2m}(\Delta_{j_2l_2})I_{mi_1k_2k_1}(\Delta_{k_1i_1})\,. \tag{2.46}$$

It is based on the completeness relation and the commutation between the I operators.

2.3. Vacuum state redefinition's approach

Dealing with many-electron ions is a difficult task due to the numerical complexity involved as well as to derive tractable formal BSQED expression. That is why *ab initio* calculations

are limited so far to a few-electron ions [67, 68, 79] and ions with single valence (or hole) electron [55, 75, 76, 83]. To facilitate the derivation of tractable formal expressions for many-electron systems the vacuum state redefinition technique is widely accepted and demonstrated within the RMBPT formalism [98–101]. However, within BSQED it is not yet broadly employed. Nevertheless, the vacuum state redefinition method was mainly utilized for single-valence electron states [85, 102–105] and recently for two-valence electron states [79]. In Ref. [85], the author considered the case of one electron over closed shells in the context of the TTGF method developed in that work. In Ref. [83], the problem of the rigorous QED formulation for many-electron systems within the S-matrix approach was considered and the usefulness of the vacuum state redefinition by analogy with the RMBPT was emphasized.

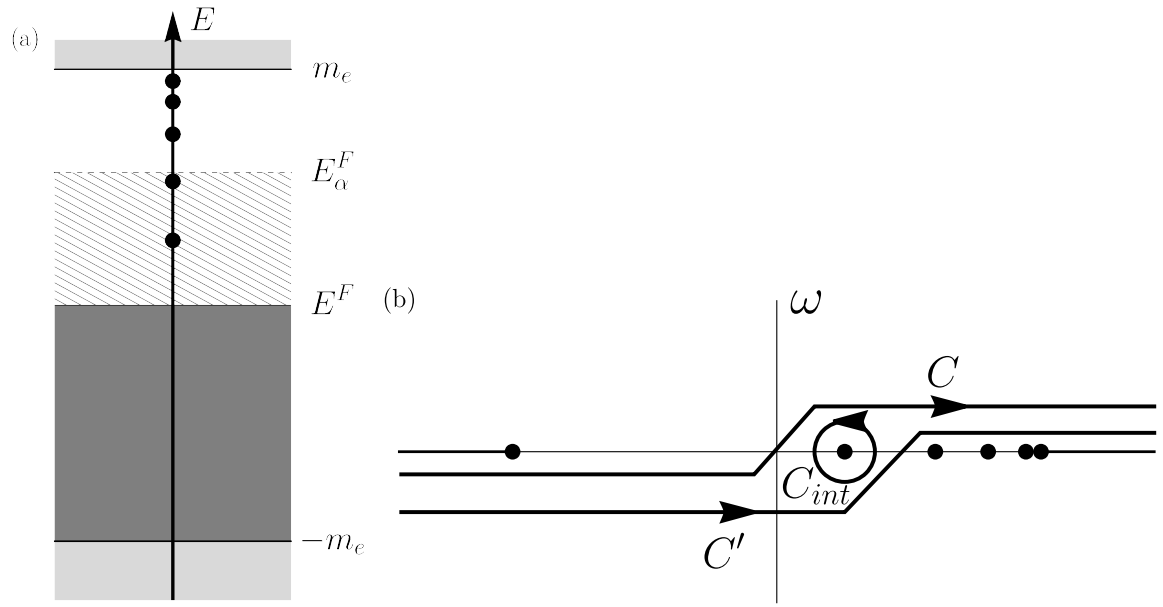

Figure 2.2.: (a) Energy spectrum of a bound system. The dots correspond to the bound energies. The light gray areas correspond to the positive and negative energy continuum, the dark gray area is the energy gap between the negative continuum and the standard vacuum state, the hatched area corresponds to the core electrons included in the redefined vacuum state. (b) Different integration paths over the electron energy ω. C is the contour of integration in the standard vacuum state according to the Feynman prescription. C' is the shifted contour of integration, where the redefined vacuum state encapsulates the $(1s)^2$ shell. $C_{\text{int}} = C' - C$ describes the interaction of the reference state (valence electron or hole state) with the $(1s)^2$-shell electrons. Other notations are identical to Fig. 2.1.

The concept of a vacuum state redefinition naturally arose in quantum field theory due to the notion of the fully occupied negative-energy continuum of spin-1/2 states, the so-called Dirac sea. The essential notion in introducing a redefined vacuum state is to separate the electron dynamics into the “core” and “valence” parts. The first part is relegated to the reference vacuum

energy [hatched area in Fig. 2.2(a)] and can be neglected when the transition energy, with a significant many-electron background remaining unchanged, is considered. The key feature is that the contributions, arising from the interaction between core electrons are canceled in the difference between the excited and the ground state energies, are not considered from the very beginning. For example, when the interest lies in the valence electron binding energy or in its excitation energy, it is convenient to employ the concept of vacuum state redefinition.

This is formulated via a new Fermi level E_α^F, which lies above all core electron states belonging to closed shells, as shown in Fig. 2.2(a). The many-electron contributions are extracted as the difference of two integrals over altering integration contours, each in link with its respective vacuum state, as shown in Fig. 2.2(b). In this way, the interaction of the reference particle (electron or hole) with core electrons is taken into account within the QED framework. The great advantage of the method is, for example, that instead of the all-electron states one deals with the few-valence-electron states, which amounts to a much smaller Hilbert space. Further elaboration on the approach based on the redefinition of the vacuum state within the QED perturbation theory is presented in the next chapter.

2.3.1. Redefined vacuum state and implications

A new vacuum state, named redefined vacuum state, is introduced in a way that all core orbitals from the closed shells belong to it [98]. Let it be denoted by $|\alpha\rangle$,

$$|\alpha\rangle = a_a^\dagger a_b^\dagger \ldots |0\rangle \,. \tag{2.47}$$

The corresponding Fermi level E_α^F precise location is determined by the redefined vacuum state $|\alpha\rangle$: E_α^F lies slightly above the energy level of the highest occupied orbital of the new vacuum state $|\alpha\rangle$. The meaning of creation and annihilation operators is changed for the core shell electrons ($a_a \to b_a^\dagger,\ a_a^\dagger \to b_a$), and the electron-positron field operator reads

$$\psi_{H,\alpha}^{(0)}(x) = \sum_{\epsilon_k > E_\alpha^F} a_k \phi_k(\boldsymbol{x}) e^{-i\epsilon_k x^0} + \sum_{\epsilon_k < E_\alpha^F} b_k^\dagger \phi_k(\boldsymbol{x}) e^{-i\epsilon_k x^0} \,. \tag{2.48}$$

Moreover, annihilation operators obey their usual rules but accordingly to their respective energy ϵ_k compared to Fermi level E_α^F [see Eq. (2.48)],

$$b_k|\alpha\rangle = 0\,, \quad a_k|\alpha\rangle = 0\,. \tag{2.49}$$

Attributing a multitude of one-electron states to the redefined vacuum state, the interest is in describing the dynamics of N-particle (electrons and holes) state A on top of the redefined vacuum state, which is defined by the expression

$$|A\rangle = a_{v_1}^\dagger a_{v_2}^\dagger \dots b_{h_{N-1}}^\dagger b_{h_N}^\dagger |\alpha\rangle \,. \tag{2.50}$$

The zeroth-order energy $E_A^{(0)}$ is thus given by the state average of the zeroth-order Hamiltonian (2.24),

$$E_A^{(0)} = \langle A|H_0|A\rangle = \sum_{v=v_1,v_2,\dots} \epsilon_v - \sum_{h=\dots,h_{N-1},h_N} \epsilon_h \,. \tag{2.51}$$

Here, one sums up the one-electron energies of the electrons and subtracts the one-electron energies of the holes. The shift of the Fermi level from E^F to E_α^F affects the electron propagator as it affected the expansion of the electron-positron field in creation and annihilation operators in Eq. (2.48). The expression presented below is suitable for both the redefined vacuum state and the standard vacuum state, with the replacement $E_\alpha^F \to E^F = 0$,

$$\langle\alpha|T\,[\psi_{H,\alpha}^{(0)}(x)\psi_{H,\alpha}^{(0)\dagger}(y)\,]|\alpha\rangle = \frac{i}{2\pi}\int d\omega \sum_k \frac{\phi_k(\boldsymbol{x})\phi_k^\dagger(\boldsymbol{y})}{\omega - \epsilon_k + i\varepsilon(\epsilon_j - E_\alpha^F)} e^{-i(x^0-y^0)\omega} \,. \tag{2.52}$$

Consequently, the expression (2.32) is adapted to

$$\frac{i}{2\pi} S_\alpha(\omega, \mathbf{x}, \mathbf{y}) = \frac{i}{2\pi}\sum_k \frac{\phi_k(\boldsymbol{x})\phi_k^\dagger(\boldsymbol{y})}{\omega - \epsilon_k + i\varepsilon(\epsilon_j - E_\alpha^F)} \,, \tag{2.53}$$

which is the electron propagator in the framework of the redefined vacuum state, highlighted by the α subscript. As stated previously, the poles of the electron propagator define the bound-states energies, but not in the full theory; recall that the interaction of the electron-positron field with the electromagnetic field was neglected in the discussion of the Furry picture (2.21), hence the use of $\psi_{H,\alpha}^{(0)}(x)$. Thus, the poles are the leading relativistic corrections but do not account for the radiative corrections arising from the quantum field description of the electromagnetic field and its interactions with the electron-positron field. In general, the energy levels for an N-electron system including QED effects are obtained from the poles of the spectral representation of N-point functions, which one comes at and discusses in details in Chapter 3.1.

2.3.2. Extraction of interelectronic interactions with core electrons

The core orbitals are by construction[1], the discrete part of the negative-energy spectrum due to the change in the poles circumvention prescription (2.53). It corresponds to a different integration path in the complex ω plane, see Fig. 2.2(b). The difference in the vacua focuses on the dynamics occurring in between them [the hatched area in Fig. 2.2(a)], which is of interest since this part of the spectrum deals with core electrons that were previously "hidden". The interelectronic interactions are retrieved as the difference between expressions in the redefined vacuum state and the ones in the standard vacuum state. Formulated in other words, the expressions obtained in the frame of the redefined vacuum state contain the same expressions, with respect to the standard vacuum state, plus interelectronic corrections between the core electrons and the reference state; one-electron radiative corrections are incorporated with the interelectronic ones in the redefined vacuum framework. Detailed examples are provided in Section 3.2.1, Eqs. (3.58, 3.59) and in Section 3.2.2, Eq. (3.67).

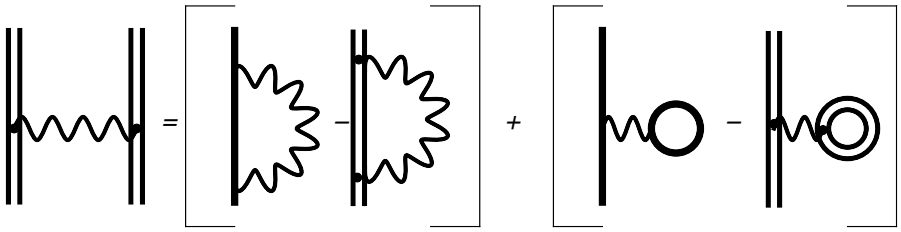

Figure 2.3.: Extraction of the one-photon-exchange correction out of the subtraction of the one-particle self-energy (SE) and one-particle vacuum-polarization (VP) Feynman diagrams in different vacua. Thick black lines denote the electron propagator in the redefined vacuum state in an external potential V. Double lines indicate the electron propagator in the standard vacuum state in an external potential V. Wavy lines correspond to the photon propagator.

The difference between the propagator in the redefined vacuum state and the propagator in the standard vacuum state corresponds to a cut of the electron line on the Feynman diagram, as shown on Fig. 2.3. The application of Sokhotski-Plemelj theorem is introduced as a tool to simplify this difference and to make the cut explicit. The following equality is meant to be understood while integrating in the complex ω plane. For $p = 1, 2, \ldots$ we have,

$$\sum_j \frac{\phi_j(\boldsymbol{x})\bar{\phi}_j(\boldsymbol{y})}{[\omega - \epsilon_j + i\varepsilon(\epsilon_j - E^F_\alpha)]^p} - \sum_j \frac{\phi_j(\boldsymbol{x})\bar{\phi}_j(\boldsymbol{y})}{[\omega - \epsilon_j + i\varepsilon(\epsilon_j - E^F)]^p} = \frac{2\pi i(-1)^p}{(p-1)!} \frac{d^{(p-1)}}{d\omega^{(p-1)}} \sum_a \delta(\omega - \epsilon_a)\phi_a(\boldsymbol{x})\bar{\phi}_a(\boldsymbol{y})\,. \quad (2.54)$$

[1] See comment below Eq.(2.47) and Fig. 2.2(a)

2.4. Perturbation Theory

Previously, the interaction term $\mathcal{L}_{\text{int}}$ was neglected in the discussion. The full theory is considered now but the highlight is on the latter term. The interaction Hamiltonian is obtained after a Legendre transformation, and encapsulates the interaction of the electron-positron field with the quantized electromagnetic field $A_\mu(x)$ and the *counterpotential* $-U(\mathbf{x})$, when one works within the extended Furry picture,

$$h_{\text{int}}(x) = \mathrm{e}\alpha^\mu A_\mu(x) - U(\boldsymbol{x}) - \delta\mathrm{m}_e\gamma^0 . \tag{2.55}$$

A mass renormalization counterterm is included as well to regularize the ultraviolet divergence occurring in self-energy loops (see Appendix A.1). The corresponding normal-ordered interaction Hamiltonian is

$$H_{\text{int}} = \int d^3x : \psi^{(0)\dagger}_{H,\alpha}(x) h_{\text{int}}(x) \psi^{(0)}_{H,\alpha}(x) : . \tag{2.56}$$

The bound-state energy corrections due to this interaction Hamiltonian are usually accounted for via the bound-state QED perturbation theory. In this context the perturbation theory is based on the fine-structure constant α as an expansion parameter, accounting for order-by-order corrections, assuming the $U(\boldsymbol{x})$ expansion converges reasonably fast. In the original Furry picture, the α perturbative expansion can be enhanced with a further $1/Z$ expansion at each order under the hypothesis $Z \gg N$, which is fulfilled for heavy few-electron ions. For an overall correction of order n, contributions range from nth order in α up to nth order in $1/Z$, with all possible intermediates fulfilling the order in α and in $1/Z$ corrections sum to n. The order in $1/Z$ indicates the number of exchanged photons, which mediates the interelectronic interaction between different electrons.

To date there are several methods employed within the BSQED perturbation theory: the adiabatic S-matrix approach [90], the two-time Green's function method [85,106], the covariant-evolution-operator method [107–109], and the line profile approach [110]. The treatment of BSQED in this thesis relies on the TTGF method, which is introduced in the next chapter. A special care is required in the treatment of the contributions where an intermediate-state energy coincides with the reference-state energy, so-called *reducible* contributions. As a side comment, the covariant-evolution-operator method mixes RMBPT with QED. It features two times as well, even thought one is sent to $t \to -\infty$, and can handle quasi-degenerate states, which is not possible with the S-matrix. The reader is referred to Ref. [107] for a detailed description of the method and its comparison with the S-matrix one and the TTGF approach.

CHAPTER 3.

TWO-TIME GREEN'S FUNCTION

Along the previous chapter, QED corrections have been teased and the reader was referred to this chapter for more detailed explanations. One shall proceed to present the two-time Green's function method devised by Shabaev [85], based on the approach of a redefined vacuum state, for both N-electronic and N-positronic (hole) states. However, before doing so, a few words on the concept of the Green's function and its use as a tool are provided, according to Ref. [111]. The chapter then goes through the consideration of a single-valence electron state over the closed shells, where interelectronic corrections are calculated up to the second order. Afterward, the first order screened radiative corrections are investigated for a single-hole state in the closed shells, a vacancy in the electronic configuration. The two-photon-exchange corrections are derived in this case too, and the matching between QED and the RMBPT is achieved as a cross-check.

The material presented in the chapter is based on the references:

> *Redefined vacuum approach and gauge-invariant subsets in two-photon-exchange diagrams for a closed-shell system with a valence electron* [112]
> R. N. Soguel, A. V. Volotka, E. V. Tryapitsyna, D. A. Glazov and S. Fritzsche
> Phys. Rev. A **103**, 042818 (2021)

> *Many-electron QED with redefined vacuum approach*[1] [113]
> R. N. Soguel, A. V. Volotka, D. A. Glazov and S. Fritzsche
> Symmetry **13(6)**, 1014 (2021)

Consider an abstract differential operator $\mathcal{D}$ acting on some state $|f\rangle$ of a linear space such that it results in the state $|g\rangle$,

$$\mathcal{D}|f\rangle = |g\rangle\,. \tag{3.1}$$

[1] Errors found in section 3 are corrected in the thesis.

The formal solution is obtained by solving the homogeneous equation $\mathcal{D}|h_i\rangle = 0$ for each linearly independent solution i, plus the particular solution associated to $|g\rangle$,

$$|f\rangle = \mathcal{D}^{-1}|g\rangle + \sum_i c_i|h_i\rangle\,. \tag{3.2}$$

It involves the inverse differential operator $\mathcal{D}^{-1}$, which meaning will become clearer after a projection on the coordinates space, and accordingly the insertion of the resolution of the identity. One arrives to

$$\langle x|f\rangle = \int_a^b dx'\langle x|\mathcal{D}^{-1}|x'\rangle\langle x'|g\rangle + \sum_i c_i\langle x|h_i\rangle\,. \tag{3.3}$$

The real variable x is taken in some interval (a,b). Per definition, the Green's function of the differential operator $\mathcal{D}$ is

$$\widetilde{G}(x,x') := \langle x|\mathcal{D}^{-1}|x'\rangle\,, \tag{3.4}$$

which corresponds to the matrix element of the inverse operator $\mathcal{D}^{-1}$ between $\langle x|$ and $|x'\rangle$. The question is, which equation does the Green's function satisfy, i.e. how to find the Green's function. A smart way to get to the result is to start with the scalar product $\langle x|x'\rangle = \delta(x-x')$, to insert the identity $\mathcal{D}\mathcal{D}^{-1} = \mathbb{1}_1$ in the left hand-side, and then the resolution of the identity

$$\begin{aligned}\delta(x-x') = \langle x|\mathcal{D}\mathcal{D}^{-1}|x'\rangle &= \int_a^b dy\langle x|\mathcal{D}|y\rangle\langle y|\mathcal{D}^{-1}|x'\rangle \\ &= D_x\int_a^b dy\,\delta(x-y)\widetilde{G}(y,x')\,.\end{aligned} \tag{3.5}$$

In the last step, $\mathcal{D}$ takes support in a suitable function space with respect to the x variable. Therefore, one gets the equation obeyed by the Green's function of some differential operator

$$D_x\widetilde{G}(x,x') = \delta(x-x')\,. \tag{3.6}$$

It turns out that the Green's function satisfies the differential equation governing the original problem, with the inhomogeneous term changed to a δ function. In other words, the Green's function describes the response of the system to an instant point source, or impulse. The previous equation happens also to be given as the defining equation of the Green's function. The problem is more conveniently solved in the Fourier space. Once the solution is found, the constants c_i are fixed by the appropriate boundary conditions on $|f\rangle$. In such a way the solution is uniquely determined. As a side comment, the solution of the problem can also be obtained

according to another methodology. The solution is obtained by taking the convolution of the Green's function with the inhomogeneous term

$$f(x) = \int_a^b dx' \widetilde{G}(x, x') g(x') \,. \tag{3.7}$$

In the literature the two-point Green's function, or two-point correlation function, $\widetilde{G}(x, x')$ and the propagator $G(x, x')$ coincide, up to an $\pm i$ factor. Thus, it may be convenient to interpret the Green's function as a correlation function. In the realm of quantum field theory, correlations functions are vacuum expectation values of time-ordered products of fields [see Eqs. (2.30, 2.33)]. The rest of this thesis considers correlation functions of $2N$ bispinor fields assessed by the vacuum state $|\Omega_0\rangle$ of the full theory [Eqs. (2.10, 2.12, 2.18)],

$$G(x_1, \ldots, x_N; y_1, \ldots, y_N) = \langle \Omega_0 | T \left[\psi_H(x_1) \cdots \psi_H(x_N) \bar{\psi}_H(y_N) \cdots \bar{\psi}_H(y_1) \right] | \Omega_0 \rangle \,. \tag{3.8}$$

The standard way to evaluate this type of expressions is to calculate it perturbatively in the interaction representation relying on the Gell-Mann-Low formula [18, 88]

$$\begin{aligned} &\langle \Omega_0 | T \left[\psi_H(x_1) \cdots \psi_H(x_N) \bar{\psi}_H(y_N) \cdots \bar{\psi}_H(y_1) \right] | \Omega_0 \rangle \\ &\qquad = \frac{\langle 0 | T \left[\psi_I(x_1) \cdots \psi_I(x_N) \bar{\psi}_I(y_N) \cdots \bar{\psi}_I(y_1) e^{-i \int dz^0 \, H_{I,\mathrm{int}}} \right] | 0 \rangle}{\langle 0 | T \left[e^{-i \int dz^0 \, H_{I,\mathrm{int}}} \right] | 0 \rangle} \,. \end{aligned} \tag{3.9}$$

The expression stated above is a great importance; it relates a quantity in the Heisenberg picture evaluated with respect to the vacuum state of the interaction theory to the same quantity in the interaction representation but evaluated with respect to the vacuum state of the free theory. Consequently, the Gell-Mann-Low formula constitutes a bridge between what one *is willing* to calculate and what one *is able* to calculate; one aims to make predictions for the realistic system (interacting theory) but the calculational abilities are limited to the independent particle approximation (free theory).

Let us pause and discuss a crucial point: the definition of the zero-point of the energy, also named the reference energy of the system. On the one side, one has the free theory described by H_0, with the eigenvalues ϵ_j and its vacuum (ground) state $|0\rangle$. The ground state energy is the vacuum expectation value $\langle 0 | H_0 | 0 \rangle = \epsilon_0$. The zero of energy is conveniently set to the vacuum energy by defining $H_0 | 0 \rangle = 0$, or equivalently $\epsilon_0 = 0$. On the other side, the interacting

theory is governed by the full Hamiltonian $H = H_0 + H_{\text{int}}$, the associated eigenvalues are $E_{\mathcal{N}}$ and its vacuum state is $|\Omega_0\rangle$. Similarly to the free theory, the ground state energy is given by $\langle\Omega_0|H|\Omega_0\rangle = E_0$. A freedom of choice is left to set the reference energy in the interacting theory; the zero-point energy is simply a constant, which cancels out in calculations of transition energies. For convenience, like in the free theory, the reference energy in the interacting system is set as the vacuum energy, $E_0 = 0$. Let us now change perspectives with the introduction of a redefinition of the vacuum state, and think from this point of view. Its effects in the free theory have been discussed above and are clear; the redefined vacuum state is $|\alpha\rangle$ and the corresponding Fermi level is E_α^F. This vacuum state shows a more involved structure; the shift in energy induces a composite vacuum state, in the sense that its spectrum encapsulates the (usual) negative-energy continuum and a discrete part due to the inclusion of the energy levels of the core electrons. A consequence, radiative and interelectronic corrections are put on the same footing. When considering the redefined vacuum state $|\alpha\rangle$ in the interaction representation, the vacuum state of the interacting theory in the Heisenberg representation is changed to $|\Omega_\alpha\rangle$. The repercussion is to introduce an increased complexity in the structure of the vacuum state. Per definition, the redefined vacuum state is the only state annihilated by the redefined annihilation operator. Therefore, consistency enforces the mapping $|\alpha\rangle$ to $|\Omega_\alpha\rangle$, which establishes the connection between the vacua of the two theories. In the remainder of this work, the subscript $_H$ is dropped and it is implicitly understood that the fields are considered within the Heisenberg representation.

3.1. Shabaev's two-time Green's function method

According to Shabaev [85], the $2N$-time Green's function Eq. (3.8) contains all the information about the energy levels of an N-electron atom. The issue is that extracting it is a tedious and laborious work as the Green's function depends on $2(N-1)$ relative times, in its time representation. The problem can be reduced to a much simpler one under an equal-time choice, i.e. keeping only two different times. Let us derive the spectral representation of the two-time Green's function within a redefined vacuum state for the case where all ψ share a common time x^0, so as for $\bar{\psi}$ but with a common time y^0. In this special case, Eq. (3.8) is changed

accordingly to

$$G_\alpha(x^0,\mathbf{x}_1,\ldots,x^0,\mathbf{x}_N;y^0,\mathbf{y}_1,\ldots,y^0,\mathbf{y}_N) = \langle\Omega_\alpha|T\left[\psi_\alpha(x^0,\mathbf{x}_1)\cdots\psi_\alpha(x^0,\mathbf{x}_N)\bar{\psi}_\alpha(y^0,\mathbf{y}_N)\cdots\bar{\psi}_\alpha(y^0,\mathbf{y}_1)\right]|\Omega_\alpha\rangle\,, \tag{3.10}$$

and the expression (3.9) is turned to

$$\langle\Omega_\alpha|T[\psi_\alpha(x^0,\mathbf{x}_1)\cdots\psi_\alpha(x^0,\mathbf{x}_N)\bar{\psi}_\alpha(y^0,\mathbf{y}_N)\cdots\bar{\psi}_\alpha(y^0,\mathbf{y}_1)]|\Omega_\alpha\rangle = \frac{\langle\alpha|T\left[\psi^{(0)}_{I,\alpha}(x^0,\mathbf{x}_1)\cdots\psi^{(0)}_{I,\alpha}(x^0,\mathbf{x}_N)\bar{\psi}^{(0)}_{I,\alpha}(y^0,\mathbf{y}_N)\cdots\bar{\psi}^{(0)}_{I,\alpha}(y^0,\mathbf{y}_1)e^{-i\int dz^0 H_{I,\mathrm{int}}}\right]|\alpha\rangle}{\langle\alpha|T\left[e^{-i\int dz^0 H_{I,\mathrm{int}}}\right]|\alpha\rangle}\,. \tag{3.11}$$

The Fourier transformed Green's function $\mathcal{G}_\alpha(E,\mathbf{x}_1,\ldots,\mathbf{x}_N;\mathbf{y}_1\ldots,\mathbf{y}_N)$ is introduced as

$$\mathcal{G}_\alpha(E;\mathbf{x}_1,\ldots,\mathbf{x}_N;\mathbf{y}_1,\ldots,\mathbf{y}_N)\delta(E-E') = \frac{1}{2\pi i}\frac{1}{N!}\int dx^0dy^0e^{iEx^0-iE'y^0}G_\alpha(x^0,\mathbf{x}_1,\ldots,x^0,\mathbf{x}_N,;y^0,\mathbf{y}_1,\ldots,y^0,\mathbf{y}_N)\,. \tag{3.12}$$

The spectral representation of Eq. (3.10) is obtained via the analysis of the Fourier transformed Green's function (3.12). A coordinate integrated Green's function, which is going to be a key instrument in the analysis, is built out of the time Fourier transformed Green's function

$$g_\alpha(E) = \frac{1}{N!}\int d^3x_1\ldots d^3x_Nd^3y_1\ldots d^3y_N : \psi^{(0)\dagger}_\alpha(0,\mathbf{x}_1)\cdots\psi^{(0)\dagger}_\alpha(0,\mathbf{x}_N) \times\mathcal{G}_\alpha(E,\mathbf{x}_1,\ldots,\mathbf{x}_N;\mathbf{y}_1,\ldots,\mathbf{y}_N)\gamma^0_1\cdots\gamma^0_N\psi^{(0)}_\alpha(0,\mathbf{y}_N)\cdots\psi^{(0)}_\alpha(0,\mathbf{y}_1) : . \tag{3.13}$$

In order to extract the energy shift, one has to consider the pole structure of the Green's function (3.13). For this purpose, let us rewrite it in term of the creation and annihilation operators:

$$g_\alpha(E) = \frac{1}{N!}\sum_{\epsilon_{i_1},\ldots,\epsilon_{i_N}>E^F_\alpha}\sum_{\epsilon_{j_1},\ldots,\epsilon_{j_N}>E^F_\alpha}a^\dagger_{i_1}\cdots a^\dagger_{i_N}a_{j_N}\cdots a_{j_1}\,g_{\alpha,i_1\ldots i_Nj_1\ldots j_N}(E) + \frac{1}{N!}\sum_{\epsilon_{i_1},\ldots,\epsilon_{i_N}<E^F_\alpha}\sum_{\epsilon_{j_1},\ldots,\epsilon_{j_N}<E^F_\alpha}b^\dagger_{i_1}\cdots b^\dagger_{i_N}b_{j_N}\cdots b_{j_1}\,g_{\alpha,i_1\ldots i_Nj_1\ldots j_N}(E)\,. \tag{3.14}$$

with

$$g_{\alpha,i_1\ldots i_N j_1\ldots j_N}(E) = \int d^3x_1\ldots d^3x_N d^3y_1\ldots d^3y_N \phi^\dagger_{i_1}(\mathbf{x}_1)\cdots\phi^\dagger_{i_N}(\mathbf{x}_N) \\ \times \mathcal{G}_\alpha(E,\mathbf{x}_1,\ldots,\mathbf{x}_N;\mathbf{y}_1,\ldots,\mathbf{y}_N)\gamma^0_1\cdots\gamma^0_N\phi_{j_1}(\mathbf{y}_1)\cdots\phi_{j_N}(\mathbf{y}_N)\,. \quad (3.15)$$

The analysis of the pole structure of $g_{\alpha,i_1\ldots i_N j_1\ldots j_N}(E)$ is conducted according to the steps shown in Ref. [85]. First, the time-ordering operator in Eq. (3.12) is expanded. The second step is to apply the time-translation rule for Heisenberg operators

$$\psi(x^0,\mathbf{x}) = e^{iHx^0}\psi(0,\mathbf{x})e^{-iHx^0}\,, \quad (3.16)$$

where the total Hamiltonian satisfies

$$H|\Omega_\mathcal{N}\rangle = (H_0 + H_{\text{int}})\,|\Omega_\mathcal{N}\rangle = E_\mathcal{N}|\Omega_\mathcal{N}\rangle\,. \quad (3.17)$$

The states $|\Omega_\mathcal{N}\rangle$ form a complete basis, $\sum_\mathcal{N}|\Omega_\mathcal{N}\rangle\langle\Omega_\mathcal{N}| = \mathbb{1}$, which is inserted to separate ψ's and $\bar\psi$'s in expression (3.10). The subscript indicating the dimensionality of the identity matrix of the Hilbert space is not displayed, as it is understood that the dimension of the Hilbert space is infinite. The integral representation of the Heaviside, Eq. (2.31), allows to simplify the expression to

$$g_{\alpha,i_1\ldots i_N j_1\ldots j_N}(E) = \sum_\mathcal{N}\frac{A_{i_1\ldots i_N j_1\ldots j_N}}{E - E_\mathcal{N} + i\varepsilon} - (-1)^N\sum_\mathcal{N}\frac{B_{i_1\ldots i_N j_1\ldots j_N}}{E + E_\mathcal{N} - i\varepsilon}\,, \quad (3.18)$$

with

$$A_{i_1\ldots i_N j_1\ldots j_N} = \frac{1}{N!}\int d^3x_1\ldots d^3x_N d^3y_1\ldots d^3y_N \phi^\dagger_{i_1}(\mathbf{x}_1)\cdots\phi^\dagger_{i_N}(\mathbf{x}_N) \\ \times\langle\Omega_\alpha|\psi_\alpha(0,\mathbf{x}_1)\cdots\psi_\alpha(0,\mathbf{x}_N)|\Omega_\mathcal{N}\rangle\langle\Omega_\mathcal{N}|\psi^\dagger_\alpha(0,\mathbf{y}_N)\cdots\psi^\dagger_\alpha(0,\mathbf{y}_1)|\Omega_\alpha\rangle \\ \times\phi_{j_1}(\mathbf{y}_1)\cdots\phi_{j_N}(\mathbf{y}_N) \quad (3.19)$$

and

$$B_{i_1\ldots i_N j_1\ldots j_N} = \frac{1}{N!}\int d^3x_1\ldots d^3x_N d^3y_1\ldots d^3y_N \phi^\dagger_{i_1}(\mathbf{x}_1)\cdots\phi^\dagger_{i_N}(\mathbf{x}_N) \\ \times\langle\Omega_\mathcal{N}|\psi_\alpha(0,\mathbf{x}_1)\cdots\psi_\alpha(0,\mathbf{x}_N)|\Omega_\alpha\rangle\langle\Omega_\alpha|\psi^\dagger_\alpha(0,\mathbf{y}_1)\cdots\psi^\dagger_\alpha(0,\mathbf{y}_N)|\Omega_\mathcal{N}\rangle \\ \times\phi_{j_1}(\mathbf{y}_N)\cdots\phi_{j_N}(\mathbf{y}_1)\,. \quad (3.20)$$

The summations run over all bound and continuum states of the interacting fields' system. A closer look to the term (3.19) informs that it contains only states with an electric charge Ne, enforced by charge conservation[2]. Hence, the first summation over $\mathcal{N}$ in Eq. (3.18) runs exclusively over the electron excitations (with respect to the redefined vacuum state in the free theory). A similar analysis for the term (3.20) leads to the conclusion that only states with an electric charge $-N$e are present, and the second summation over $\mathcal{N}$ in Eq. (3.18) runs exclusively over states with vacancy excitations (from the redefined vacuum state, in the free theory) . If the vacuum state of the free theory were not shifted above a closed shell, one could refer to $B_{i_1\ldots i_N j_1\ldots j_N}$ as the positronic term. The terminology hole is rather used, since an electronic vacancy in a shell resembles a lot to the charge transfer in a p-n junction, where such a vacancy is called a hole state.

An detailed discussion of the analytical continuation[3] to the complex energy plane of Eq. (3.18) is not compulsory to note that the positions of the poles for the electron and hole states are essentially different, and in what follows a distinction among these two cases will be made. The poles of the electronic term are located below the right-hand real axis and the ones of the hole (or positronic) term are located above the left-hand real axis. Nevertheless, it is important to notice that the analytical continuation of the Green's function has cuts $(-\infty, E_{\min}^{(-)}]$ and $[E_{\min}^{(+)}, +\infty)$, where $E_{\min}^{(\pm)}$ is the minimal energy of the states with electric charge $\pm N$e. The poles of the Green's function correspond to the bound states of the system. Their locations depend on whether the interest lies on electronic or hole states. A crucial point to emphasis on is that, as long as the interaction between the electromagnetic field and the electron-positron field is turned off, the poles are isolated. Switching on the interaction changes the poles to branch points, due to the zero mass of the photon. In order to proceed with the formulation of the perturbation theory, the poles corresponding to the bound states have to be isolated from the related cuts. The isolation of the poles is carried out by the formal introduction of a photon mass μ. The photon mass is assumed to be larger than the energy shift of the level under consideration but smaller than the distance to the other levels. It is then set to zero in the final expression. As a side remark, the cuts below Eq. (2.34) are affected as follow $\omega = -\mu + i\varepsilon$ and $\omega = \mu - i\varepsilon$. The prescription opens a gap where the integration path can be squeezed in [see Fig. 2.1(b)], and ensures the regularization of infrared divergences at the individual Feynman diagram level. The instabilities of the excited states are not accounted for, which is equivalent to neglecting their imaginary component of the energy.

[2]The charge operator is $Q = \int d^3x \psi^\dagger(\mathbf{x})\psi(\mathbf{x})$. Its commutation relation with ψ and $\bar{\psi}$ reads, respectively, $[Q, \psi(\mathbf{x})] = -\mathrm{e}\psi(\mathbf{x})$ and $[Q, \bar{\psi}(\mathbf{x})] = \mathrm{e}\bar{\psi}(\mathbf{x})$.

[3]The extension of the domain of a function from the (energy) real axis to the whole (energy) complex plane.

3.1.1. Electron states

The integral formalism developed in operator theory by Szökefalvi-Nagy [114] and Kato [115, 116] is applied to generate the perturbation series in E. The focus is on the state $|A\rangle$ (2.50) involving only electron states, $A \equiv A_v$. An integration contour Γ_{A_v} is chosen such that it surrounds anticlockwise only the pole $E = E^{(0)}_{A_v}$, while other singularities are kept outside. In such a way, one ends up with

$$\frac{1}{2\pi i}\oint_{\Gamma_{A_v}} dE\, E\langle A_v|g_\alpha(E)|A_v\rangle = E_{A_v} A_{i_1\ldots i_N j_1\ldots j_N}\,, \tag{3.21}$$

owing to the fact that the spectral representation (3.18) has the characteristic

$$\langle A_v|g_\alpha(E)|A_v\rangle = \frac{A_{i_1\ldots i_N j_1\ldots j_N}}{E - E_{A_v}} + \text{regular terms at } E \sim E^{(0)}_{A_v}\,. \tag{3.22}$$

Similarly, one has

$$\frac{1}{2\pi i}\oint_{\Gamma_{A_v}} dE\, \langle A_v|\, g_\alpha(E)|A_v\rangle = A_{i_1\ldots i_N j_1\ldots j_N}\,. \tag{3.23}$$

Dividing Eq. (3.21) by Eq. (3.23) leads to

$$E_{A_v} = \frac{\dfrac{1}{2\pi i}\oint_{\Gamma_{A_v}} dE\, E\langle A_v|g_\alpha(E)|A_v\rangle}{\dfrac{1}{2\pi i}\oint_{\Gamma_{A_v}} dE\, \langle A_v|g_\alpha(E)|A_v\rangle}\,. \tag{3.24}$$

It is more convenient to deal with a formula yielding directly the energy shift $\Delta E_A = E_A - E^{(0)}_A$. The zeroth-order term is the energy obtained by solving the Dirac equation, Eq. (2.51). At the zeroth-order, the expansion of the electron-positron field in creation and annihilation operators (2.48) can be inserted in (3.19). Then, the zeroth-order Green's function is

$$\langle A_v|g^{(0)}_\alpha(E)|A_v\rangle = \frac{1}{E - E^{(0)}_{A_v}}\,. \tag{3.25}$$

Denoting $\Delta g_\alpha(E) = g_\alpha(E) - g_\alpha^{(0)}(E)$, the energy shift is given by the cornerstone formula

$$\Delta E_{A_v} = \frac{\frac{1}{2\pi i}\oint_{\Gamma_{A_v}} dE \left(E - E_{A_v}^{(0)}\right) \langle A_v|\Delta g_\alpha(E)|A_v\rangle}{1 + \frac{1}{2\pi i}\oint_{\Gamma_{A_v}} dE \, \langle A_v|\Delta g_\alpha(E)|A_v\rangle} . \tag{3.26}$$

Here, one should note that in contrast to the expression given in Ref. [85], the matrix elements in Eq. (3.26) are understood as the matrix elements in the Fock space. One is in position to develop the perturbation series in the energy E. Replacing the exponentials in Eq. (3.11) by its Taylor series, one obtains the perturbation expansion in the fine-structure constant α. As a result, one also finds for the Green's function $\Delta g_\alpha(E)$ and the energy shift ΔE_{A_v}

$$\Delta g_\alpha(E) = \langle A_v|\Delta g_\alpha^{(1)}(E)|A_v\rangle + \langle A_v|\Delta g_\alpha^{(2)}(E)|A_v\rangle + \langle A_v|\Delta g_\alpha^{(3)}(E)|A_v\rangle \ldots , \tag{3.27}$$

$$\Delta E_{A_v} = \Delta E_{A_v}^{(1)} + \Delta E_{A_v}^{(2)} + \Delta E_{A_v}^{(3)} \ldots . \tag{3.28}$$

The expression for the energy corrections $\Delta E_{A_v}^{(i)}$ at each order is attained by developing Eq. (3.26) in a geometric series, substituting Eq. (3.27) and Eq. (3.28) and separating out the individual orders in α. The first order is given by

$$\Delta E_{A_v}^{(1)} = \frac{1}{2\pi i}\oint_{\Gamma_{A_v}} dE \left(E - E_{A_v}^{(0)}\right) \langle A_v|\Delta g_\alpha^{(1)}(E)|A_v\rangle , \tag{3.29}$$

the second order reads

$$\begin{aligned}\Delta E_{A_v}^{(2)} = &\frac{1}{2\pi i}\oint_{\Gamma_{A_v}} dE \left(E - E_{A_v}^{(0)}\right) \langle A_v|\Delta g_\alpha^{(2)}(E)|A_v\rangle \\ &- \frac{1}{2\pi i}\oint_{\Gamma_{A_v}} dE \left(E - E_{A_v}^{(0)}\right) \langle A_v|\Delta g_\alpha^{(1)}(E)|A_v\rangle \frac{1}{2\pi i}\oint_{\Gamma_{A_v}} dE' \langle A_v|\Delta g_\alpha^{(1)}(E')|A_v\rangle .\end{aligned} \tag{3.30}$$

and the third order is

$$\begin{aligned}\Delta E_v^{(3)} = &\frac{1}{2\pi i}\oint_{\Gamma_{A_v}} dE\left(E - E_{A_v}^{(0)}\right)\langle A_v|\Delta g_\alpha^{(3)}(E)|A_v\rangle \\ &- \frac{1}{2\pi i}\oint_{\Gamma_{A_v}} dE\left(E - E_{A_v}^{(0)}\right)\langle A_v|\Delta g_\alpha^{(2)}(E)|A_v\rangle \frac{1}{2\pi i}\oint_{\Gamma_{A_v}} dE'\langle A_v|\Delta g_\alpha^{(1)}(E')|A_v\rangle \\ &- \frac{1}{2\pi i}\oint_{\Gamma_{A_v}} dE\left(E - E_{A_v}^{(0)}\right)\langle A_v|\Delta g_\alpha^{(1)}(E)|A_v\rangle \\ &\times\left\{\frac{1}{2\pi i}\oint_{\Gamma_{A_v}} dE'\langle A_v|\Delta g_\alpha^{(2)}(E')|A_v\rangle - \left[\frac{1}{2\pi i}\oint_{\Gamma_{A_v}} dE'\langle A_v|\Delta g_\alpha^{(1)}(E')|A_v\rangle\right]^2\right\}.\end{aligned} \tag{3.31}$$

The terms in the second line of Eq. (3.30) and the three last lines of Eq. (3.31) are referred to as disconnected contributions, and are generally merged with the corresponding irreducible diagrams. Note that all one-particle-irreducible (1PI) diagrams, any diagram that cannot be split in two by removing a single line, do not have disconnected contributions. Thus, one has expressed the energy shift in terms of the matrix elements of the Green's function $g_\alpha(E)$ in the occupation number space. In the following, particular examples of the state A_v are considered.

The first illustrative example is the well-known single-valence-electron state. Consider an electronic configuration, which has one valence electron above closed shells. After the assignment of the closed shells to the redefined vacuum state $|\alpha\rangle$, the one-valence-electron state is described by

$$|v\rangle = a_v^\dagger|\alpha\rangle\,. \tag{3.32}$$

Expressing the Green's function by Eq. (3.14), it is now easy to evaluate the Fock-space matrix elements $\langle A_v|\Delta g_\alpha(E)|A_v\rangle$ with $A_v = v$, which enters the expression for the determination of the energy shift (3.26). The expectation value of the one-particle Green's function [$N = 1$, Eq. (3.14)] with respect to the one-valence-electron state is evaluated and the matrix element is just

$$\langle v|\Delta g_\alpha(E)|v\rangle = \Delta g_{\alpha,vv}(E)\,, \tag{3.33}$$

where $\Delta g_{\alpha,ij}(E)$ is given by Eq. (3.15). Substituting this expression into Eq. (3.26), one easily gets,

$$\Delta E_v = \frac{\dfrac{1}{2\pi i}\oint_{\Gamma_v} dE\,(E-\epsilon_v)\,\Delta g_{\alpha,vv}(E)}{1+\dfrac{1}{2\pi i}\oint_{\Gamma_v} dE\,\Delta g_{\alpha,vv}(E)}\,, \tag{3.34}$$

where Γ_v surrounds only the pole $E=\epsilon_v$. This expression coincides with the one-valence-electron result of Ref. [85].

The second example discussed is the two-valence-electron state formed by the one-electron orbitals v_1 and v_2. In this case, the first issue to consider is the construction of a coupled two-electron state. Employing the jj-coupling scheme, the state with the total angular momentum J and its projection M is built. Thus, the two-valence-electron state under consideration is given by

$$|(v_1v_2)_{JM}\rangle = \eta \sum_{m_{v_1}m_{v_2}} \langle j_{v_1}m_{v_1}j_{v_2}m_{v_2}|JM\rangle a^\dagger_{v_1}a^\dagger_{v_2}|\alpha\rangle \equiv F_{v_1v_2}a^\dagger_{v_1}a^\dagger_{v_2}|\alpha\rangle\,, \tag{3.35}$$

where j_{v_i} and m_{v_i} are the one-electron total angular momentum and its projection, the Clebsch-Gordan coefficient is $\langle j_{v_1}m_{v_1}j_{v_2}m_{v_2}|JM\rangle$, and η is the normalization factor, which depends on the degeneracy of the orbitals forming the jj-coupled state [99],

$$\eta = \begin{cases} 1 & \text{if } \epsilon_{v_1} \neq \epsilon_{v_2} \\ 1/\sqrt{2} & \text{if } \epsilon_{v_1} = \epsilon_{v_2} \end{cases}\,. \tag{3.36}$$

Then, the expectation value of the two-particle Green's function [Eq. (3.14), $N=2$] with the state (3.35) reads,

$$\langle (v_1v_2)_{JM}|\Delta g_\alpha(E)|(v_1v_2)_{JM}\rangle = F_{v_1v_2}F_{v_1v_2}\left[\Delta g_{\alpha,v_1v_2v_1v_2}(E) - \Delta g_{\alpha,v_1v_2v_2v_1}(E)\right]\,. \tag{3.37}$$

Substituting this expression into Eq. (3.26) , one easily obtains,

$$\Delta E_{v_1v_2} = \frac{\dfrac{1}{2\pi i}\oint_{\Gamma_{v_1v_2}} dE\left(E-\epsilon_{v_1}-\epsilon_{v_2}\right)F_{v_1v_2}F_{v_1v_2}\left[\Delta g_{\alpha,v_1v_2v_1v_2}(E) - \Delta g_{\alpha,v_1v_2v_2v_1}(E)\right]}{1+\dfrac{1}{2\pi i}\oint_{\Gamma_{v_1v_2}} dE\,F_{v_1v_2}F_{v_1v_2}\left[\Delta g_{\alpha,v_1v_2v_1v_2}(E) - \Delta g_{\alpha,v_1v_2v_2v_1}(E)\right]}\,, \tag{3.38}$$

where $\Gamma_{v_1 v_2}$ surrounds only the pole $E = \epsilon_{v_1} + \epsilon_{v_2}$. As one can see from the above formulas, Eqs. (3.34) and (3.38), the energy shifts are expressed in terms of the one- and two-electron matrix elements $\Delta g_{\alpha,ij}(E)$ and $\Delta g_{\alpha,ijkl}(E)$, for which the Feynman rules formulated in Ref. [85] can be used. The only difference to keep in mind is that the electron propagator has to be replaced by the one in the redefined vacuum state, defined by Eq. (2.52). Consequences of the employment of the redefined vacuum state's propagator will become clear in the next section. A generalization to three and more valence-electron state is straightforward in terms of N-particle Green's function (3.14) and the energy shift (3.26).

3.1.2. Hole states

In order to extract the energy shift for the hole states, one has to consider the second sum in Eq. (3.18). The state $|A\rangle$ is considered to be of hole type $A \equiv A_h$. Following the same path as in the electron's case, the expression for the energy shift $\Delta E_{A_h} = E_{A_h} - E^{(0)}_{A_h}$ is derived. The contour of integration Γ_{A_h} surrounds anticlockwise only the pole $E = -E^{(0)}_{A_h}$ and keeps all other singularities outside. One has to pay attention that the zeroth-order Green's function (3.25) is changed accordingly to

$$\langle A_h | g^{(0)}_\alpha | A_h \rangle = -\frac{(-1)^N}{E + E^{(0)}_{A_h}} \,. \tag{3.39}$$

Therefore, the cornerstone expression for the energy shift ΔE_{A_h} is

$$\Delta E_{A_h} = \frac{\frac{1}{2\pi i} \oint_{\Gamma_{A_h}} dE \left(E + E^{(0)}_{A_h} \right) \langle A_h | (-1)^N \Delta g_\alpha(E) | A_h \rangle}{1 - \frac{1}{2\pi i} \oint_{\Gamma_{A_h}} dE \, \langle A_h | (-1)^N \Delta g_\alpha(E) | A_h \rangle} \,. \tag{3.40}$$

As previously, replacing the exponentials in Eq. (3.11) by its Taylor series generates the perturbation expansion in the fine-structure constant α. Hence, the first-order and second-order corrections to the energy shift ΔE_{A_h} are found

$$\Delta E^{(1)}_{A_h} = \frac{1}{2\pi i} \oint_{\Gamma_{A_h}} dE \left(E + E^{(0)}_{A_h} \right) \langle A_h | (-1)^N \Delta g^{(1)}_\alpha(E) | A_h \rangle \,, \tag{3.41}$$

$$\Delta E^{(2)}_{A_h} = \frac{1}{2\pi i}\oint_{\Gamma_{A_h}} dE\left(E + E^{(0)}_{A_h}\right)\langle A_h|(-1)^N \Delta g^{(2)}_\alpha(E)|A_h\rangle + \frac{1}{2\pi i}\oint_{\Gamma_{A_h}} dE\left(E + E^{(0)}_{A_h}\right)\langle A_h|(-1)^N \Delta g^{(1)}_\alpha(E)|A_h\rangle \times \frac{1}{2\pi i}\oint_{\Gamma_{A_h}} dE'\langle A_h|(-1)^N \Delta g^{(1)}_\alpha(E')|A_h\rangle\,. \tag{3.42}$$

Note that from Eq. (3.18), $g_{\alpha,i_1\ldots i_N j_1\ldots j_N}(E)$ contains a $-(-1)^N$ factor in front of the hole term, thus

$$(-1)^N \Delta g^{(i)}_\alpha(E) \equiv -\Delta\widetilde{g}^{(i)}_\alpha(E) \tag{3.43}$$

is always negative whatever the number N of holes considered.

Let us now consider some examples. The first case is the mirror image of the single-valence-electron configuration, termed as the one-hole state: closed shells with a single electronic vacancy. In this case, symmetrical to the one-valence-electron state considered above, the Fock state is defined as follows [98]:

$$|h\rangle = (-1)^{j_h - m_h} b^\dagger_h |\alpha\rangle\,, \tag{3.44}$$

with the phase factor introduced to restore the rotational invariance of the matrix elements. j_h and m_h are the hole total angular momentum and its projection. The zeroth-order energy $E^{(0)}_h$, given by Eq. (2.51), for one-hole state reads

$$E^{(0)}_h = \langle A_h|H_0|A_h\rangle = -\epsilon_h\,. \tag{3.45}$$

Obviously, $E^{(0)}_h$ is negative since the hole dynamics occurs below the zero-point energy assigned to the redefined vacuum state $|\alpha\rangle$. Evaluating now the matrix element [$N = 1$, Eq. (3.14)],

$$\langle h|(-1)\Delta g_\alpha(E)|h\rangle = -\Delta\widetilde{g}_{\alpha,hh}(E)\,, \tag{3.46}$$

with emphasis on the negative sign as stated in Eq. (3.43), one gets the cornerstone expression for the energy shift of the one-hole state:

$$\Delta E_h = -\frac{\frac{1}{2\pi i}\oint_{\Gamma_h} dE\,(E-\epsilon_h)\,\Delta\widetilde{g}_{\alpha,hh}(E)}{1+\frac{1}{2\pi i}\oint_{\Gamma_h} dE\,\Delta\widetilde{g}_{\alpha,hh}(E)}\,, \tag{3.47}$$

where Γ_h surrounds only the pole $E=\epsilon_h$. It should be highlighted that the single-valence cornerstone expression Eq. (3.34) and the single-hole cornerstone expression Eq. (3.47) are related by an odd-parity symmetry with respect to the redefined vacuum state. In Ref. [101], it was stated that within the RMBPT framework **the expressions for the corrections to the energy level of a single-hole state are obtained from the formulas of the single-valence electron under the replacement v to h and each term enters with the opposite sign**. Here, we manifest that **such an odd parity symmetry with respect to the redefined Fermi level also holds within the QED framework**. This statement, and its extension to any N-particle states [electrons: Eq. (3.26), holes: Eq. (3.43) in Eq. (3.40)], is one of the major results of this thesis.

The second example considered is the two-hole state. Similar to the case of the two-valence-electron state, the angular momenta of the two holes are coupled via the jj-coupling scheme, which leads to the following two-hole state,

$$\begin{aligned}|(h_1h_2)_{JM}\rangle &= \eta\sum_{m_{h_1}m_{h_2}}(-1)^{j_{h_1}+j_{h_2}-m_{h_1}-m_{h_2}}\langle j_{h_1}-m_{h_1}j_{h_2}-m_{h_2}|JM\rangle b^\dagger_{h_1}b^\dagger_{h_2}|\alpha\rangle \\ &\equiv F_{h_1h_2}b^\dagger_{h_1}b^\dagger_{h_2}|\alpha\rangle\,,\end{aligned} \tag{3.48}$$

where j_{h_i} and m_{h_i} are the one-hole total angular momentum and its projection, and the normalization factor η is defined by Eq. (3.36). Then, the matrix element of the two-particle Green's function [Eq. (3.14), $N=2$] is evaluated for the two-hole state (3.48) with the result,

$$\langle(h_1h_2)_{JM}|\Delta g_\alpha(E)|(h_1h_2)_{JM}\rangle = F_{h_1h_2}F_{h_1h_2}\left[\Delta\widetilde{g}_{\alpha,h_1h_2h_1h_2}(E)-\Delta\widetilde{g}_{\alpha,h_1h_2h_2h_1}(E)\right]\,. \tag{3.49}$$

Substituting this expression into Eq. (3.40) and using $E^{(0)}_{h_1h_2} = -\epsilon_{h_1} - \epsilon_{h_2}$, one easily gets

$$\Delta E_{h_1h_2} = -\frac{\dfrac{1}{2\pi i}\oint_{\Gamma_{h_1h_2}} dE\left(E-\epsilon_{h_1}-\epsilon_{h_2}\right) F_{h_1h_2}F_{h_1h_2}\left[\Delta\widetilde{g}_{\alpha,h_1h_2h_1h_2}(E) - \Delta\widetilde{g}_{\alpha,h_1h_2h_2h_1}(E)\right]}{1+\dfrac{1}{2\pi i}\oint_{\Gamma_{h_1h_2}} dE\, F_{h_1h_2}F_{h_1h_2}\left[\Delta\widetilde{g}_{\alpha,h_1h_2h_1h_2}(E) - \Delta\widetilde{g}_{\alpha,h_1h_2h_2h_1}(E)\right]}, \tag{3.50}$$

where $\Gamma_{h_1h_2}$ surrounds only the pole $E = \epsilon_{h_1} + \epsilon_{h_2}$. As one can see from above equations, the energy shifts of the holes states are expressed in terms of the matrix element of the Green's function $\Delta g_\alpha(E)$. These matrix elements can be evaluated according to the same Feynman rules as in the electron-state case.

Concluding this section, one notices that despite the arbitrary number of the core electrons, the energy shift of the electron A_v (or hole A_h) state is reduced to the matrix elements of corresponding valence electrons (or holes).

3.2. Single-valence electron over closed shells

The focus of the section is on the single-electron case [$N = 1$, $A_v \equiv v$], with the energy shift given by Eq. (3.34). The investigation is carried out on the interelectronic-interaction corrections to binding energies, namely, one- and two-photon-exchange, and how they can be extracted from the one-particle diagrams in the redefined vacuum state formalism. To make it clear, starting from the first-order correction in α, a subdivision among different terms of the same order is made, as introduced in Section 2.4. The one-particle loop diagrams are denoted by (L), the interelectronic-interaction diagrams by (I) and the screened loop diagrams by (S). The latter will only start to occur to the second order. The first-order correction,

$$\Delta E^{(1)}_v = \Delta E^{(1\mathrm{L})}_v + \Delta E^{(1\mathrm{I})}_v\,, \tag{3.51}$$

contains the self-energy (SE) and vacuum-polarization (VP) graphs in the first term, and the counterpotential (CP) as well as the one-photon exchange in the second one. The second-order correction,

$$\Delta E^{(2)}_v = \Delta E^{(2\mathrm{L})}_v + \Delta E^{(2\mathrm{I})}_v + \Delta E^{(2\mathrm{S})}_v\,, \tag{3.52}$$

provides the one-particle two-loop terms, the two-photon-exchange and the screened one-loop terms, in the respective order. The focus is in the two-photon-exchange term $\Delta E_v^{(2\mathrm{I})}$. In the next part, one demonstrates how to extract the interelectronic-interaction correction on an example of the one-photon-exchange.

3.2.1. One-photon-exchange corrections

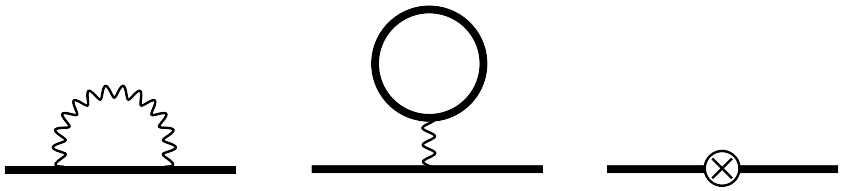

Figure 3.1.: First-order one-particle (valence electron or hole state) one-loop Feynman diagrams corresponding (from left to right) to SE, VP, and CP corrections in the redefined vacuum state formalism. The cross inside a circle represents a counterpotential term, $-U$. Other notations are the same as in Fig. 2.3

In this subsection, the method and techniques presented above are illustrated by an example of first-order one-particle diagrams, which are depicted in Fig. 3.1. The matrix elements of the Green's function for SE and VP are, using the Feynman rules provided in [85], respectively, given by

$$\Delta g^{(1)\mathrm{SE}}_{\alpha,vv}(E) = \frac{1}{(E-\epsilon_v)^2}\frac{i}{2\pi}\int d\omega \sum_j \frac{I_{vjjv}(\omega)}{E-\omega-\epsilon_j+i\varepsilon(\epsilon_j-E^F_\alpha)}\,, \tag{3.53}$$

$$\Delta g^{(1)\mathrm{VP}}_{\alpha,vv}(E) = \frac{-1}{(E-\epsilon_v)^2}\frac{i}{2\pi}\int d\omega \sum_j \frac{I_{vjvj}(0)}{\omega-\epsilon_j+i\varepsilon(\epsilon_j-E^F_\alpha)}\,. \tag{3.54}$$

They are used as inputs to calculate the energy correction according to Eq. (3.29). The contour integral contains a first order pole in $E=\epsilon_v$, thus the Green's functions are evaluated at $E=\epsilon_v$ leading to

$$\Delta E^{(1)\mathrm{SE}}_v = \frac{i}{2\pi}\int d\omega \sum_j \frac{I_{vjjv}(\omega)}{\epsilon_v-\omega-\epsilon_j+i\varepsilon(\epsilon_j-E^F_\alpha)} \equiv \langle v|\Sigma_\alpha(\epsilon_v)|v\rangle\,, \tag{3.55}$$

$$\Delta E^{(1)\mathrm{VP}}_v = -\frac{i}{2\pi}\int d\omega \sum_j \frac{I_{vjvj}(0)}{\omega-\epsilon_j+i\varepsilon(\epsilon_j-E^F_\alpha)} \equiv \langle v|\Upsilon_\alpha|v\rangle\,. \tag{3.56}$$

Hence, one got the first-order self-energy and vacuum-polarization energy corrections in the redefined vacuum state framework. The SE operator Σ_α and the VP operator Υ_α, in the

redefined vacuum state denoted by the subscript $_\alpha$, are introduced. Both contain ultraviolet (UV) divergences and should be regularized. The renormalization procedure is discussed in details in Appendix A.1. The problem is cured with the consideration of the mass counterterm in Eq. (2.55), so that the renormalized SE operator is

$$\Sigma_{\alpha,R}(\epsilon_v) = \Sigma_\alpha(\epsilon_v) - \delta \mathrm{m}_e \gamma^0 \,. \tag{3.57}$$

The equality is obviously valid in the standard vacuum state [Eq. (102) in Ref. [85]] but remains true in the redefined vacuum state, since it amounts to a shift in the energy. The charge renormalization ensures that the UV divergence in the VP loop is cured, see also Appendix A.1. The formulas (3.55, 3.56) encapsulate not only the one-particle one-loop corrections, but also the one-photon-exchange, see also Fig. (2.3). According to Eq. (3.51), in order to obtain the one-photon-exchange contribution, one should subtract SE and VP corrections calculated in the framework of the standard vacuum state. With the help of Eq. (2.54), one obtains for the SE part,

$$\begin{aligned}
\Delta E_v^{(1\mathrm{I})\mathrm{SE}} &= \Delta E_v^{(1)\mathrm{SE}} - \Delta E_v^{(1\mathrm{L})\mathrm{SE}} \\
&= \frac{i}{2\pi} \int d\omega \sum_j \left[\frac{I_{vjjv}(\omega)}{\epsilon_v - \omega - \epsilon_j + i\varepsilon(\epsilon_j - E_\alpha^F)} - \frac{I_{vjjv}(\omega)}{\epsilon_v - \omega - \epsilon_j u} \right] \\
&= -\sum_a I_{vaav}(\Delta_{va}) \,,
\end{aligned} \tag{3.58}$$

and for the VP part,

$$\begin{aligned}
\Delta E_v^{(1\mathrm{I})\mathrm{VP}} &= \Delta E_v^{(1)\mathrm{VP}} - \Delta E_v^{(1\mathrm{L})\mathrm{VP}} \\
&= -\frac{i}{2\pi} \int d\omega \sum_j \left[\frac{I_{vjvj}(0)}{\omega - \epsilon_j + i\varepsilon(\epsilon_j - E_\alpha^F)} - \frac{I_{vjvj}(0)}{\omega - \epsilon_j u} \right] \\
&= \sum_a I_{vava}(0) \,.
\end{aligned} \tag{3.59}$$

It is left to evaluate the counterpotential graph. Let us define $\int d^3x \phi_i^\dagger(\boldsymbol{x}) U(\boldsymbol{x}) \phi_j(\boldsymbol{x}) \equiv U_{ij}$, then the corresponding Green's function takes the form

$$\Delta g_{\alpha,vv}^{(1)\mathrm{CP}}(E) = \frac{-U_{vv}}{(E - \epsilon_v)^2} \,. \tag{3.60}$$

Following the same line as before, the evaluation of the contour integral in Eq. (3.29) provides

$$\Delta E_v^{(1\mathrm{I})\mathrm{CP}} = \Delta E_v^{(1)\mathrm{CP}} = -U_{vv}\,, \tag{3.61}$$

since CP does not participate in radiative corrections belonging to $\Delta E_v^{(1\mathrm{L})}$. The total first-order correction $\Delta E_v^{(1\mathrm{I})}$ is found to be

$$\Delta E_v^{(1\mathrm{I})} = \sum_a \left[I_{vava}(0) - I_{vaav}(\Delta_{va})\right] - U_{vv}\,. \tag{3.62}$$

Let proceed to demonstrate the gauge invariance of the first-order interelectronic correction $\Delta E_v^{(1\mathrm{I})}$. The CP term is obviously gauge invariant. The starting point for the two remaining terms is Eq. (2.42). Straightforward application of this formula gives

$$\delta\Delta E_v^{(1\mathrm{I})} \;=\; \sum_a \left[(0^2 + \Delta_{vv}\Delta_{aa})\widetilde{I}_{vava}(0) - (\Delta_{va}^2 + \Delta_{va}\Delta_{av})\widetilde{I}_{vaav}(\Delta_{va})\right] = 0\,, \tag{3.63}$$

thus, showing its gauge invariance.

3.2.2. Two-photon-exchange corrections

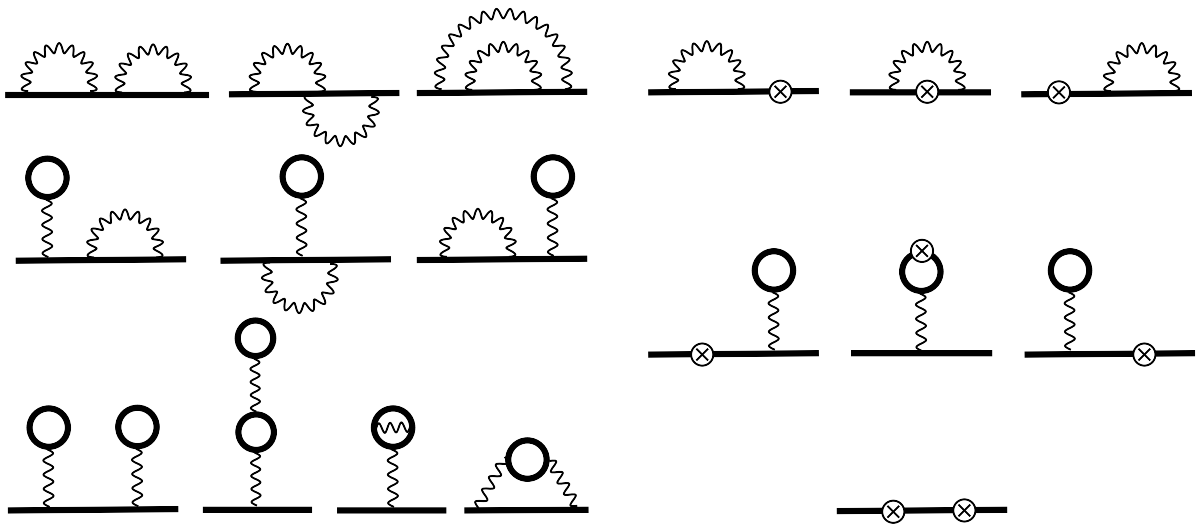

Figure 3.2.: One-particle two-loop (left group) and one-particle one-loop counterpotential (right group) Feynman diagrams representing the second-order corrections to the energy shift of a single-particle (valence or hole) state in the redefined vacuum state formalism. Notations for the diagrams are as follows, left group: SESE (first row); SEVP (second row); VPVP, V(VP)P, V(SE)P, and S(VP)E from left to right in the last row; right group: SECP (first row); VPCP (second row); CPCP (third row). Other notations are same as in Fig. 2.3.

In order to derive the expressions of the matrix elements for the two-photon-exchange corrections in the redefined vacuum state framework, one has to start with the complete set of second-order one-particle diagrams. There are ten two-loop diagrams, which are presented in Fig. 3.2, left panel. In the extended Furry picture, one has to consider also seven counterpotential diagrams depicted in Fig. 3.2, right panel. Already such a decomposition allows to identify nine GI subsets based on the gauge invariance of the one-particle two-loop diagrams [117]. Here are the subsets with labeling presented in Figs. 3.2: SESE, SEVP, VPVP, V(VP)P, V(SE)P, S(VP)E, SECP, VPCP, and CPCP. The identified subsets should be gauge invariant in both redefined and standard vacuum state frameworks. This means that the many-electron diagrams obtained as a difference between redefined and standard vacuum state diagrams can be also divided according to these subsets. In the following, this statement will be illustrated by the rigorous derivation and direct proof of the gauge invariance.

To keep track of the source of generated reducible contributions, a subscript is used with previous notation; for example v_1, a_1, b_1, where $\epsilon_{i_1} = \epsilon_i$.

SESE subset

The Green's function for the SESE subset can be cast in the form

$$\Delta g^{(2)\mathrm{SESE}}_{\alpha,vv}(E) = \frac{1}{(E-\epsilon_v)^2}\left(\frac{i}{2\pi}\right)^2 \sum_{i,j,k}\int d\omega_1 d\omega_2 \times \left\{ \frac{I_{viij}(\omega_1) I_{jkkv}(\omega_2)}{[E-\omega_1-\epsilon_i+i\varepsilon(\epsilon_i-E^F_\alpha)][E-\epsilon_j+i\varepsilon(\epsilon_j-E^F_\alpha)][E-\omega_2-\epsilon_k+i\varepsilon(\epsilon_k-E^F_\alpha)]} + \frac{I_{vjik}(\omega_1) I_{ikjv}(\omega_2)}{[E-\omega_1-\epsilon_i+i\varepsilon(\epsilon_i-E^F_\alpha)][E-\omega_1-\omega_2-\epsilon_j+i\varepsilon(\epsilon_j-E^F_\alpha)][E-\omega_2-\epsilon_k+i\varepsilon(\epsilon_k-E^F_\alpha)]} + \frac{I_{vkiv}(\omega_1) I_{ijjk}(\omega_2)}{[E-\omega_1-\epsilon_i+i\varepsilon(\epsilon_i-E^F_\alpha)][E-\omega_1-\omega_2-\epsilon_j+i\varepsilon(\epsilon_j-E^F_\alpha)][E-\omega_1-\epsilon_k+i\varepsilon(\epsilon_k-E^F_\alpha)]} \right\}, \tag{3.64}$$

with the corresponding energy correction [see Eq. (3.30)],

$$\Delta E^{(2)\mathrm{SESE}}_v = \frac{1}{2\pi i}\oint_{\Gamma_v} dE(E-\epsilon_v)\Delta g^{(2)\mathrm{SESE}}_{\alpha,vv}(E) - \frac{1}{2\pi i}\oint_{\Gamma_v} dE(E-\epsilon_v)\Delta g^{(1)\mathrm{SE}}_{\alpha,vv}(E)\,\frac{1}{2\pi i}\oint_{\Gamma_v} dE'\Delta g^{(1)\mathrm{SE}}_{\alpha,vv}(E')\,. \tag{3.65}$$

Let us now work through the two-photon-exchange extraction procedure,

$$\Delta E_v^{(2)\mathrm{SESE}} - \Delta E_v^{(2\mathrm{L})\mathrm{SESE}} = \Delta E_v^{(2\mathrm{I})\mathrm{SESE}} + \Delta E_v^{(2\mathrm{S})\mathrm{SESE}}\,, \tag{3.66}$$

for the last term of $\Delta g_{\alpha,vv}^{(2)\mathrm{SESE}}(E)$ in Eq. (3.64) as an example. In order to not overload the following steps, the integrals and associated prefactors are ignored for the time being; however, signs are taken into account accordingly:

$$\begin{aligned}
&\sum_{i,j,k}\left\{\frac{I_{vkiv}(\omega_1)I_{ijjk}(\omega_2)}{[E-\omega_1-\epsilon_i+i\varepsilon(\epsilon_i-E_\alpha^F)][E-\omega_1-\omega_2-\epsilon_j+i\varepsilon(\epsilon_j-E_\alpha^F)][E-\omega_1-\epsilon_k+i\varepsilon(\epsilon_k-E_\alpha^F)]}\right.\\
&\quad\left.-\frac{I_{vkiv}(\omega_1)I_{ijjk}(\omega_2)}{[E-\omega_1-\epsilon_i u][E-\omega_1-\omega_2-\epsilon_j u][E-\omega_1-\epsilon_k u]}\right\}\\
&=2\pi i\sum_{a,j,k}^{k\neq a}\frac{I_{vkav}(\omega_1)I_{ajjk}(\omega_2)\delta(E-\omega_1-\epsilon_a)}{(E-\omega_1-\omega_2-\epsilon_j u)(E-\omega_1-\epsilon_k u)}\\
&\quad+2\pi i\sum_{i,a,k}\frac{I_{vkiv}(\omega_1)I_{iaak}(\omega_2)\delta(E-\omega_1-\omega_2-\epsilon_a)}{(E-\omega_1-\epsilon_i u)(E-\omega_1-\epsilon_k u)}\\
&\quad+2\pi i\sum_{i,j,a}^{i\neq a}\frac{I_{vaiv}(\omega_1)I_{ijja}(\omega_2)\delta(E-\omega_1-\epsilon_a)}{(E-\omega_1-\epsilon_i u)(E-\omega_1-\omega_2-\epsilon_j u)}\\
&\quad+(2\pi i)^2\sum_{a,b,k}^{k\neq a}\frac{I_{vkav}(\omega_1)I_{abbk}(\omega_2)\delta(E-\omega_1-\epsilon_a)\delta(E-\omega_1-\omega_2-\epsilon_b)}{(E-\omega_1-\epsilon_k u)}\\
&\quad+(2\pi i)^2\sum_{a,j,a_1}\frac{I_{va_1av}(\omega_1)I_{ajja_1}(\omega_2)}{(E-\omega_1-\omega_2-\epsilon_j u)}\frac{d}{d\omega_1}\delta(E-\omega_1-\epsilon_a)\\
&\quad+(2\pi i)^2\sum_{i,a,b}^{i\neq b}\frac{I_{vbiv}(\omega_1)I_{iaab}(\omega_2)\delta(E-\omega_1-\omega_2-\epsilon_a)\delta(E-\omega_1-\epsilon_b)}{(E-\omega_1-\epsilon_i u)}\\
&\quad+(2\pi i)^2\sum_{a,b,a_1}I_{va_1av}(\omega_1)I_{abba_1}(\omega_2)\delta(E-\omega_1-\omega_2-\epsilon_b)\frac{d}{d\omega_1}\delta(E-\omega_1-\epsilon_a)\,.
\end{aligned}\tag{3.67}$$

After one cut, one gets the first three terms with only one delta function. The first and third of them correspond to the screened radiative diagrams, while the second one gives the crossed diagram of the two-photon exchange. At the two-cut level, two three-electron contributions are found; the fourth and sixth terms with two delta functions. The term which has a derivative acting on the delta function gives rise to the reducible part of the screened radiative diagram. The reducible three-electron part is provided by the three-cut term displayed on the last line of Eq. (3.67). Thus, separating only the interelectronic-interaction terms, one gets for the last

term of Eq. (3.64):

$$\begin{aligned}\Delta E_v^{(2\mathrm{I})\mathrm{SESE}} \sim 2\pi i \sum_{i,a,k} \frac{I_{vkiv}(\omega_1) I_{iaak}(\omega_2)\delta(E-\omega_1-\omega_2-\epsilon_a)}{(E-\omega_1-\epsilon_i u)(E-\omega_1-\epsilon_k u)} \\ + (2\pi i)^2 \sum_{a,b,k}^{k\neq a} \frac{I_{vkav}(\omega_1) I_{abbk}(\omega_2)\delta(E-\omega_1-\epsilon_a)\delta(E-\omega_1-\omega_2-\epsilon_b)}{(E-\omega_1-\epsilon_k u)} \\ + (2\pi i)^2 \sum_{i,a,b}^{i\neq b} \frac{I_{vbiv}(\omega_1) I_{iaab}(\omega_2)\delta(E-\omega_1-\omega_2-\epsilon_a)\delta(E-\omega_1-\epsilon_b)}{(E-\omega_1-\epsilon_i u)} \\ + (2\pi i)^2 \sum_{a,b,a_1} I_{va_1av}(\omega_1) I_{abba_1}(\omega_2)\delta(E-\omega_1-\omega_2-\epsilon_b)\frac{d}{d\omega_1}\delta(E-\omega_1-\epsilon_{a_1}) \\ + \ldots . \end{aligned} \tag{3.68}$$

Notice that one obtains different types of contribution arising when the same diagram in the standard vacuum is subtracted: two-electron and three-electron, which are additionally divided into irreducible and reducible parts. The disconnected SESE part, the second term of Eq. (3.65), is incorporated into the three-electron reducible part.

In the rest of the section one summarizes the results for the SESE subset. The two-electron irreducible part $\Delta E_v^{(2\mathrm{I})\mathrm{SESE,2e,irr}}$ is given by

$$\begin{aligned}\Delta E_v^{(2\mathrm{I})\mathrm{SESE,2e,irr}} = -\frac{i}{2\pi}\int d\omega \left[\sum_{a,i,j}{}' \frac{I_{vjiv}(\omega) I_{iaaj}(\Delta_{va}-\omega)}{(\epsilon_v-\omega-\epsilon_i u)(\epsilon_v-\omega-\epsilon_j u)} \right. \\ \left. + \sum_{a,i,j}^{(i,j)\neq(a,v)} \frac{I_{vaij}(\omega) I_{ijav}(\Delta_{va}-\omega)}{(\epsilon_v-\omega-\epsilon_i u)(\epsilon_a+\omega-\epsilon_j u)} \right], \end{aligned} \tag{3.69}$$

where the first term resembles the crossed-exchange graph considered above in details, while the second one gives the ladder-exchange diagram. Following Ref. [72], one excludes (prime on the sum) from the crossed irreducible term the contributions with $\epsilon_i+\epsilon_j = 2\epsilon_v$ and $\epsilon_i+\epsilon_j = 2\epsilon_a$ and attribute them to the reducible term. The two-electron reducible part $\Delta E_v^{(2\mathrm{I})\mathrm{SESE,2e,red}}$, which corresponds to $\epsilon_i+\epsilon_j = \epsilon_a+\epsilon_v$ restriction in the ladder term and the contributions

excluded in the irreducible crossed term, reads

$$\begin{aligned}\Delta E_v^{(2\mathrm{I})\mathrm{SESE,2e,red}} = \frac{i}{2\pi}\int \frac{d\omega}{(\omega+i\varepsilon)^2}\Bigg\{ &- \sum_{a,v_1,v_2} I_{vv_2v_1v}(\omega) I_{v_1aav_2}(\Delta_{va}+\omega) \\ &+ \sum_{a,a_1,v_1}\Big[I_{vav_1a_1}(\omega) I_{v_1a_1av}(\Delta_{va}+\omega) + I_{vaa_1v_1}(\Delta_{va}-\omega) I_{a_1v_1av}(\omega)\Big] \\ &- \sum_{a,a_1,a_2} I_{va_2a_1v}(\Delta_{va}-\omega) I_{a_1aaa_2}(\omega)\Bigg\}\,. \end{aligned} \tag{3.70}$$

The three-electron irreducible part $\Delta E_v^{(2\mathrm{I})\mathrm{SESE,3e,irr}}$ is given by

$$\begin{aligned}\Delta E_v^{(2\mathrm{I})\mathrm{SESE,3e,irr}} = &\sum_{a,b,i}^{i\neq b} \frac{I_{vibv}(\Delta_{vb}) I_{baai}(\Delta_{ba}) + I_{vbiv}(\Delta_{vb}) I_{iaab}(\Delta_{ab})}{(\epsilon_b-\epsilon_i)} \\ &+ \sum_{a,b,i}^{(i,b)\neq(v,a)} \frac{I_{vabi}(\Delta_{vb}) I_{biav}(\Delta_{ba}) + I_{vaib}(\Delta_{ba}) I_{ibav}(\Delta_{vb})}{(\epsilon_v+\epsilon_a-\epsilon_b-\epsilon_i)} \\ &+ \sum_{a,b,i}^{i\neq v} \frac{I_{vaai}(\Delta_{va}) I_{ibbv}(\Delta_{vb})}{(\epsilon_v-\epsilon_i)} + \sum_{a,b,i} \frac{I_{viab}(\Delta_{va}) I_{abiv}(\Delta_{vb})}{(\epsilon_a+\epsilon_b-\epsilon_v-\epsilon_i)}\,. \end{aligned} \tag{3.71}$$

The derivative term arising from the ladder-exchange graph as well as the disconnected SESE part from the second term in Eq. (3.65) are merged into the reducible part, leading to

$$\begin{aligned}\Delta E_v^{(2\mathrm{I})\mathrm{SESE,3e,red}} = &\sum_{a,b,a_1}\Big[I_{va_1av}(\Delta_{va}) I'_{abba_1}(\Delta_{ab}) - I'_{va_1av}(\Delta_{va}) I_{abba_1}(\Delta_{ab})\Big] \\ &+ \sum_{a,b,v_1} I'_{vaav_1}(\Delta_{va}) I_{v_1bbv}(\Delta_{vb}) + \sum_{a,a_1,v_1} I'_{vaa_1v_1}(\Delta_{va}) I_{a_1v_1av}(0)\,. \end{aligned} \tag{3.72}$$

Since the contributions summarized above are derived from the GI SESE subset, one assumes that they form a GI subset as well. Moreover, the gauge invariance also persists for two- and three-electron contributions independently. The gauge invariance of the three-electron SESE subset can be demonstrated analytically. With the help of Eq. (2.45), once the denominators have been canceled and the sum completed with the appropriated missing terms, the gauge

difference $\delta\Delta E_v^{(2),\mathrm{SESE,3e,irr}}$ is turned into

$$\begin{aligned}\delta\Delta E_v^{(2\mathrm{I})\mathrm{SESE,3e,irr}} &= \frac{1}{2}\sum_{a,b,i}\Big[\Delta_{bv}\widetilde{I}_{vibv}(\Delta_{vb})I^F_{baai}(\Delta_{ba}) + \Delta_{ba}I^C_{vibv}(\Delta_{vb})\widetilde{I}_{baai}(\Delta_{ba}) \\ &+ \Delta_{vb}\widetilde{I}_{ibav}(\Delta_{vb})I^F_{vaib}(\Delta_{ab}) + \Delta_{ab}I^C_{ibav}(\Delta_{vb})\widetilde{I}_{vaib}(\Delta_{ab}) \\ &+ \Delta_{bv}\widetilde{I}_{vbiv}(\Delta_{vb})I^F_{iaab}(\Delta_{ab}) + \Delta_{ba}I^C_{vbiv}(\Delta_{vb})\widetilde{I}_{iaab}(\Delta_{ab}) \\ &+ \Delta_{vb}\widetilde{I}_{vabi}(\Delta_{vb})I^F_{biav}(\Delta_{ba}) + \Delta_{ab}I^C_{vabi}(\Delta_{vb})\widetilde{I}_{biav}(\Delta_{ba}) \\ &+ \Delta_{va}\widetilde{I}_{vaai}(\Delta_{va})I^F_{ibbv}(\Delta_{vb}) + \Delta_{vb}I^C_{vaai}(\Delta_{va})\widetilde{I}_{ibbv}(\Delta_{vb}) \\ &+ \Delta_{av}\widetilde{I}_{viab}(\Delta_{va})I^F_{abiv}(\Delta_{vb}) + \Delta_{bv}I^C_{viab}(\Delta_{va})\widetilde{I}_{abiv}(\Delta_{vb})\Big] \\ &+ F \leftrightarrow C - \delta^{\mathrm{SESE}}_{\mathrm{completion}}\,. \end{aligned} \tag{3.73}$$

Applying then Eq. (2.46) on the first and second terms with appropriate use of symmetry property (2.38) allows to rewrite them exactly as the third and fourth terms but with an opposite sign, therefore canceling them. And doing similar for other terms shows the absence of contribution coming from the complete sum. The remaining terms arising from the completion of the sum are given by the expression

$$\begin{aligned}\delta^{\mathrm{SESE}}_{\mathrm{completion}} &= \sum_{a,b,a_1}\Big[\Delta_{av}\widetilde{I}_{va_1av}(\Delta_{va})I^F_{abba_1}(\Delta_{ab}) + \Delta_{ab}I^C_{va_1av}(\Delta_{va})\widetilde{I}_{abba_1}(\Delta_{ab})\Big] \\ &+ \frac{1}{2}\sum_{a,b,v_1}\Big[\Delta_{va}\widetilde{I}_{vaav_1}(\Delta_{va})I^F_{v_1bbv}(\Delta_{vb}) + \Delta_{vb}I^C_{vaav_1}(\Delta_{va})\widetilde{I}_{v_1bbv}(\Delta_{vb})\Big] \\ &+ \sum_{a,b,v_1}\Delta_{vb}\widetilde{I}_{vabv_1}(\Delta_{vb})I^F_{bv_1av}(0) + F \leftrightarrow C\,. \end{aligned} \tag{3.74}$$

The contribution from the reducible part reads

$$\begin{aligned}\delta\Delta E_v^{(2\mathrm{I})\mathrm{SESE,3e,red}} &= \sum_{a,b,a_1}\Big[\Delta_{av}\widetilde{I}_{va_1av}(\Delta_{va})I^F_{abba_1}(\Delta_{ab}) + \Delta_{ab}I^C_{va_1av}(\Delta_{va})\widetilde{I}_{abba_1}(\Delta_{ab})\Big] \\ &+ \sum_{a,b,v_1}\Big[\Delta_{vb}\widetilde{I}_{vabv_1}(\Delta_{vb})I^F_{bv_1av}(0) + \Delta_{va}\widetilde{I}_{vaav_1}(\Delta_{va})I^F_{v_1bbv}(\Delta_{vb})\Big] \\ &+ F \leftrightarrow C\,. \end{aligned} \tag{3.75}$$

One can see that the first, second and fifth terms of the completion term cancel out the first three terms of the reducible part. The remaining ones vanish when their counterparts in $F \leftrightarrow C$ are taken into account, which leads to the desired result.

SEVP subset

The SEVP subset contains only three-electron contribution, which gives the following irreducible part $\Delta E_v^{(2\mathrm{I})\mathrm{SEVP,3e,irr}}$,

$$\Delta E_v^{(2\mathrm{I})\mathrm{SEVP,3e,irr}} = -\sum_{a,b,i}^{i\neq v} \frac{I_{vaai}(\Delta_{va})I_{ibvb}(0) + I_{ibbv}(\Delta_{vb})I_{vaia}(0)}{(\epsilon_v - \epsilon_i)} - \sum_{a,b,i}^{i\neq a} \frac{I_{viav}(\Delta_{va})I_{abib}(0) + I_{vaiv}(\Delta_{va})I_{ibab}(0)}{(\epsilon_a - \epsilon_i)}\,, \tag{3.76}$$

and the reducible part being merged with the disconnected SEVP one yields

$$\Delta E_v^{(2\mathrm{I})\mathrm{SEVP,3e,red}} = -\sum_{a,b,v_1} I'_{vaav_1}(\Delta_{va})I_{v_1bvb}(0) + \sum_{a,b,a_1} I'_{va_1av}(\Delta_{va})I_{aba_1b}(0)\,. \tag{3.77}$$

In order to show its gauge invariance, the first thing one has to do after using Eq. (2.45) and canceling the denominator is to complete the sum. These extra terms cancel the reducible part after simple $a \leftrightarrow b$ renaming where necessary. One is left with

$$\delta\Delta E_v^{(2\mathrm{I})\mathrm{SEVP,3e,irr}} = -\frac{1}{2}\sum_{a,b,i}\Big[\Delta_{va}\widetilde{I}_{vaan}(\Delta_{va})I^F_{nbvb}(0) + \Delta_{vb}\widetilde{I}_{nbbv}(\Delta_{vb})I^F_{vana}(0) + \Delta_{av}\widetilde{I}_{vnav}(\Delta_{va})I^F_{abnb}(0) + \Delta_{av}\widetilde{I}_{vanv}(\Delta_{va})I^F_{nbab}(0) + F \leftrightarrow C\Big]\,. \tag{3.78}$$

Applying Eq. (2.46) on the two first terms and after minor rewriting based on the symmetry property, it gives exactly the same terms as the two last ones but with an opposite sign. Thus, the complete sum gives zero contribution and the subset is gauge invariant.

S(VP)E subset

Two-electron contribution is also found in the S(VP)E subset, in addition to the three-electron one. Let us now consider them separately and start with the first one. The two-electron irreducible part $\Delta E_v^{(2\mathrm{I})\mathrm{S(VP)E,2e,irr}}$ reads

$$\Delta E_v^{(2\mathrm{I})\mathrm{S(VP)E,2e,irr}} = \frac{i}{2\pi}\int d\omega \left[\sum_{a,i,j}{}' \frac{I_{vjia}(\omega)I_{iavj}(\omega)}{(\epsilon_v - \omega - \epsilon_i u)(\epsilon_a - \omega - \epsilon_j u)} + \sum_{a,i,j}^{(i,j)\neq(a,v)} \frac{I_{vaij}(\omega)I_{ijva}(\omega)}{(\epsilon_v - \omega - \epsilon_i u)(\epsilon_a + \omega - \epsilon_j u)}\right]\,, \tag{3.79}$$

where one again excludes the contribution with $\epsilon_i = \epsilon_v$ and $\epsilon_j = \epsilon_a$ from the crossed-direct term (first item) by hand and note this by the prime on the sum. The two-electron reducible part $\Delta E_v^{(2I)S(VP)E,2e,red}$, coming from the ladder direct restriction $\epsilon_i + \epsilon_j = \epsilon_a + \epsilon_v$ together with the excluded part from the irreducible crossed-direct term, yields[4]

$$\begin{aligned}\Delta E_v^{(2I)S(VP)E,2e,red} = &-\frac{i}{4\pi}\int d\omega \left[\frac{1}{(\omega+i\varepsilon)^2}+\frac{1}{(-\omega+i\varepsilon)^2}\right] \\ &\times \sum_{a,a_1,v_1} I_{vaa_1v_1}(\Delta_{va}-\omega) I_{a_1v_1va}(\Delta_{va}-\omega)\,. \end{aligned} \tag{3.80}$$

The three-electron irreducible part $\Delta E_v^{(2I)S(VP)E,3e,irr}$ yields

$$\begin{aligned}\Delta E_v^{(2I)S(VP)E,3e,irr} = &-\sum_{a,b,i}^{(i,b)\neq(v,a)} \frac{I_{vabi}(\Delta_{vb}) I_{biva}(\Delta_{vb}) + I_{vaib}(\Delta_{ba}) I_{ibva}(\Delta_{ba})}{(\epsilon_v+\epsilon_a-\epsilon_b-\epsilon_i)} \\ &-\sum_{a,b,i} \frac{I_{viba}(\Delta_{vb}) I_{bavi}(\Delta_{vb})}{(\epsilon_a+\epsilon_b-\epsilon_v-\epsilon_i)}\,, \end{aligned} \tag{3.81}$$

together with the corresponding reducible part,

$$\Delta E_v^{(2I)S(VP)E,3e,red} = -\sum_{a,a_1,v_1} I_{vaa_1v_1}(\Delta_{va}) I'_{a_1v_1va}(\Delta_{va})\,. \tag{3.82}$$

The recipe to show gauge invariance is always the same: apply Eq. (2.45), cancel the denominators, and complete the sum. One obtains afterward for the three-electron part

$$\begin{aligned}\delta\Delta E_v^{(2I)S(VP)E,3e,irr} = &-\frac{1}{2}\sum_{a,b,i}\Big\{\Delta_{bv}\left[\widetilde{I}_{viba}(\Delta_{vb}) I^F_{bavi}(\Delta_{vb}) + I^C_{viba}(\Delta_{vb})\widetilde{I}_{bavi}(\Delta_{vb})\right] \\ &+\Delta_{vb}\left[\widetilde{I}_{vabi}(\Delta_{vb}) I^F_{biva}(\Delta_{vb}) + I^C_{vabi}(\Delta_{vb})\widetilde{I}_{biva}(\Delta_{vb})\right] \\ &+\Delta_{ab}\left[\widetilde{I}_{vaib}(\Delta_{ba}) I^F_{ibva}(\Delta_{ba}) + I^C_{vaib}(\Delta_{ba})\widetilde{I}_{ibva}(\Delta_{ba})\right]\Big\} \\ &+F\leftrightarrow C - \delta^{S(VP)E}_{completion}\,. \end{aligned} \tag{3.83}$$

The first two terms of the sum are rewritten with the help of Eq. (2.46) and symmetry property as the third and fourth terms. Only the prefactor differs by the sign, leading to their cancellation. The part proportional to Δ_{ab} is canceled in the same way, the major difference lies in the fact

[4] The expression $\frac{-1}{(x+i\varepsilon)^2}+\frac{1}{(-x+i\varepsilon)^2} = \frac{2\pi}{i}\partial_x\delta(x)$ was used to symmetrize the ω-flow in the VP loop, or in other words, to symmetrize the pole structure with respect to the real-line axis.

that they will be cancelled by their counterpart in $F \leftrightarrow C$. The same applies to the reducible part in order to cancel the completion term $\delta^{\mathrm{S(VP)E}}_{\mathrm{completion}}$.

VPVP subset

The VPVP graph provides only one term, a three-electron contribution,

$$\Delta E_v^{(2\mathrm{I})\mathrm{VPVP,3e}} = \sum_{a,b,i}^{i\neq v} \frac{I_{vaia}(0) I_{ibvb}(0)}{(\epsilon_v - \epsilon_i)} \,. \tag{3.84}$$

As has been shown in the one-photon exchange section, it is straightforward to see that the difference between Feynman and Coulomb gauges vanishes since the argument of the photon propagator is zero.

V(VP)P subset

In the case of the V(VP)P graph, there is also only a three-electron contribution which can be found,

$$\Delta E_v^{(2\mathrm{I})\mathrm{V(VP)P,3e}} = \sum_{a,b,i}^{i\neq a} \frac{I_{vavi}(0) I_{ibab}(0) + I_{viva}(0) I_{abib}(0)}{(\epsilon_a - \epsilon_i)} \,. \tag{3.85}$$

Similar as in the previous subset, the difference between Feynman and Coulomb gauges is zero due to the zero argument of the photon propagator.

V(SE)P subset

The V(SE)P subset contains the three-electron irreducible contribution $\Delta E_v^{(2\mathrm{I})\mathrm{V(SE)P,3e,irr}}$,

$$\Delta E_v^{(2\mathrm{I})\mathrm{V(SE)P,3e,irr}} = -\sum_{a,b,i}^{i\neq b} \left[\frac{I_{vbvi}(0) I_{aiba}(\Delta_{ba}) + I_{vivb}(0) I_{abia}(\Delta_{ba})}{(\epsilon_b - \epsilon_i)} \right] , \tag{3.86}$$

together with the three-electron reducible term $\Delta E_v^{(2\mathrm{I})\mathrm{V(SE)P,3e,red}}$,

$$\Delta E_v^{(2\mathrm{I})\mathrm{V(SE)P,3e,red}} = -\sum_{a,b,a_1} I_{vava_1}(0) I'_{ba_1ab}(\Delta_{ab}) \,. \tag{3.87}$$

As the reducible part arises from the excluded term in the sum, completing the sum will automatically cancel the reducible part. The only subtlety is to break the reducible contribution into two pieces and use the symmetry property to rewrite it in proper shape.

SECP subset

Let us turn now to the counterpotential terms and its previously proposed decomposition. Since, after extraction of the interelectronic-interaction parts, all diagrams will be either two-electron (SECP and VPCP subsets) or one-electron (CPCP subset), one does not identify this superscript directly. In the case of the SECP subset, it is easy to obtain the following expression for the corresponding irreducible part $\Delta E_v^{(2\mathrm{I})\mathrm{SECP,irr}}$,

$$\Delta E_v^{(2\mathrm{I})\mathrm{SECP,irr}} = \sum_{a,i}^{i\neq v} \frac{U_{vi} I_{iaav}(\Delta_{va}) + I_{vaai}(\Delta_{va}) U_{iv}}{(\epsilon_v - \epsilon_i)} + \sum_{a,i}^{i\neq a} \frac{I_{vaiv}(\Delta_{va}) U_{ia} + I_{viav}(\Delta_{va}) U_{ai}}{(\epsilon_a - \epsilon_i)} \,. \tag{3.88}$$

The reducible part, which encapsulates also the disconnected SECP part of the second term of Eq. (3.30), can be written as

$$\Delta E_v^{(2\mathrm{I})\mathrm{SECP,red}} = \sum_{a,v_1} I'_{vaav_1}(\Delta_{va}) U_{v_1 v} - \sum_{a,a_1} I'_{vaa_1 v}(\Delta_{va}) U_{a_1 a} \,. \tag{3.89}$$

It is left to demonstrate the gauge invariance of this subset. As previously, use Eq. (2.42), cancel the denominators, and complete the sum one gets for the gauge difference

$$\begin{aligned} \delta\Delta E_v^{(2\mathrm{I})\mathrm{SECP,irr}} = & 2 \sum_{a,i} \left[\Delta_{va} \widetilde{I}_{vaai}(\Delta_{va}) U_{iv} + \Delta_{av} \widetilde{I}_{viav}(\Delta_{va}) U_{ai} \right] \\ & - 2 \sum_{a,v_1} \Delta_{va} \widetilde{I}_{vaav_1}(\Delta_{va}) U_{v_1 v} - 2 \sum_{a,a_1} \Delta_{av} \widetilde{I}_{va_1 av}(\Delta_{va}) U_{aa_1} \,. \end{aligned} \tag{3.90}$$

Then Eq. (2.44) applied on the reducible part will provide the appropriate terms to cancel the second line of the previous equation. With $[I(\boldsymbol{x}-\boldsymbol{y}), V(\boldsymbol{z})] = 0$ in mind, a similar formula as Eq. (2.46) shows that the complete sum vanishes; therefore, this ends the proof of the gauge invariance.

VPCP subset

The diagrams of the VPCP subset give only one term, which yields

$$\Delta E_v^{(2\mathrm{I})\mathrm{VPCP}} = -\sum_{a,i}^{i\neq v} \frac{I_{vaia}(0)U_{iv} + U_{vi}I_{iava}(0)}{(\epsilon_v - \epsilon_i)} - \sum_{a,i}^{i\neq a} \frac{I_{vavi}(0)U_{ia} + U_{ai}I_{viva}(0)}{(\epsilon_a - \epsilon_i)}. \quad (3.91)$$

As the argument of the photon propagator is zero and the counterpotential is not influenced by any gauge change, the gauge invariance of this term is straightforwardly guaranteed.

CPCP subset

The CPCP subset contains only one term, which corresponds to the diagram itself,

$$\Delta E_v^{(2\mathrm{I})\mathrm{CPCP}} = \sum_{i}^{i\neq v} \frac{U_{vi}U_{iv}}{(\epsilon_v - \epsilon_i)}, \quad (3.92)$$

since as in the case of the one-photon exchange, there is no such term in the radiative correction set. By the construction it is gauge invariant.

Final expressions

Thus, in the previous section, one identified eight GI subsets in the original Furry picture: SESE (two- and three-electron subsets), SEVP, S(VP)E (two- and three-electron subsets), VPVP, V(VP)P, and V(SE)P. In an extended Furry picture, they are completed by three additional counterpotential subsets: SECP, VPCP, and CPCP. The final expression for the total two-photon exchange correction $\Delta E_v^{(2\mathrm{I})}$,

$$\begin{aligned}\Delta E_v^{(2\mathrm{I})} = &\left(\Delta E_v^{(2\mathrm{I})\mathrm{SESE,2e,irr}} + \Delta E_v^{(2\mathrm{I})\mathrm{SESE,2e,red}}\right) + \left(\Delta E_v^{(2\mathrm{I})\mathrm{SESE,3e,irr}} + \Delta E_v^{(2\mathrm{I})\mathrm{SESE,3e,red}}\right) \\ &+ \left(\Delta E_v^{(2\mathrm{I})\mathrm{SEVP,3e,irr}} + \Delta E_v^{(2\mathrm{I})\mathrm{SEVP,3e,red}}\right) + \left(\Delta E_v^{(2\mathrm{I})\mathrm{S(VP)E,2e,irr}} + \Delta E_v^{(2\mathrm{I})\mathrm{S(VP)E,2e,red}}\right) \\ &+ \left(\Delta E_v^{(2\mathrm{I})\mathrm{S(VP)E,3e,irr}} + \Delta E_v^{(2\mathrm{I})\mathrm{S(VP)E,3e,red}}\right) + \Delta E_v^{(2\mathrm{I})\mathrm{VPVP,3e}} + \Delta E_v^{(2\mathrm{I})\mathrm{V(VP)P,3e,irr}} \\ &+ \left(\Delta E_v^{(2\mathrm{I})\mathrm{V(SE)P,3e,irr}} + \Delta E_v^{(2\mathrm{I})\mathrm{V(SE)P,3e,red}}\right) + \left(\Delta E_v^{(2\mathrm{I})\mathrm{SECP,irr}} + \Delta E_v^{(2\mathrm{I})\mathrm{SECP,red}}\right) \\ &+ \Delta E_v^{(2\mathrm{I})\mathrm{VPCP}} + \Delta E_v^{(2\mathrm{I})\mathrm{CPCP}}, \end{aligned} \quad (3.93)$$

is given by a sum of equations (3.69) – (3.72), (3.76), (3.77), (3.79) – (3.82), (3.84) – (3.89), (3.91), and (3.92). The terms in Eq. (3.93) are grouped into the GI subsets.

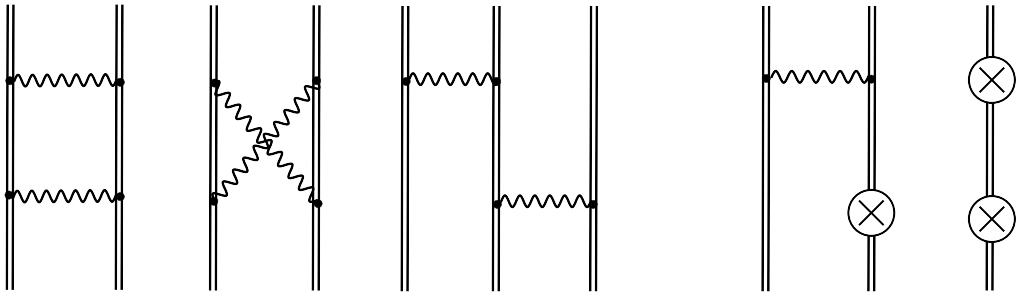

Figure 3.3.: Feynman diagrams representing the two-photon-exchange corrections to the energy shift of a single-particle (valence or hole) state. Notations for the diagrams are as follows, from left to right: two-particle ladder, two-particle crossed, three-particle, and two counterpotential graphs. Other notations are the same as in Fig. 2.3.

The two-photon-exchange corrections can be also identified by the many-electron diagrams depicted in Fig. 3.3. All of the contributions originated from these diagrams have been obtained within the redefined vacuum state approach and are presented with Eq. (3.93). To compare these results based on the effective one-particle approach with the ones obtained within consideration of many-electron diagrams, one gathers them in accordance with the separation published previously [72, 73, 82]. First, the expression for the two-electron irreducible contribution $\Delta E_v^{(2\mathrm{I})2\mathrm{e,irr}}$, which is obtained by summing up Eqs. (3.69) and (3.79), is presented

$$\begin{aligned}\Delta E_v^{(2\mathrm{I})2\mathrm{e,irr}} = \frac{i}{2\pi}\int d\omega \left\{ \sum_{a,i,j}^{(i,j)\neq(a,v)} \frac{I_{vaij}(\omega) I_{ijva}(\omega)}{(\epsilon_v - \omega - \epsilon_i u)(\epsilon_a + \omega - \epsilon_j u)} \right. \\ + \sum_{a,i,j}{}' \frac{I_{vjia}(\omega) I_{iavj}(\omega)}{(\epsilon_v - \omega - \epsilon_i u)(\epsilon_a - \omega - \epsilon_j u)} - \sum_{a,i,j}^{(i,j)\neq(a,v)} \frac{I_{vaij}(\omega) I_{ijav}(\Delta_{va} - \omega)}{(\epsilon_v - \omega - \epsilon_i u)(\epsilon_a + \omega - \epsilon_j u)} \\ \left. - \sum_{a,i,j}{}' \frac{I_{vjiv}(\omega) I_{iaaj}(\Delta_{va} - \omega)}{(\epsilon_v - \omega - \epsilon_i u)(\epsilon_v - \omega - \epsilon_j u)} \right\} . \end{aligned} \tag{3.94}$$

The first two terms are direct parts [Eq. (3.79)], ladder and crossed, respectively, while the second two are the exchange counterparts [Eq. (3.69)], again ladder and crossed, respectively. The primes on the sums are meant for the omitted terms, namely, $i = v$ and $j = a$ for the crossed-direct term and $(i, j) = \{(a, a), (v, v)\}$ for the crossed-exchange term. The two-

electron reducible contribution $\Delta E_v^{(2\mathrm{I})2\mathrm{e,red}}$ is given by a sum of Eqs. (3.70) and (3.80),

$$\begin{aligned}\Delta E_v^{(2\mathrm{I})2\mathrm{e,red}} = \frac{i}{2\pi}\int \frac{d\omega}{(\omega+i\varepsilon)^2}\Bigg\{ \sum_{a,a_1,v_1} \Big[& I_{vav_1a_1}(\omega) I_{v_1a_1av}(\Delta_{va}+\omega) \\ & + I_{vaa_1v_1}(\Delta_{va}-\omega) I_{a_1v_1av}(\omega) - \frac{1}{2} I_{vaa_1v_1}(\Delta_{va}-\omega) I_{a_1v_1va}(\Delta_{va}-\omega) \\ & - \frac{1}{2} I_{vaa_1v_1}(\Delta_{va}+\omega) I_{a_1v_1va}(\Delta_{va}+\omega) \Big] - \sum_{a,a_1,a_2} I_{va_2a_1v}(\Delta_{va}-\omega) I_{a_1aaa_2}(\omega) \\ & - \sum_{a,v_1,v_2} I_{vv_2v_1v}(\omega) I_{v_1aav_2}(\omega+\Delta_{va}) \Bigg\} . \end{aligned} \tag{3.95}$$

The expressions of the two-electron contribution presented in such a way agree with the results of Refs. [72, 73, 82]. In Refs. [76, 83], the two-electron contribution is not separated into irreducible and reducible parts and given as in Eq. (3.94) but without any sums' restrictions. One recalls the separations made between irreducible and reducible parts. Concerning the two-electron crossed terms, the reducible parts are separated artificially and can be added back, thus, removing the restrictions in the second and fourth sums in Eq. (3.94). In contrast, the two-electron ladder term is leading to a discrepancy. In order to restore the completeness of the first and third sums in Eq. (3.94), the omitted terms $(i,j) = (a,v)$ should have the pole structure $(\omega+i\varepsilon)(\omega-i\varepsilon)$. However, as one can see from Eq. (3.95) all contributions have a different pole topology, namely, $(\omega+i\varepsilon)^2$.

Collecting all three-electron irreducible terms given by Eqs. (3.71), (3.76), (3.81), (3.84), (3.85), and (3.86) together with the counterpotential irreducible terms, Eqs. (3.88), (3.91), and

(3.92), one comes to the following total three-electron contribution:

$$\begin{aligned}
\Delta E_v^{(2\mathrm{I})3\mathrm{e,irr}} = &\sum_{a,b,i}^{i\neq a}\left\{\frac{\left[I_{ibab}(0)-I_{ibba}(\Delta_{ab})\right]\left[I_{vavi}(0)-I_{vaiv}(\Delta_{va})\right]}{\epsilon_a-\epsilon_i}\right.\\
&\left.+\frac{\left[I_{abib}(0)-I_{baib}(\Delta_{ab})\right]\left[I_{viva}(0)-I_{viav}(\Delta_{va})\right]}{\epsilon_a-\epsilon_i}\right\}\\
&+\sum_{a,b,i}^{i\neq v}\frac{\left[I_{vaai}(\Delta_{va})-I_{vaia}(0)\right]\left[I_{ibbv}(\Delta_{vb})-I_{ibvb}(0)\right]}{\epsilon_v-\epsilon_i}\\
&+\sum_{a,b,i}\frac{\left[I_{abiv}(\Delta_{vb})-I_{abvi}(\Delta_{va})\right]I_{viab}(\Delta_{va})}{\epsilon_a+\epsilon_b-\epsilon_v-\epsilon_i}\\
&+\sum_{a,b,i}^{(i,b)\neq(v,a)}\frac{\left[I_{vabi}(\Delta_{vb})-I_{vaib}(\Delta_{ba})\right]\left[I_{biav}(\Delta_{ba})-I_{biva}(\Delta_{vb})\right]}{\epsilon_v+\epsilon_a-\epsilon_b-\epsilon_i}\\
&+\sum_{a,i}^{i\neq v}\frac{U_{vi}\left[I_{iaav}(\Delta_{va})-I_{iava}(0)\right]+\left[I_{vaai}(\Delta_{va})-I_{vaia}(0)\right]U_{iv}}{\epsilon_v-\epsilon_i}\\
&+\sum_{a,i}^{i\neq a}\frac{U_{ai}\left[I_{viav}(\Delta_{va})-I_{viva}(0)\right]+\left[I_{vaiv}(\Delta_{va})-I_{vavi}(0)\right]U_{ia}}{\epsilon_a-\epsilon_i}+\sum_{i}^{i\neq v}\frac{U_{vi}U_{iv}}{\epsilon_v-\epsilon_i}\,.
\end{aligned}\tag{3.96}$$

In the same way, summing Eqs. (3.72), (3.77), (3.82), (3.87), and (3.89) one derives the total three-electron reducible contribution:

$$\begin{aligned}
\Delta E_v^{(2\mathrm{I})3\mathrm{e,red}} = &\sum_{a,b,a_1}\left\{I'_{va_1av}(\Delta_{va})\left[I_{aba_1b}(0)-I_{abba_1}(\Delta_{ab})\right]\right.\\
&\left.+I'_{abba_1}(\Delta_{ab})\left[I_{va_1av}(\Delta_{va})-I_{va_1va}(0)\right]\right\}\\
&+\sum_{a,b,v_1}I'_{vaav_1}(\Delta_{va})\left[I_{v_1bbv}(\Delta_{vb})-I_{v_1bvb}(0)\right]-\sum_{a,a_1}I'_{vaa_1v}(\Delta_{va})U_{a_1a}\\
&+\sum_{a,v_1}I'_{vaav_1}(\Delta_{va})U_{v_1v}+\sum_{a,a_1,v_1}I'_{vaa_1v_1}(\Delta_{va})\left[I_{a_1v_1av}(0)-I_{a_1v_1va}(\Delta_{va})\right]\,.
\end{aligned}\tag{3.97}$$

In contrast to the two-electron contribution, the three-electron contribution has a more complicated structure and can not be easily generalized. Therefore, they were mainly derived for a particular state, e.g., for Li-like ions in Refs. [72, 73] or B-like ions in Ref. [82], and for these special cases the presented expressions agree with the mentioned papers. However, in Refs. [76, 83], the general expressions for the three-electron terms are given, e.g., E_{2F} as the irreducible part and $E_{2F'}$ as the reducible part in accordance with Ref. [83]. Comparing the

derived expressions (3.96) and (3.97) with those of Sapirstein and Cheng, one finds an almost perfect agreement for the irreducible part, except for an absence of a restriction in the fourth sum in Eq. (3.96). Whereas, the reducible part strongly disagrees. Comparing term by term, one notices problems with expressions in the first and third lines of Eq. (3.97). For example, the last expression is written with b state instead of a_1, meaning the summations over all core electrons independently. The first expression in the first line is written with apparent misprints (odd number of electron states in matrix elements). Moreover, there is no expression like the second term in the first line in Ref. [83]. Here, one should note that the gauge invariance condition dictates the exact form of the reducible part. The detailed analysis of gauge invariance for each subset of diagrams performed here makes one believe that this result is more reliable.

3.2.3. Numerical evaluation for Lithium-like ions

One is now in a position to support numerically the gauge invariance of the identified subsets – the strength of the developed approach. The computations are performed for the $2s$, $2p_{1/2}$, and $2p_{3/2}$ binding energies in Li-like tin ion. The finite nuclear size is accounted for by using the Fermi model for the nucleus charge distribution with the root-mean-square radius of 4.6519 fm [118]. The ω integration in the two-electron terms was performed with the Wick rotation to the integration contours chosen as in Ref. [64]. The infinite summations over the whole Dirac spectrum are performed using the dual-kinetic-balance finite basis set method [119] for the Dirac equation. The basis functions are constructed from B-splines [120]. The number of basis functions is systematically increased to achieve a clear convergence pattern of the calculated results. Then the extrapolation to an infinite number of basis functions is undertaken. The partial wave summation over the Dirac quantum number κ was terminated at $\kappa_{\max} = 8$, and the remainder was estimated by the least-squares inverse polynomial fitting. More details on the numerical convergence are provided in appendix A.3. The numerical uncertainty is estimated to be less than 3×10^{-6} atomic units.

The numerical evaluations are performed in both Feynman and Coulomb gauges to demonstrate the gauge invariance of the identified subsets. The individual contributions and sums for each subset are presented in Tables 3.1 and A.1 in atomic units. In Table 3.1, the results for the case of Coulomb potential (original Furry picture) are presented. As one can see from the table, the values for each of eight identified subsets are gauge invariant within the numerical uncertainty. Notice that the term $\Delta E^{(2\mathrm{I})\mathrm{V(SE)P,3el,red}}$ is not displayed, since it gives zero contribution in the case of Li-like ions, i.e., ions with only one closed shell. For a comparison, results from Ref. [72] for the $2s$ and $2p_{1/2}$ states and from Ref. [73] for the $2p_{3/2}$ state are

presented. The comparison shows an excellent agreement with values obtained in the present work. In Table A.1, the results for the extended Furry picture are displayed. The self-consistent core-Hartree potential has been used in this case. In addition to the subsets presented already in the original Furry picture case, three additional subsets coming from the counterpotential diagrams are present. Again, as in the former case, the values presented in this table confirm all identified subsets' gauge invariance.

Presenting now the accurate control on numerical results, calculations are performed for the most compelling experimental cases; Li-like bismuth and uranium ions are presented. In Table 3.2, the ionization potentials and transition energies for the $2s$ and $2p_{3/2}$ states in the case of Li-like Bi and for the $2s$ and $2p_{1/2}$ states in the case of Li-like U ions are displayed. The following nuclear radii 5.531 fm and 5.860 fm are employed for bismuth and uranium, respectively, following Ref. [76]. As in Ref. [76] the Kohn-Sham potential is used as the starting potential and compared term by term the zeroth-order energy E^0 as well as the first-order $\Delta E^{(1)}$ and second-order $\Delta E^{(2)}$ corrections. As one can see from the table, the zeroth- and first-order terms are in perfect agreement to all given digits. At the same time, the two-photon exchange (second-order) correction is slightly different. The reason for this may be precisely the discrepancy in the reducible two- and three-electron contributions stated above. Since the reducible terms are always much smaller than the dominant irreducible one, it is rather difficult to identify the correctness of its calculation. Here, one should emphasize again that the reducible terms are responsible for restoring the gauge invariance, and within the developed method, one has excellent control on this issue.

To compare with the experiments, one has to add additional correction ΔE_{rest}, which incorporates three-photon-exchange, recoil, radiative, and screened-radiative contributions. These contributions are taken directly from Ref. [76]. Comparing now the total values of the energies for the $2p_{3/2} - 2s$ transition in bismuth and the $2p_{1/2} - 2s$ transition in uranium, one can see overall good agreement between both theoretical calculations and experimental results within the given error bars. Nevertheless, the conviction is that these independent calculations are essential for future more precise comparisons.

	$2s$		$2p_{1/2}$		$2p_{3/2}$	
	Feynman	Coulomb	Feynman	Coulomb	Feynman	Coulomb
SESE,2e,irr	0.026650	0.029926	0.022374	0.025697	0.027738	0.031426
SESE,2e,red	0.003036	-0.000240	0.002901	-0.000422	0.003839	0.000151
SESE,2e	0.029686	0.029686	0.025275	0.025275	0.031578	0.031578
	0.02968[a]	0.02967[a,*]	0.02528[a]	0.02529[a]	0.03156[b]	
S(VP)E,2e,irr	-0.187925	-0.187589	-0.323212	-0.323137	-0.212025	-0.211837
S(VP)E,2e,red	0.000338	0.000001	0.000052	-0.000022	0.000187	-0.000002
S(VP)E,2e	-0.187588	-0.187587	-0.323159	-0.323159	-0.211838	-0.211838
	-0.18759[a]	-0.18759[a]	-0.32317[a]	-0.32317[a]	-0.21185[b]	
SESE,3e,irr	-0.026028	-0.027012	-0.015884	-0.017989	-0.022614	-0.024791
SESE,3e,red	-0.000933	0.000052	-0.002146	-0.000041	-0.002602	-0.000424
SESE,3e	-0.026960	-0.026960	-0.018030	-0.018030	-0.025215	-0.025215
SEVP,3e,irr	0.035264	0.037506	0.018094	0.022872	0.037953	0.042854
SEVP,3e,red	0.002122	-0.000120	0.004866	0.000088	0.005850	0.000949
SEVP,3e	0.037386	0.037386	0.022960	0.022960	0.043803	0.043803
S(VP)E,3e,irr	0.176478	0.176348	0.305829	0.305787	0.197613	0.197495
S(VP)E,3e,red	-0.000130	0.000000	-0.000041	0.000001	-0.000140	-0.000022
S(VP)E,3e	0.176348	0.176348	0.305788	0.305788	0.197473	0.197473
VPVP,3e	-0.302978	-0.302978	-0.483510	-0.483510	-0.430804	-0.430804
V(VP)P,3e	-0.050230	-0.050230	-0.038836	-0.038836	-0.029621	-0.029621
V(SE)P,3e,irr	0.021757	0.021757	0.017132	0.017132	0.013100	0.013100
Total 3-electron	-0.144678	-0.144678	-0.194497	-0.194497	-0.231265	-0.231265
	-0.14468[a]	-0.14468[a]	-0.19450[a]	-0.19449[a]	-0.23126[b]	
Total	-0.302579	-0.302579	-0.492381	-0.492381	-0.411525	-0.411526
	-0.30259[a]	-0.30259[a]	-0.49239[a]	-0.49237[a]	-0.41156[b]	

[a] Yerokhin *et al.* [72]; sphere model for the nuclear charge distribution used.

[b] Artemyev *et al.* [73]; sphere model for the nuclear charge distribution used.

[*] Misprint corrected: Table III, $\Delta E^{2\mathrm{el}}_{\mathrm{ir}}$(exch) 0.02995 a.u. is used instead of 0.02595 a.u.

Table 3.1.: Contributions of the identified gauge-invariant subsets to the two-photon-exchange corrections for the $2s$, $2p_{1/2}$, and $2p_{3/2}$ states of the Li-like Sn ($Z = 50$) ion, in atomic units. The values are obtained within the original Furry picture (Coulomb potential). The results of the Feynman and Coulomb gauges are given. The Fermi model of the nuclear charge distribution is employed.

	$2s$		$2p_{3/2}$		$2p_{3/2} - 2s$	
$Z = 83$	Ref. [76]	This work	Ref. [76]	This work	Ref. [76]	This work
$E^{(0)}$	−937.4309	−937.43089	−833.7473	−833.74735	103.6836	103.68354
$\Delta E^{(1)}$	−6.5674	−6.56746	−6.8275	−6.82756	−0.2601	−0.26010
$\Delta E^{(2)}$	−0.0178	−0.01725	−0.0159	−0.01491	0.0019	0.00234
ΔE_{rest}	1.1413	1.1413	0.1747	0.1747	−0.9666(18)	−0.9666(18)
E_{theo}	−942.8748	−942.87431	−840.4160	−840.41512	102.4588(18)	102.4592(18)
E_{exp} [121]					102.4622(14)	
	$2s$		$2p_{1/2}$		$2p_{1/2} - 2s$	
$Z = 92$	Ref. [76]	This work	Ref. [76]	This work	Ref. [76]	This work
$E^{(0)}$	−1201.067	−1201.06660	−1192.233	−1192.23254	8.834	8.83406
$\Delta E^{(1)}$	−7.360	−7.36038	−4.305	−4.30548	3.055	3.05490
$\Delta E^{(2)}$	−0.023	−0.02187	−0.070	−0.06914	−0.047	−0.04727
ΔE_{rest}	1.731	1.731	0.202	0.202	−1.529(3)	−1.529(3)
E_{theo}	−1206.719	−1206.71785	−1196.406	−1196.40515	10.313(3)	10.3127(30)
E_{exp} [44]					10.3135(5)	

Table 3.2.: Individual contributions to the ionization potentials (a.u.) and transition energies (a.u.) for the $2s$ and $2p_{3/2}$ states in the case of Li-like Bi (upper half) and for the $2s$ and $2p_{1/2}$ states in case of the Li-like U (lower half). The Dirac energy $E^{(0)}$, one-photon $\Delta E^{(1)}$ and two-photon $\Delta E^{(2)}$ exchange corrections are compared with the results of Ref. [76]. The Kohn-Sham potential is employed as the starting potential. Other correction ΔE_{rest}, which includes three-photon-exchange, recoil, radiative, and screened-radiative contributions, is taken from Ref. [76] and also used for calculation of our total theory results. A comparison with existing experimental values is given.

3.3. Single-hole (electronic vacancy) in closed shells

The investigations are focused on the one-hole state [$N = 1$, $A_h \equiv h$]. Such an example is chosen due to the fact that two-photon-exchange correction is still uncalculated for fluorine-like ions [54–56] as well as due to recent experimental efforts for such systems [51, 52]. Having derived the formal expressions for the energy shift, Eq. (3.47), in this section the formalism is applied for the derivation of the first- and second-order corrections. Special attention is paid to

the allocation of the GI subsets, which is the key aspect of the developed formalism, as was demonstrated previously for the one-valence-electron case in Section 3.2.2 .

3.3.1. One- and two-photon-exchange corrections

The separation of different contributions to the energy shift at each perturbative order is done exactly as in Eqs. (3.51, 3.52). Owing to the symmetry argument developed below Eq. (3.47), the derivation of the one-photon-exchange correction $\Delta E_h^{(1\mathrm{I})}$ and two-photon-exchange correction $\Delta E_h^{(2\mathrm{I})}$ is straightforward; for every expression previously derived, the hole's case is obtained under the change of labelling $v \to h$ and each formula enters with the opposite sign. Therefore, those steps are spared but the end result is recalled. The one-photon-exchange corrections is

$$\Delta E_h^{(1\mathrm{I})} = -\sum_a \left[I_{haha}(0) - I_{haah}(\Delta_{ha}) \right] + U_{hh} \,, \tag{3.98}$$

and final expression for the total two-photon-exchange correction, $\Delta E_h^{(2\mathrm{I})}$, reads,

$$\begin{aligned} \Delta E_h^{(2\mathrm{I})} = {} & \Delta E_h^{(2\mathrm{I})\mathrm{SESE,2e}} + \Delta E_h^{(2\mathrm{I})\mathrm{SESE,3e}} + \Delta E_h^{(2\mathrm{I})\mathrm{SEVP,3e}} + \Delta E_h^{(2\mathrm{I})\mathrm{S(VP)E,2e}} + \Delta E_h^{(2\mathrm{I})\mathrm{S(VP)E,3e}} \\ & + \Delta E_h^{(2\mathrm{I})\mathrm{V(SE)P,3e}} + \Delta E_h^{(2\mathrm{I})\mathrm{VPVP,3e}} + \Delta E_h^{(2\mathrm{I})\mathrm{V(VP)P,3e}} + \Delta E_h^{(2\mathrm{I})\mathrm{SECP}} + \Delta E_h^{(2\mathrm{I})\mathrm{VPCP}} \\ & + \Delta E_h^{(2\mathrm{I})\mathrm{CPCP}} \,, \end{aligned} \tag{3.99}$$

which is given by a sum of Eqs. (3.69)–(3.92), presented in section 3.2.2 (under the sign flip and the exchange of labels). The expressions in Eq. (3.99) are derived for the first time and require a critical view. Therefore, the Breit approximation is applied to these results, in Appendix A.4, and the outcome compared with the RMBPT expressions of Ref. [101]. A full agreement is encountered. Each term in Eq. (3.99) is individually GI. Generally, this statement is based on the gauge invariance of the corresponding subsets of one-electron diagrams [117] depicted in Fig. 3.2.

3.3.2. Screened-radiative corrections

The interest is, thus, focused on the many-electron term not treated so far, the screened-radiative corrections $\Delta E_h^{(2\mathrm{S})}$. Some of these terms were presented in Eq. (3.67) but no further comments were made. The procedure goes as before, first applying the Feynman rules for each of the

diagrams depicted in Fig. 3.2, one writes down the expression for the second-order Green's function $\Delta g^{(2)}_{\alpha,hh}(E)$. The next step is the identification of the two-particle one-loop radiative corrections. Details concerning this procedure are similar to the one-valence-electron case, which was already provided in great details in Section 3.2.2. For this reason, the full-length derivation is not provided here and one restricts itself to the presentation of final formulas.

Let us start with the two terms, which originate from the one-particle diagrams with a VP loop only: VPVP and V(VP)P,

$$\Delta E_h^{(2S)\mathrm{VPVP}} = \frac{i}{2\pi}\int d\omega \sum_{a,i,j}^{i\neq h} \frac{2I_{haia}(0)I_{ijhj}(0)}{(\epsilon_h-\epsilon_i)(\omega-\epsilon_j u)} \tag{3.100}$$

and

$$\Delta E_h^{(2S)\mathrm{V(VP)P}} = \frac{i}{2\pi}\int d\omega \left[\sum_{a,i,j}^{i\neq a} \frac{2I_{hahi}(0)I_{ijaj}(0)}{(\epsilon_a-\epsilon_i)(\omega-\epsilon_j u)} + \sum_{a,i,j} \frac{I_{hihj}(0)I_{jaia}(0)}{(\omega-\epsilon_i u)(\omega-\epsilon_j u)}\right], \tag{3.101}$$

respectively. The next three subsets displayed come from the diagrams with both SE and VP loops. One begins with the SEVP term, where the disconnected SEVP part [second term in Eq. (3.42)] is included,

$$\begin{aligned}\Delta E_h^{(2S)\mathrm{SEVP}} = &-\frac{i}{2\pi}\int d\omega \left\{\sum_{a,i,j}^{i\neq h} \frac{2I_{haai}(\Delta_{ha})I_{ijhj}(0)}{(\epsilon_h-\epsilon_i)(\omega-\epsilon_j u)} + \sum_{a,i,j}^{i\neq a} \frac{2I_{haih}(\Delta_{ha})I_{ijaj}(0)}{(\epsilon_a-\epsilon_i)(\omega-\epsilon_j u)}\right.\\
&+ \sum_{a,i,j}^{j\neq h} \frac{2I_{hiij}(\omega)I_{jaha}(0)}{(\epsilon_h-\omega-\epsilon_i u)(\epsilon_h-\epsilon_j)} + \sum_{a,i,j} \frac{I_{hjih}(\omega)I_{iaja}(0)}{(\epsilon_h-\omega-\epsilon_i u)(\epsilon_h-\omega-\epsilon_j u)}\\
&+ \sum_{a,i,h_1}\left[\frac{I'_{haah_1}(\Delta_{ha})I_{h_1ihi}(0)}{(\omega-\epsilon_i u)} - \frac{I_{hiih_1}(\omega)I_{h_1aha}(0)}{(\epsilon_h-\omega-\epsilon_i u)^2}\right]\\
&\left.- \sum_{a,i,a_1} \frac{I'_{haa_1h}(\Delta_{ha})I_{a_1iai}(0)}{(\omega-\epsilon_i u)}\right\}.\end{aligned} \tag{3.102}$$

The second subset falling into this category is the V(SE)P one,

$$\begin{aligned}\Delta E_h^{(2S)\mathrm{V(SE)P}} = &-\frac{i}{2\pi}\int d\omega \left[\sum_{a,i,j}^{j\neq a} \frac{2I_{aiij}(\omega)I_{hjha}(0)}{(\epsilon_a-\omega-\epsilon_i u)(\epsilon_a-\epsilon_j)}\right.\\
&\left.+ \sum_{a,i,j} \frac{I_{ajia}(\omega)I_{hihj}(0)}{(\epsilon_a-\omega-\epsilon_i u)(\epsilon_a-\omega-\epsilon_j u)} - \sum_{a,i,a_1} \frac{I_{aiia_1}(\omega)I_{ha_1ha}(0)}{(\epsilon_a-\omega-\epsilon_i u)^2}\right],\end{aligned} \tag{3.103}$$

and finally the S(VP)E graph yields

$$\Delta E_h^{(2S)S(VP)E} = -\frac{i}{2\pi}\int d\omega \sum_{a,i,j} \frac{I_{hjai}(\Delta_{ha})I_{aihj}(\Delta_{ha})}{(\omega-\epsilon_i u)(\omega-\Delta_{ha}-\epsilon_j u)}\,. \tag{3.104}$$

Last, but not least, the SESE subset comes from the diagrams involving only self-energy loops. It includes also the SESE disconnected part [second term in Eq. (3.42)], and leads to the following expression,

$$\begin{aligned}\Delta E_h^{(2S)SESE} = \frac{i}{2\pi}\int d\omega \Bigg\{ &\sum_{a,i,j}^{j\neq h} \frac{2I_{hiij}(\omega)I_{jaah}(\Delta_{ha})}{(\epsilon_h-\omega-\epsilon_i u)(\epsilon_h-\epsilon_j)} + \sum_{a,i,j}^{j\neq a} \frac{2I_{aiij}(\omega)I_{hjah}(\Delta_{ha})}{(\epsilon_a-\omega-\epsilon_i u)(\epsilon_a-\epsilon_j)} \\ &+ \sum_{a,i,j} \frac{2I_{ajih}(\omega)I_{hiaj}(\Delta_{ha})}{(\epsilon_a-\omega-\epsilon_i u)(\epsilon_h-\omega-\epsilon_j u)} + \sum_{a,i,h_1} \Bigg[\frac{I_{hiih_1}(\omega)I'_{h_1aah}(\Delta_{ha})}{(\epsilon_h-\omega-\epsilon_i u)} \\ &- \frac{I_{hiih_1}(\omega)I_{h_1aah}(\Delta_{ha})}{(\epsilon_h-\omega-\epsilon_i u)^2}\Bigg] - \sum_{i,a,a_1}\left[\frac{I_{aiia_1}(\omega)I'_{ha_1ah}(\Delta_{ha})}{(\epsilon_a-\omega-\epsilon_i u)} + \frac{I_{ha_1ah}(\Delta_{ha})I_{aiia_1}(\omega)}{(\epsilon_a-\omega-\epsilon_i u)^2}\right]\Bigg\}.\end{aligned} \tag{3.105}$$

Furthermore, in the extended Furry picture, two counterpotential subsets emerge. The first one, VPCP, is associated to a vacuum-polarization loop,

$$\Delta E_h^{(2S)VPCP} = -\frac{i}{2\pi}\int d\omega \left[\sum_{a,i,j}\frac{I_{hjhi}(0)U_{ij}}{(\omega-\epsilon_i u)(\omega-\epsilon_j u)} + \sum_{a,i,j}^{i\neq h}\frac{2U_{hi}I_{ijhj}(0)}{(\epsilon_h-\epsilon_i)(\omega-\epsilon_j u)}\right], \tag{3.106}$$

while the second, SECP, arises from the diagram with a self-energy loop and the disconnected SECP part [second term in Eq. (3.42)],

$$\begin{aligned}\Delta E_h^{(2S)SECP} = \frac{i}{2\pi}\int d\omega \Bigg[&\sum_{a,i,j}\frac{I_{hjih}(\omega)U_{ij}}{(\epsilon_h-\omega-\epsilon_i u)(\epsilon_h-\omega-\epsilon_j u)} \\ &+ \sum_{a,i,j}^{i\neq h}\frac{2U_{hi}I_{ijjh}(\omega)}{(\epsilon_h-\epsilon_i)(\epsilon_h-\omega-\epsilon_j u)} - \sum_{a,i,h_1}\frac{U_{hh_1}I_{h_1iih}(\omega)}{(\epsilon_h-\omega-\epsilon_i u)^2}\Bigg]\,.\end{aligned} \tag{3.107}$$

Finals expressions

The eight different GI subsets for the screened-radiative corrections are identified from the general expression for each diagram and presented here

$$\Delta E_h^{(2S)} = \Delta E_h^{(2S)\mathrm{VPVP}} + \Delta E_h^{(2S)\mathrm{V(VP)P}} + \Delta E_h^{(2S)\mathrm{SEVP}} + \Delta E_h^{(2S)\mathrm{V(SE)P}} + \Delta E_h^{(2S)\mathrm{S(VP)E}} + \Delta E_h^{(2S)\mathrm{SESE}} + \Delta E_h^{(2S)\mathrm{VPCP}} + \Delta E_h^{(2S)\mathrm{SECP}}, \quad (3.108)$$

where corresponding terms were explicitly given above by Eqs. (3.100)–(3.105) and by Eqs. (3.106) and (3.107) for the counterpotential terms. The identified subsets should be gauge invariant in both redefined and standard vacuum state frameworks. It implies that the screened-radiative contributions obtained as a difference between the redefined and the standard vacuum state expressions also form the same GI subsets. Explicit proof of this statement has been performed for the two-photon-exchange subsets in the case of one-valence-electron in Section 3.2.2.

In what follows, one also rearranges the screened-radiative corrections according to its usual representation by the many-electron diagrams in the ordinary vacuum formalism, displayed in Fig. 3.4:

$$\Delta E_h^{(2S)} = \Delta E_h^{(2S)\mathrm{SE,ver}} + \Delta E_h^{(2S)\mathrm{SE,wf}} + \Delta E_h^{(2S)\mathrm{VP,wf}} + \Delta E_h^{(2S)\mathrm{VP,int}} + \Delta E_h^{(2S)\mathrm{CP}}, \quad (3.109)$$

where $\Delta E_h^{(2S)\mathrm{SE,ver}}$ and $\Delta E_h^{(2S)\mathrm{SE,wf}}$ represent the screened self-energy correction (vertex

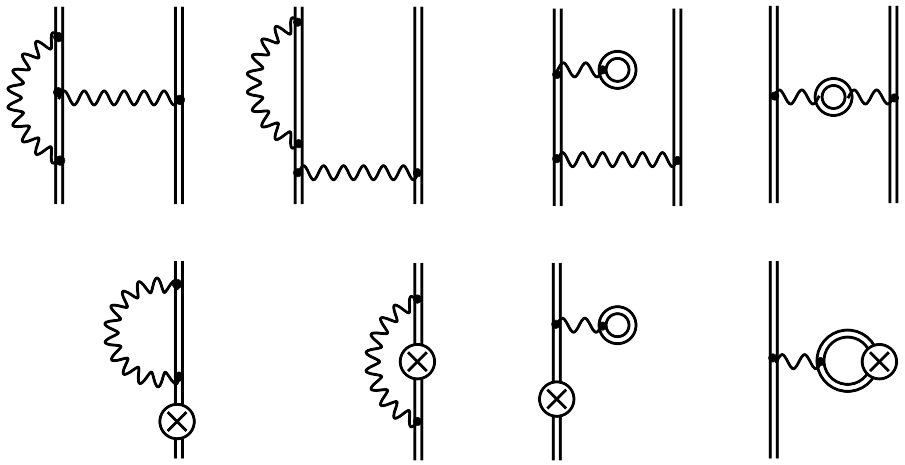

Figure 3.4.: Feynman diagrams representing the one-particle screened self-energy and one-particle screened vacuum-polarization corrections to the energy shift of single-particle (valence or hole) state. Notations for the diagrams are as follows, SE,ver, SE,wf, VP,wf, and VP,int (upper raw) and CP (lower raw). Other notations are the same as in Fig. 2.3

and wave function parts), $\Delta E_h^{(2S)\mathrm{VP,wf}}$ and $\Delta E_h^{(2S)\mathrm{VP,int}}$ correspond to the screened vacuum-polarization correction (wave function and internal-loop parts), and, finally, $\Delta E_h^{(2S)\mathrm{CP}}$ is the counterpotential term. The self-energy vertex part is given by the expression,

$$\Delta E_h^{(2S)\mathrm{SE,ver}} = -\frac{i}{2\pi}\int d\omega \sum_{a,i,j}\left[\frac{I_{hjih}(\omega)I_{iaja}(0)}{(\epsilon_h-\omega-\epsilon_i u)(\epsilon_h-\omega-\epsilon_j u)}\right. \tag{3.110}$$
$$\left. + \frac{I_{ajia}(\omega)I_{hihj}(0)}{(\epsilon_a-\omega-\epsilon_i u)(\epsilon_a-\omega-\epsilon_j u)} - \frac{2I_{ajih}(\omega)I_{hiaj}(\Delta_{ha})}{(\epsilon_a-\omega-\epsilon_i u)(\epsilon_h-\omega-\epsilon_j u)}\right],$$

which arises from the fourth sum in Eq. (3.102), the second one in Eq. (3.103), and the third one in Eq. (3.105). The self-energy wave function part reads

$$\begin{aligned}\Delta E_h^{(2S)\mathrm{SE,wf}} = -\frac{i}{2\pi}\int d\omega \Bigg\{ &\sum_{a,i,j}^{j\neq h}\frac{2I_{hiij}(\omega)\left[I_{jaha}(0)-I_{jaah}(\Delta_{ha})\right]}{(\epsilon_h-\omega-\epsilon_i u)(\epsilon_h-\epsilon_j)} \\ &- \sum_{a,i,h_1}\frac{I_{hiih_1}(\omega)I'_{h_1aah}(\Delta_{ha})}{(\epsilon_h-\omega-\epsilon_i u)} + \sum_{a,i,j}^{j\neq a}\frac{2I_{aiij}(\omega)\left[I_{hjha}(0)-I_{hjah}(\Delta_{ha})\right]}{(\epsilon_a-\omega-\epsilon_i u)(\epsilon_a-\epsilon_j)} \\ &+ \sum_{a,i,a_1}\frac{I_{aiia_1}(\omega)I'_{ha_1ah}(\Delta_{ha})}{(\epsilon_a-\omega-\epsilon_i u)} - \sum_{a,i,h_1}\frac{I_{hiih_1}(\omega)\left[I_{h_1aha}(0)-I_{h_1aah}(\Delta_{ha})\right]}{(\epsilon_h-\omega-\epsilon_i u)^2} \\ &- \sum_{a,i,a_1}\frac{I_{aiia_1}(\omega)\left[I_{ha_1ha}(0)-I_{ha_1ah}(\Delta_{ha})\right]}{(\epsilon_a-\omega-\epsilon_i u)^2}\Bigg\},\end{aligned} \tag{3.111}$$

where the third sum and second term of the fifth sum in Eq. (3.102), the first and third sums in Eq. (3.103), as well as the first, second, fourth and fifth sums in Eq. (3.105) are added together. The vacuum-polarization wave function part reads,

$$\begin{aligned}\Delta E_h^{(2S)\mathrm{VP,wf}} = \frac{i}{2\pi}\int d\omega \Bigg\{ &\sum_{a,i,j}^{i\neq h}\frac{2\left[I_{haia}(0)-I_{haai}(\Delta_{ha})\right]I_{ijhj}(0)}{(\epsilon_h-\epsilon_i)(\omega-\epsilon_j u)} - \sum_{a,h_1,j}\frac{I'_{haah_1}(\Delta_{ha})I_{h_1jhj}(0)}{(\omega-\epsilon_j u)} \\ &+ \sum_{a,i,j}^{i\neq a}\frac{2\left[I_{hahi}(0)-I_{haih}(\Delta_{ha})\right]I_{ijaj}(0)}{(\epsilon_a-\epsilon_i)(\omega-\epsilon_j u)} + \sum_{a,a_1,j}\frac{I'_{haa_1h}(\Delta_{ha})I_{a_1jaj}(0)}{(\omega-\epsilon_j u)}\Bigg\},\end{aligned} \tag{3.112}$$

which comes from Eq. (3.100), the first sum in Eq. (3.101), and the first and second sums as well as the first term in fifth sum and the sixth sum in Eq. (3.102). For the vacuum-polarization

internal-loop term one obtains,

$$\Delta E_h^{(2S)\mathrm{VP,int}} = \frac{i}{2\pi}\int d\omega \sum_{a,i,j}\left[\frac{I_{hihj}(0)I_{jaia}(0)}{(\omega-\epsilon_i u)(\omega-\epsilon_j u)} - \frac{I_{hjai}(\Delta_{ha})I_{aihj}(\Delta_{ha})}{(\omega-\epsilon_i u)(\omega-\Delta_{ha}-\epsilon_j u)}\right] \tag{3.113}$$

by adding the second sum in Eq. (3.101) and Eq. (3.104). Finally, the counterpotential term reads,

$$\begin{aligned}\Delta E_h^{(2S)\mathrm{CP}} = \frac{i}{2\pi}\int d\omega \Bigg\{ &\sum_{a,i,j}\left[\frac{I_{hjih}(\omega)U_{ij}}{(\epsilon_h-\omega-\epsilon_i u)(\epsilon_h-\omega-\epsilon_j u)} - \frac{I_{hjhi}(0)U_{ij}}{(\omega-\epsilon_i u)(\omega-\epsilon_j u)}\right] \\ &+ \sum_{a,i,j}^{i\neq h}\left[\frac{2U_{hi}I_{ijjh}(\omega)}{(\epsilon_h-\epsilon_i)(\epsilon_h-\omega-\epsilon_j u)} - \frac{2U_{hi}I_{ijhj}(0)}{(\epsilon_h-\epsilon_i)(\omega-\epsilon_j u)}\right] \\ &- \sum_{a,h_1,j}\frac{U_{hh_1}I_{h_1jjh}(\omega)}{(\epsilon_h-\omega-\epsilon_j u)^2}\Bigg\}\,,\end{aligned} \tag{3.114}$$

found as the sums of Eqs. (3.106) and (3.107). The expressions above provide all contributions to the screened self-energy and screened vacuum-polarization. Both type of screened corrections should be renormalized; the reader is referred to Ref. [55] and references therein for more details. Here, one notes that the screened self-energy formulas perfectly agree with the ones of Ref. [55], where they were obtained by considering the diagrams depicted in Fig. 3.4 directly.

3.4. Discussion

The redefined vacuum state approach within BSQED was presented in details and applied to the derivation of the one- and two-photon-exchange corrections for atoms with a single-valence electron over closed shells. The general formulas for the two-photon-exchange correction are presented. The employment of the redefined vacuum state approach allows to identify GI subsets at two- and three-electron diagrams and to separate between the direct and exchange parts at two-electron graphs. Such separation was observed numerically in Ref. [72]. The redefined vacuum state formalism has furnished the explanation for this GI separation; they originate from different one-particle two-loop Feynman diagrams. In total, eight GI subsets were identified in the case of the original Furry picture. In the case of the screening potential involved, an additional three subsets are originated from the counterpotential diagrams. The gauge invariance of the identified subsets is verified analytically for three-electron contribution

and numerically for all of the subsets on the example of Li-like ions. The possibility of checking the gauge invariance allows to control the correctness of the derived expressions and verify the numerical calculations by comparing the results for each identified subset in different gauges.

As a second example, the method is applied to atoms with a single-hole electronic configuration, which occurs in halogen atoms such as fluorine, chlorine, etc. The particular interest in this system is twofold. First, in Refs. [54–56] it was demonstrated that highly accurate theoretical predictions are possible in such atoms, and thus accurate tests of the QED effects become feasible. The reason for this is a drastic reduction of the correlations due to Layzer quenching effects [122]. Second, recent measurements of the fine-structure splitting in fluorine-like systems [51, 52] emphasize the necessity of improvement in theoretical predictions for such systems. The accuracy of experimental results is at least of the same order as that of the theoretical predictions, while for some ions it is an order of magnitude better. Moreover, an improvement in the experimental precision is foreseen in the near future [51]. The formulas for the QED corrections up to second order in α for the single-hole configuration have been derived. The screened radiative and two-photon-exchange corrections have been carefully extracted from the rigorous formulas obtained within the redefined vacuum state formalism. In the extended Furry picture, eight different GI subsets have been identified in the screened-radiative corrections, based on the corresponding subsets of one-particle diagrams. It highlights the advantage of the employed formalism. The two-photon-exchange corrections have been checked, by the comparison of the Breit approximation applied to the derived expression, with the RMBPT expressions previously obtained.

CHAPTER 4.

VALENCE-HOLE EXCITATION IN CLOSED-SHELL SYSTEMS

So far the TTFG method was applied to electronic structures generalised to either N-valence-electrons or N-hole states. Thus, the situation when both valence electrons and holes are involved in the description of a state has not been considered yet within the vacuum state redefinition method. The aim of this chapter is to provide a rigorous *ab initio* derivation of the BSQED perturbation theory for a valence-hole excitation in a closed shell system with the redefined vacuum state approach. It is shown that with the appropriate initial equal-time-choice conditions a Green's function with the proper two-body state normalization in the non-interacting field limit can be constructed. Its spectral representation identifies poles at the valence-hole excitation energies and the integral formula for the energy shift to the binding energy is obtained. The latter expression is expanded to the first order, where one-particle radiative and one-photon-exchange corrections are explicitly derived. Reduction to the standard vacuum electron propagator is shown, which agrees in the Breit approximation with the RMBPT expressions for the valence-hole excitation energy.

The material presented in the chapter is based on the reference:

QED approach to valence-hole excitation in closed-shell systems [123]
R. N. Soguel, A. V. Volotka and S. Fritzsche
Phys. Rev. A **106**, 012802 (2022)

4.1. Devise the valence-hole two-time Green's function

Let us derive the Green's function describing the valence-hole excitation in a closed shell system and show that its spectral representation indeed has poles at valence-hole excitation energies. To begin, consider the general four-point Green's function [$N = 2$, Eq. (3.8)]

$$G(x_1, x_2; y_1, y_2) = \langle \Omega_0 | T \left[\psi_H(x_1) \psi_H(x_2) \bar{\psi}_H(y_2) \bar{\psi}_H(y_1) \right] | \Omega_0 \rangle \,. \tag{4.1}$$

As stated previously, this Green's function contains all the information about the two-particle dynamics in presence of the nuclear Coulomb field. To get the energy levels it is enough to consider a two-time Green's function. In the original work [85], Shabaev proposed considering the following equal-time choices $x_1^0 = x_2^0 = x^0$ and $y_1^0 = y_2^0 = y^0$:

$$\begin{aligned} &G(x^0,\mathbf{x}_1,x^0,\mathbf{x}_2;y^0,\mathbf{y}_1,y^0,\mathbf{y}_2) \\ &\qquad = \langle\Omega_0|T\left[\psi_H(x^0,\mathbf{x}_1)\psi_H(x^0,\mathbf{x}_2)\bar{\psi}_H(y^0,\mathbf{y}_2)\bar{\psi}_H(y^0,\mathbf{y}_1)\right]|\Omega_0\rangle\,. \end{aligned} \tag{4.2}$$

However, the spectral representation of the Green's function for this particular choice of times unambiguously reveals poles only for pure electron (charge 2e) or positron (charge -2e) states[1]. This is a clear message that such an equal-time Green's function cannot deal with valence-hole excitation. Thus, one has to come up with a different Green's function to describe such a system. Notice that although the choice of times was motivated and justified *a posteriori* when the spectral representation is derived, it is nevertheless an arbitrary choice. *A priori* one can also choose to have equal times such as $x_1^0 = y_1^0 = x^0$ and $x_2^0 = y_2^0 = y^0$; then the resulting Green's function reads

$$\begin{aligned} &G(x^0,\mathbf{x}_1,y^0,\mathbf{x}_2;x^0,\mathbf{y}_1,y^0,\mathbf{y}_2) \\ &\qquad = \langle\Omega_0|T\left[\psi_H(x^0,\mathbf{x}_1)\psi_H(y^0,\mathbf{x}_2)\bar{\psi}_H(y^0,\mathbf{y}_2)\bar{\psi}_H(x^0,\mathbf{y}_1)\right]|\Omega_0\rangle\,. \end{aligned} \tag{4.3}$$

Similar Green's functions were studied previously by Logunov and Tavkhelidze [23], Fetter and Walecka [124], Oddershede and Jörgensen [125] and Liegener [126]. The subscript $_H$ denoting the Heisenberg representation is dropped in the rest of the chapter. In order to achieve the desired structure and for normalization reasons, as can be seen in Appendix A.5, one has to take into account three extra terms. One might argue that other structures are possible; by virtue of Ockham's razor the one proposed here is, to our view, the simplest one. Hence, the Green's function one has to consider takes the following form in the redefined vacuum state:

$$\begin{aligned} G_\alpha(x^0,\mathbf{x}_1,y^0,\mathbf{x}_2;x^0,\mathbf{y}_1,y^0,\mathbf{y}_2) = \langle\Omega_\alpha|T\Big[&\psi_\alpha(x^0,\mathbf{x}_1)\psi_\alpha(y^0,\mathbf{x}_2)\bar{\psi}_\alpha(y^0,\mathbf{y}_2)\bar{\psi}_\alpha(x^0,\mathbf{y}_1) \\ &- \psi_\alpha(x^0,\mathbf{x}_2)\psi_\alpha(y^0,\mathbf{x}_1)\bar{\psi}_\alpha(y^0,\mathbf{y}_2)\bar{\psi}_\alpha(x^0,\mathbf{y}_1) \\ &- \psi_\alpha(x^0,\mathbf{x}_1)\psi_\alpha(y^0,\mathbf{x}_2)\bar{\psi}_\alpha(y^0,\mathbf{y}_1)\bar{\psi}_\alpha(x^0,\mathbf{y}_2) \\ &+ \psi_\alpha(x^0,\mathbf{x}_2)\psi_\alpha(y^0,\mathbf{x}_1)\bar{\psi}_\alpha(y^0,\mathbf{y}_1)\bar{\psi}_\alpha(x^0,\mathbf{y}_2)\Big]|\Omega_\alpha\rangle\,. \end{aligned} \tag{4.4}$$

[1] See Eq. (3.18) and analysis below.

To demonstrate that this Green's function has the expected pole structure, one has to consider its spectral representation, which is obtained by taking the Fourier transform of the Green's function. For the sake of clarity, the steps that need to be performed are briefly described. The first one is to rearrange the Dirac spinors to get identical times close to each other, keeping in mind that for equal time the only non-zero anti-commutator is $\{\psi_\alpha(x^0,\mathbf{x}),\psi^\dagger_\alpha(x^0,\mathbf{y})\}=\delta^{(3)}(\mathbf{x}-\mathbf{y})$. The next step is to proceed with the time ordering. Once that is done, a completeness relation, $\mathbb{1}=\sum_{\mathcal{N}}|\Omega_{\mathcal{N}}\rangle\langle\Omega_{\mathcal{N}}|$, is inserted to separate terms with different times within the time-ordered product. Then, the Heisenberg's time translation rule for the field operator is used (3.16) and the integral representation of the Heaviside function (2.31) is applied. One ends up with

$$\begin{aligned}
&\mathcal{G}_\alpha(E;\mathbf{x}_1,\mathbf{x}_2;\mathbf{y}_1,\mathbf{y}_2)\delta(E-E') \\
&\qquad=\frac{1}{2\pi i}\frac{1}{2!}\int dx^0dy^0e^{iEx^0-iE'y^0}G_\alpha(x^0,\mathbf{x}_1,y^0,\mathbf{x}_2;x^0,\mathbf{y}_1,y^0,\mathbf{y}_2) \\
&\qquad=\frac{1}{4\pi^2}\frac{1}{2!}\int dx^0dy^0e^{iEx^0-iE'y^0}\int d\omega e^{-i\omega(x^0-y^0)} \\
&\qquad\quad\times\left\{\sum_{\mathcal{N}}\frac{\mathcal{A}(\mathbf{x}_1,\mathbf{x}_2;\mathbf{y}_1,\mathbf{y}_2)}{\omega-E_{\mathcal{N}}+i\varepsilon}-\sum_{\mathcal{N}}\frac{\mathcal{B}(\mathbf{x}_1,\mathbf{x}_2;\mathbf{y}_1,\mathbf{y}_2)}{\omega+E_{\mathcal{N}}-i\varepsilon}\right\} \\
&\qquad=\frac{\delta(E-E')}{2!}\left\{\sum_{\mathcal{N}}\frac{\mathcal{A}(\mathbf{x}_1,\mathbf{x}_2;\mathbf{y}_1,\mathbf{y}_2)}{E-E_{\mathcal{N}}+i\varepsilon}-\sum_{\mathcal{N}}\frac{\mathcal{B}(\mathbf{x}_1,\mathbf{x}_2;\mathbf{y}_1,\mathbf{y}_2)}{E+E_{\mathcal{N}}-i\varepsilon}\right\}, \qquad (4.5)
\end{aligned}$$

where the $\mathcal{A}$ term is given by

$$\begin{aligned}
\mathcal{A}(\mathbf{x}_1,\mathbf{x}_2;\mathbf{y}_1,\mathbf{y}_2)=\langle\Omega_\alpha|\,[&\psi_\alpha(0,\mathbf{x}_1)\bar\psi_\alpha(0,\mathbf{y}_1)|\Omega_{\mathcal{N}}\rangle\langle\Omega_{\mathcal{N}}|\psi_\alpha(0,\mathbf{x}_2)\bar\psi_\alpha(0,\mathbf{y}_2) \\
&-\psi_\alpha(0,\mathbf{x}_2)\bar\psi_\alpha(0,\mathbf{y}_1)|\Omega_{\mathcal{N}}\rangle\langle\Omega_{\mathcal{N}}|\psi_\alpha(0,\mathbf{x}_1)\bar\psi_\alpha(0,\mathbf{y}_2) \\
&-\psi_\alpha(0,\mathbf{x}_1)\bar\psi_\alpha(0,\mathbf{y}_2)|\Omega_{\mathcal{N}}\rangle\langle\Omega_{\mathcal{N}}|\psi_\alpha(0,\mathbf{x}_2)\bar\psi_\alpha(0,\mathbf{y}_1) \\
&+\psi_\alpha(0,\mathbf{x}_2)\bar\psi_\alpha(0,\mathbf{y}_2)|\Omega_{\mathcal{N}}\rangle\langle\Omega_{\mathcal{N}}|\psi_\alpha(0,\mathbf{x}_1)\bar\psi_\alpha(0,\mathbf{y}_1)]\,|\Omega_\alpha\rangle\,, \qquad (4.6)
\end{aligned}$$

and the $\mathcal{B}$ one is

$$\begin{aligned}
\mathcal{B}(\mathbf{x}_1,\mathbf{x}_2;\mathbf{y}_1,\mathbf{y}_2)=\langle\Omega_\alpha|\,[&\psi_\alpha(0,\mathbf{x}_2)\bar\psi_\alpha(0,\mathbf{y}_2)|\Omega_{\mathcal{N}}\rangle\langle\Omega_{\mathcal{N}}|\psi_\alpha(0,\mathbf{x}_1)\bar\psi_\alpha(0,\mathbf{y}_1) \\
&-\psi_\alpha(0,\mathbf{x}_1)\bar\psi_\alpha(0,\mathbf{y}_2)|\Omega_{\mathcal{N}}\rangle\langle\Omega_{\mathcal{N}}|\psi_\alpha(0,\mathbf{x}_2)\bar\psi_\alpha(0,\mathbf{y}_1) \\
&-\psi_\alpha(0,\mathbf{x}_2)\bar\psi_\alpha(0,\mathbf{y}_1)|\Omega_{\mathcal{N}}\rangle\langle\Omega_{\mathcal{N}}|\psi_\alpha(0,\mathbf{x}_1)\bar\psi_\alpha(0,\mathbf{y}_2) \\
&+\psi_\alpha(0,\mathbf{x}_1)\bar\psi_\alpha(0,\mathbf{y}_1)|\Omega_{\mathcal{N}}\rangle\langle\Omega_{\mathcal{N}}|\psi_\alpha(0,\mathbf{x}_2)\bar\psi_\alpha(0,\mathbf{y}_2)]\,|\Omega_\alpha\rangle\,. \qquad (4.7)
\end{aligned}$$

As previously, the summations run over all bound and continuum states of the interacting fields' system. Thus, the spectral representation of expression (4.4) was derived. Under the assumption

of non-interacting electron-positron fields and their expansion in creation and annihilation operators, as in Eq. (2.48), the only consistent zeroth-order $|0_{\mathcal{N}}\rangle$ states are found to be

$$|0_{\mathcal{N}}\rangle = \left\{ |vh\rangle = a_v^\dagger b_h^\dagger |\alpha\rangle,\ |\alpha\rangle \right\} . \tag{4.8}$$

Now that the Green's function spectral representation is obtained as a function of E, one can define its analytic continuation in the complex E plane. Some remarks are important here. First, although Eq. (4.5) looks similar to the one obtained in Eq. (3.18), it has poles at essentially different energies. In analogy to the discussion held in Chapter 3.1, the poles at the valence-hole excitation energies are located below the right-hand real axis for the former term and above the left-hand real axis for the latter one. Second, despite the structure of $\mathcal{A}$ and $\mathcal{B}$ looks complicated, in the non-interacting case it contains neutral charged states corresponding to valence-hole excitations of a closed shell. Hence, the analytical continuation of the Green's function has cuts $(-\infty, -E^{(0)}_{\rm min}]$ and $[E^{(0)}_{\rm min}, +\infty)$, where $E^{(0)}_{\rm min}$ is the minimal energy of the states with zero total electric charge, and one sees the presence of poles at the valence-hole excitation energies E_{vh} and $-E_{vh}$ as well as at the zero (vacuum energy). Third and most important, it leads to normalized two-particle wave functions in the zeroth order, as can be seen in appendix A.5. A coordinate integrated Green's function is built out of spectral representation of the Green's function, as in Eq. (3.13),

$$\begin{aligned} g_\alpha(E) = \frac{1}{2!} \int & d^3x_1 d^3x_2 d^3y_1 d^3y_2 \\ & \times :\psi^{(0)\dagger}_\alpha(\mathbf{x}_1)\psi^{(0)\dagger}_\alpha(\mathbf{x}_2)\mathcal{G}_\alpha(E;\mathbf{x}_1,\mathbf{x}_2;\mathbf{y}_1,\mathbf{y}_2)\gamma_1^0\gamma_2^0\psi^{(0)}_\alpha(\mathbf{y}_2)\psi^{(0)}_\alpha(\mathbf{y}_1): . \end{aligned} \tag{4.9}$$

Accordingly to the two-particle cases treated in Section 3.1 [Eqs. (3.35, 3.48)], one employs the occupation number representation as in the RMBPT description provided by Lindgren [127] to construct the two-particle operator. Since the interest lies in the valence-hole state described by [100, 101]

$$|(vh)_{JM}\rangle = \sum_{m_v, m_h} \langle j_v m_v j_h - m_h | JM\rangle (-1)^{j_h - m_h} a_v^\dagger b_h^\dagger |\alpha\rangle \equiv F_{vh} a_v^\dagger b_h^\dagger |\alpha\rangle , \tag{4.10}$$

where the jj-coupling scheme is applied to form a state with total angular momentum J and its projection M, one works out and retains only the six terms involving two a and two b operators.

After normal ordering one arrives to the expression

$$
\begin{aligned}
g_\alpha(E) \cong & \left\{ \sum_{\epsilon_i,\epsilon_j>E_\alpha^F,\epsilon_k,\epsilon_l<E_\alpha^F} a_i^\dagger a_j^\dagger b_l^\dagger b_k^\dagger - \sum_{\epsilon_k,\epsilon_l>E_\alpha^F,\epsilon_i,\epsilon_j<E_\alpha^F} a_k a_l b_i b_j + \sum_{\epsilon_i,\epsilon_l>E_\alpha^F,\epsilon_j,\epsilon_k<E_\alpha^F} a_i^\dagger a_l b_k^\dagger b_j \right. \\
& \left. + \sum_{\epsilon_j,\epsilon_k>E_\alpha^F,\epsilon_i,\epsilon_l<E_\alpha^F} a_j^\dagger a_k b_l^\dagger b_i - \sum_{\epsilon_i,\epsilon_k>E_\alpha^F,\epsilon_j,\epsilon_l<E_\alpha^F} a_i^\dagger a_k b_l^\dagger b_j - \sum_{\epsilon_j,\epsilon_l>E_\alpha^F,i,k<E_\alpha^F} a_j^\dagger a_l b_k^\dagger b_i \right\} \\
& \times \frac{1}{2!} g_{\alpha,ijkl}(E)\,,
\end{aligned}
\tag{4.11}
$$

with

$$
\begin{aligned}
g_{\alpha,ijkl}(E) = & \int d^3x_1 d^3x_2 d^3y_1 d^3y_2 \\
& \times \phi_i^\dagger(\mathbf{x}_1)\phi_j^\dagger(\mathbf{x}_2)\mathcal{G}_\alpha(E;\mathbf{x}_1,\mathbf{x}_2;\mathbf{y}_1,\mathbf{y}_2)\gamma_1^0\gamma_2^0\phi_k(\mathbf{y}_1)\phi_l(\mathbf{y}_2)\,.
\end{aligned}
\tag{4.12}
$$

Further, one has to evaluate the matrix element of $g_\alpha(E)$ with the valence-hole state defined by Eq. (4.10). The first two terms in Eq. (4.11) do not contribute as they cannot be fully contracted with the valence-hole state. Computing the matrix element, one gets

$$
\langle (vh)_{JM}|g_\alpha(E)|(vh)_{JM}\rangle = F_{v_1h_1}F_{v_2h_2}\left[g_{\alpha,v_1h_2h_1v_2}(E) - g_{\alpha,v_1h_2v_2h_1}(E)\right]\,. \tag{4.13}
$$

Note that whereas in the two-valence case [Eq. (3.37)] and two-hole case [Eq. (3.49)], the matrix elements read "direct - exchange" part, the above expression is "exchange - direct" part. Now all the necessary pieces are available to derive the formula for the energy shift to the valence-hole binding energy. Applying the integral formalism introduced in Section 3.1 and focusing only on the first term with the integral contour Γ_{vh} surrounding anticlockwise only the pole $E \sim E_{vh}^{(0)}$,

$$
E_{vh}^{(0)} = \langle vh|H_0|vh\rangle = \epsilon_v - \epsilon_h\,, \tag{4.14}
$$

while all others singularities are kept outside, one ends up to the expression

$$
E_{vh} = \frac{\frac{1}{2\pi i}\oint_{\Gamma_{vh}} dE\, E\langle (vh)_{JM}|g_\alpha(E)|(vh)_{JM}\rangle}{\frac{1}{2\pi i}\oint_{\Gamma_{vh}} dE\,\langle (vh)_{JM}|g_\alpha(E)|(vh)_{JM}\rangle}\,. \tag{4.15}
$$

Evaluating the zeroth-order Green's function

$$\langle (vh)_{JM}|g_\alpha^{(0)}(E)|(vh)_{JM}\rangle = \frac{1}{E - E_{vh}^{(0)}} \tag{4.16}$$

(the detailed calculation is presented in appendix A.5), the cornerstone expression for the energy shift $\Delta E_{vh} = E_{vh} - E_{vh}^{(0)}$ is derived:

$$\Delta E_{vh} = \frac{\frac{1}{2\pi i}\oint_{\Gamma_{vh}} dE \left(E - E_{vh}^{(0)}\right) \langle (vh)_{JM}|\Delta g_\alpha(E)|(vh)_{JM}\rangle}{1 + \frac{1}{2\pi i}\oint_{\Gamma_{vh}} dE \, \langle (vh)_{JM}|\Delta g_\alpha(E)|(vh)_{JM}\rangle}, \tag{4.17}$$

where $\Delta g_\alpha(E) = g_\alpha(E) - g_\alpha^{(0)}(E)$. A similar equation to Eq. (3.11) exists for the valence-hole excitation case. Taylor expanding its exponential into a series in the fine-structure constant α leads to the perturbative expansion, $\Delta g_\alpha(E) = \Delta g_\alpha^{(1)}(E) + \Delta g_\alpha^{(2)}(E) + ...$, and combining the terms of the same order, one easily obtains the BSQED perturbation expansion for the valence-hole energy shift $\Delta E_{vh} = \Delta E_{vh}^{(1)} + \Delta E_{vh}^{(2)} + ...$ Thus, in this section the TTGF suited for the treatment of valence-hole states is obtained and the cornerstone expression for the energy shift to the binding energy, as contour integrals of the Green's function, is derived. In the next section, the formalism is applied to evaluate the first-order correction to the energy of the valence-hole excitation.

4.2. First-order shift to valence-hole binding energy

The first-order energy correction, obtained from the expansion of Eq. (4.17), yields

$$\Delta E_{vh}^{(1)} = \frac{1}{2\pi i} F_{v_1 h_1} F_{v_2 h_2} \oint_{\Gamma_{vh}} dE \left(E - E_{vh}^{(0)}\right) \left[\Delta g^{(1)}_{\alpha, v_1 h_2 h_1 v_2}(E) - \Delta g^{(1)}_{\alpha, v_1 h_2 v_2 h_1}(E)\right] . \tag{4.18}$$

The energy correction can be split into one-particle ($\Delta E_{vh}^{(1)1}$) and two-particle ($\Delta E_{vh}^{(1)2}$) terms:

$$\Delta E_{vh}^{(1)} = \Delta E_{vh}^{(1)1} + \Delta E_{vh}^{(1)2} . \tag{4.19}$$

In turn, the one-particle contribution originates from three Feynman diagrams: self-energy, vacuum-polarization, and counterpotential, which are depicted in Fig. 3.1 and give rise to the

following terms in the Green's function:

$$\Delta g_\alpha^{(1)1}(E) = \Delta g_\alpha^{(1)\mathrm{SE}}(E) + \Delta g_\alpha^{(1)\mathrm{VP}}(E) + \Delta g_\alpha^{(1)\mathrm{CP}}(E)\,. \tag{4.20}$$

The two-particle contribution corresponds to the Green's function $\Delta g_\alpha^{(1)2}$ and the valence-hole one-photon exchange diagram presented in Fig. 4.1. The one-particle diagrams are considered first.

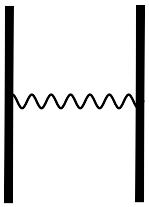

Figure 4.1.: Valence-hole one-photon-exchange Feynman diagram. Notations are the same as in Fig. 2.3.

4.2.1. One-particle contributions

Formally, for single particle graphs, SE, VP or CP, a second disconnected line (propagator) is present. However, these diagrams reduce to the single-particle case since the disconnected line can be integrated out, as it will be shown below. In what follows the SE correction is considered in details, which can be further divided into two terms, one in which the SE loop is located on the valence electron line $\Delta g_\alpha^{(1)\mathrm{SE}v}$ and one in which it is located on the hole line $\Delta g_\alpha^{(1)\mathrm{SE}h}$. Let us consider the valence SE graph with disconnected hole line first. The Feynman rules, according to Ref. [85] but noting that *hole's energy formally flows in the negative x^0 direction while being a positive quantity*, provides the following expression:

$$\begin{aligned}
\Delta g^{(1)\mathrm{SE}v}_{\alpha,v_1h_2v_2h_1}(E)\delta(E-E') &= e^2\left(\frac{i}{2\pi}\right)^2\int d^3x d^3y dp_1^0 dp_2^0 d\omega dk^0 \\
&\times \delta(E-p_1^0+p_2^0)\delta(E'-p_1^0+p_2^0)\delta(p_1^0-\omega-k^0) \\
\times \frac{\bar\psi_{v_1}(\mathbf{y})}{p_1^0-\epsilon_v+i\varepsilon}\gamma^\mu\sum_j\frac{\psi_j(\mathbf{y})\bar\psi_j(\mathbf{x})}{k^0-\epsilon_j+i\varepsilon(\epsilon_j-E_\alpha^F)}D_{\mu\nu}(\omega,\mathbf{y}-\mathbf{x})\gamma^\nu\frac{\psi_{v_2}(\mathbf{x})}{p_1^0-\epsilon_v+i\varepsilon}\frac{\delta_{h_1h_2}}{p_2^0-\epsilon_h-i\varepsilon} \\
= \left(\frac{i}{2\pi}\right)^2\int dp_1^0 d\omega\sum_j\frac{I_{v_1jjv_2}(\omega)}{p_1^0-\omega-\epsilon_j+i\varepsilon(\epsilon_j-E_\alpha^F)}\frac{\delta(E-E')}{\left[p_1^0-\epsilon_v+i\varepsilon\right]^2}\frac{\delta_{h_1h_2}}{p_1^0-E-\epsilon_h-i\varepsilon}\,,
\end{aligned} \tag{4.21}$$

where two momentum integrations have been carried out with the help of δ-functions and further simplified due to the orthogonality of the wave functions. One should highlight the fact that p_2^0 and $p_2'^0$ *are the hole's energy in all calculations and that the* δ*- functions taking care of the energy conservation of initial and final states are affected*, as can be expected from Eq. (4.14). Notice also that the zeroth-order energy of each particle does not depend on its spin projection, i.e., $\epsilon_{v_1} = \epsilon_{v_2} = \epsilon_v$, $\epsilon_{h_1} = \epsilon_{h_2} = \epsilon_h$. Since the integration over energy E is the next step, the singularities in $E - E_{vh}^{(0)}$ should be analyzed. Notice that

$$\begin{aligned}\frac{1}{\left[p_1^0 - \epsilon_v + i\varepsilon\right]^2}\frac{1}{p_1^0 - E - \epsilon_h - i\varepsilon} &= \frac{1}{(E - E_{vh}^{(0)})^2}\left[\frac{1}{p_1^0 - E - \epsilon_h - i\varepsilon} - \frac{1}{p_1^0 - \epsilon_v + i\varepsilon}\right] \\ &\quad - \frac{1}{E - E_{vh}^{(0)}}\frac{1}{\left[p_1^0 - \epsilon_v + i\varepsilon\right]^2}\,. \end{aligned} \tag{4.22}$$

Only the most singular part is to retain to access the irreducible contribution[2]. It leads to

$$\begin{aligned}\Delta E_{vh}^{(1)\mathrm{SE}v} &= -\frac{1}{2\pi i}F_{v_1h_1}F_{v_2h_2}\oint_{\Gamma_{vh}} dE(E - E_{vh}^{(0)})\Delta g_{\alpha,v_1h_2v_2h_1}^{(1)\mathrm{SE}v}(E) \\ &= \frac{i}{2\pi}F_{v_1h_1}F_{v_2h_2}\int d\omega \sum_j \frac{I_{v_1jjv_2}(\omega)\delta_{h_1h_2}}{\epsilon_v - \omega - \epsilon_j + i\varepsilon(\epsilon_j - E_\alpha^F)} \\ &\equiv F_{v_1h_1}F_{v_2h_2}\delta_{h_1h_2}\langle v_1|\Sigma_\alpha(\epsilon_v)|v_2\rangle\,, \end{aligned} \tag{4.23}$$

and the identity

$$\delta(x) = \frac{i}{2\pi}\left(\frac{1}{x + i\varepsilon} + \frac{1}{-x + i\varepsilon}\right) \tag{4.24}$$

was utilized. Since the investigated graph is the SE matrix element for a single valence electron, there is no need to distinguish between the initial state v_1 and the final state v_2 because the SE operator preserves the spin projection, which was the sole difference between them. Hence, one can write $\delta_{v_1v_2}$, and the previous prefactor is then $F_{v_1h_1}F_{v_2h_2}\delta_{v_1v_2}\delta_{h_1h_2} = 1$ [100]. The same calculation is performed for the SE graph located on the hole line, and the electron line is

[2]Reducible contributions give rise to higher-order poles, hence, derivative terms of the evaluated expressions, especially for high-order diagrams.

integrated out this time:

$$\Delta g^{(1)\mathrm{SE}h}_{\alpha,v_1h_2v_2h_1}(E) = \left(\frac{i}{2\pi}\right)^2 \int dp_2^0 d\omega \sum_j \frac{I_{h_2jjh_1}(\omega)}{p_2^0 - \omega - \epsilon_j + i\varepsilon(\epsilon_j - E_\alpha^F)} \frac{1}{\left[p_2^0 - \epsilon_h - i\varepsilon\right]^2} \times \frac{\delta_{v_1v_2}}{E + p_2^0 - \epsilon_v + i\varepsilon}\,. \tag{4.25}$$

As previously, one isolates the most singular part to get

$$\begin{aligned}
\Delta E^{(1)\mathrm{SE}h}_{vh} &= -\frac{1}{2\pi i} F_{v_1h_1}F_{v_2h_2} \oint_{\Gamma_{vh}} dE (E - E^{(0)}_{vh}) \Delta g^{(1)\mathrm{SE}h}_{\alpha,v_1h_2v_2h_1}(E) \\
&= -\frac{i}{2\pi} F_{v_1h_1}F_{v_2h_2} \int d\omega \sum_j \frac{I_{h_2jjh_1}(\omega)\delta_{v_1v_2}}{\epsilon_{h_1} - \omega - \epsilon_j + i\varepsilon(\epsilon_j - E_\alpha^F)} \\
&\equiv -F_{v_1h_1}F_{v_2h_2}\delta_{v_1v_2}\langle h_2|\Sigma_\alpha(\epsilon_h)|h_1\rangle\,.
\end{aligned} \tag{4.26}$$

As before, the SE contribution to a single hole state is considered, thus $\delta_{h_1h_2}$ and the prefactor reduces to 1. The one-particle result is recovered in both cases. Such calculations can be extended to the VP graph under the modification $\langle v_1|\Sigma_\alpha(\epsilon_v)|v_2\rangle$ to

$$\begin{aligned}
\langle v_1|\mathrm{Y}_\alpha|v_2\rangle &= -\frac{ie^2}{2\pi} \int d^3x d^3y \psi^\dagger_{v_1}(\mathbf{y}) \alpha^\mu D_{\mu\nu}(0, \mathbf{y} - \mathbf{x}) \\
&\quad \times \int d\omega \mathrm{Tr}\left[\sum_j \frac{\psi_j(\mathbf{x})\psi_j^\dagger(\mathbf{x})}{\omega - \epsilon_j + i\varepsilon(\epsilon_j - E_\alpha^F)} \alpha^\nu\right] \psi_{v_2}(\mathbf{y}) \\
&\equiv -\frac{i}{2\pi} \int d\omega \sum_j \frac{I_{v_1jv_2j}(0)}{\omega - \epsilon_j + i\varepsilon(\epsilon_j - E_\alpha^F)}
\end{aligned} \tag{4.27}$$

and accordingly for the hole case: $\langle h_2|\Sigma_\alpha(\epsilon_h)|h_1\rangle$ to $\langle h_2|\mathrm{Y}_\alpha|h_1\rangle$. Hence, the one-particle graph contributions in the redefined vacuum state framework are given by[3]

$$\begin{aligned}
\Delta E^{(1)1}_{vh} &= F_{v_1h_1}F_{v_2h_2}\delta_{v_1v_2}\delta_{h_1h_2}\Big[\langle v_1|\Sigma_\alpha(\epsilon_v)|v_2\rangle + \langle v_1|\mathrm{Y}_\alpha|v_2\rangle - U_{v_1v_2} \\
&\quad - \langle h_2|\Sigma_\alpha(\epsilon_h)|h_1\rangle - \langle h_2|\mathrm{Y}_\alpha|h_1\rangle + U_{h_2h_1}\Big] \\
&= \langle v|\Sigma_\alpha(\epsilon_v)|v\rangle + \langle v|\mathrm{Y}_\alpha|v\rangle - U_{vv} - \langle h|\Sigma_\alpha(\epsilon_h)|h\rangle - \langle h|\mathrm{Y}_\alpha|h\rangle + U_{hh}\,.
\end{aligned} \tag{4.28}$$

[3]The renormalization procedure for the self-energy and vacuum-polarization loops is found in Appendix A.1, and the renormalized self-energy operator is given in Eq. (3.57).

Two counterpotential terms $U_{ij} = \langle i|U|j\rangle$ are added into the formula above to accommodate for the extended Furry picture. Their treatment is straightforward and does not need to be given in details.

4.2.2. Two-particle contributions

The only two-particle correction found at this order is the valence-hole one-photon-exchange, with exchange part $\Delta E_{vh}^{(1)2\mathrm{exc}}$ minus direct part $\Delta E_{vh}^{(1)2\mathrm{dir}}$ according to Eq. (4.18):

$$\Delta E_{vh}^{(1)2\mathrm{exc}} = \frac{1}{2\pi i} F_{v_1 h_1} F_{v_2 h_2} \oint_{\Gamma_{vh}} dE (E - E_{vh}^{(0)}) \Delta g^{(1)2\mathrm{exc}}_{\alpha, v_1 h_2 h_1 v_2}(E)\,, \tag{4.29}$$

$$\Delta E_{vh}^{(1)2\mathrm{dir}} = -\frac{1}{2\pi i} F_{v_1 h_1} F_{v_2 h_2} \oint_{\Gamma_{vh}} dE (E - E_{vh}^{(0)}) \Delta g^{(1)2\mathrm{dir}}_{\alpha, v_1 h_2 v_2 h_1}(E)\,. \tag{4.30}$$

Let us tackle first the direct graph, keeping in mind that the hole's energies are flowing backward in time. Similar to previous calculations, trivial steps are already performed, and the expression is given by

$$\begin{aligned}
\Delta g^{(1)\mathrm{dir}}_{\alpha, v_1 h_2 v_2 h_1}(E)\delta(E - E') &= e^2 \left(\frac{i}{2\pi}\right)^2 \int d^3x d^3y dp_1^0 dp_1'^0 dp_2^0 dp_2'^0 d\omega \\
&\times \delta(E - p_1^0 + p_2^0)\delta(E' - p_1'^0 + p_2'^0)\delta(p_1^0 - \omega - p_1'^0)\delta(p_2'^0 + \omega - p_2^0) \\
&\times \frac{\bar\psi_{v_1}(\mathbf{x})}{p_1'^0 - \epsilon_v + i\varepsilon} \frac{\bar\psi_{h_2}(\mathbf{y})}{p_2'^0 - \epsilon_h - i\varepsilon} \gamma^\mu \gamma^\nu D_{\mu\nu}(\omega, \mathbf{x} - \mathbf{y}) \frac{\psi_{v_2}(\mathbf{x})}{p_1^0 - \epsilon_v + i\varepsilon} \frac{\psi_{h_1}(\mathbf{y})}{p_2^0 - \epsilon_h - i\varepsilon} \\
= \left(\frac{i}{2\pi}\right)^2 \int dp_2^0 dp_2'^0 &\frac{I_{v_1 h_2 v_2 h_1}(p_2^0 - p_2'^0)}{E + p_2'^0 - \epsilon_v + i\varepsilon} \frac{1}{p_2'^0 - \epsilon_h - i\varepsilon} \frac{\delta(E - E')}{E + p_2^0 - \epsilon_v + i\varepsilon} \frac{1}{p_2^0 - \epsilon_h - i\varepsilon}\,.
\end{aligned} \tag{4.31}$$

Rewriting the denominators to pull out the singular part as

$$\begin{aligned}
\frac{1}{E + p_2'^0 - \epsilon_v + i\varepsilon} \frac{1}{p_2'^0 - \epsilon_h - i\varepsilon} &= \frac{1}{E - E_{vh}^{(0)}} \left(\frac{1}{p_2'^0 - \epsilon_h - i\varepsilon} - \frac{1}{E + p_2'^0 - \epsilon_v + i\varepsilon} \right), \\
\frac{1}{E + p_2^0 - \epsilon_v + i\varepsilon} \frac{1}{p_2^0 - \epsilon_h - i\varepsilon} &= \frac{1}{E - E_{vh}^{(0)}} \left(\frac{1}{p_2^0 - \epsilon_h - i\varepsilon} - \frac{1}{E + p_2^0 - \epsilon_v + i\varepsilon} \right),
\end{aligned} \tag{4.32}$$

one gets to

$$\Delta E^{(1)2\mathrm{dir}}_{vh} = -F_{v_1h_1}F_{v_2h_2}I_{v_1h_2v_2h_1}(0)\,. \tag{4.33}$$

Last, but not least, is the exchange graph . The partially simplified expression is found to be

$$\begin{aligned}\Delta g^{(1)2\mathrm{exc}}_{\alpha,v_1h_2h_1v_2}(E)\delta(E-E') &= e^2\left(\frac{i}{2\pi}\right)^2\int d^3x d^3y dp_1^0 dp_1'^0 dp_2^0 dp_2'^0 d\omega \\ &\times \delta(E-p_1^0+p_2^0)\delta(E'-p_1'^0+p_2'^0)\delta(p_2^0-\omega-p_1'^0)\delta(p_2'^0+\omega-p_1^0) \\ &\times \frac{\bar\psi_{v_1}(\mathbf{x})}{p_1'^0-\epsilon_v+i\varepsilon}\frac{\bar\psi_{h_2}(\mathbf{y})}{p_2'^0-\epsilon_h-i\varepsilon}\gamma^\mu\gamma^\nu D_{\mu\nu}(\omega,\mathbf{x}-\mathbf{y})\frac{\psi_{h_1}(\mathbf{x})}{p_2^0-\epsilon_h-i\varepsilon}\frac{\psi_{v_2}(\mathbf{y})}{p_1^0-\epsilon_v+i\varepsilon} \\ = \left(\frac{i}{2\pi}\right)^2\int dp_1^0 dp_2'^0 &\frac{I_{v_1h_2h_1v_2}(p_2'^0-p_1^0)}{E+p_2'^0-\epsilon_v+i\varepsilon}\frac{1}{p_2'^0-\epsilon_h-i\varepsilon}\frac{\delta(E-E')}{p_1^0-E-\epsilon_h-i\varepsilon}\frac{1}{p_1^0-\epsilon_v+i\varepsilon}\,.\end{aligned} \tag{4.34}$$

As before, the singular part of the denominators are separated. Hence, the energy integration gives

$$\Delta E^{(1)2\mathrm{exc}}_{vh} = F_{v_1h_1}F_{v_2h_2}I_{v_1h_2h_1v_2}(\Delta_{hv})\,, \tag{4.35}$$

and the total two-particle contribution is

$$\Delta E^{(1)2}_{vh} = F_{v_1h_1}F_{v_2h_2}\left[I_{v_1h_2h_1v_2}(\Delta_{hv}) - I_{v_1h_2v_2h_1}(0)\right]\,. \tag{4.36}$$

4.2.3. Standard vacuum description

So far the formulas for the first-order energy corrections obtained in the previous subsections,

$$\begin{aligned}\Delta E^{(1)}_{vh} &= F_{v_1h_1}F_{v_2h_2}\left[I_{v_1h_2h_1v_2}(\Delta_{hv}) - I_{v_1h_2v_2h_1}(0)\right] \\ &+ \langle v|\Sigma_\alpha(\epsilon_v)|v\rangle + \langle v|\Upsilon_\alpha|v\rangle - U_{vv} - \langle h|\Sigma_\alpha(\epsilon_h)|h\rangle - \langle h|\Upsilon_\alpha|h\rangle + U_{hh}\,,\end{aligned} \tag{4.37}$$

have been written for the case when the redefined vacuum state is employed in the electron propagator [see Eq. (2.53)]. In Eq. (4.37) the first term in square brackets corresponds to the interelectronic interaction between valence and hole particles taken with a minus sign; the next two blocks of three terms are the one-particle corrections (self-energy, vacuum-polarization, and counterterm) for the valence and hole particles, respectively. It is clear that excitation of an electron from state h to v leads to the subtraction of an one-electron hole energy and

addition of an one-electron valence energy [See Eq. (4.14)]. The interelectronic interaction between valence (hole) particle with core electrons is not explicitly recognizable in Eq. (4.37). In fact, the SE and VP terms with the redefined vacuum state propagator contain also the interelectronic interaction with the core electrons. The redefined vacuum state expressions are linked to the usual ones for the valence SE and VP contributions. One has the following relationship [Eqs. (3.58, 3.59)]:

$$\langle v|\Sigma_\alpha(\epsilon_v)|v\rangle = \langle v|\Sigma(\epsilon_v)|v\rangle - \sum_a I_{vaav}(\Delta_{va})\,, \tag{4.38}$$

$$\langle v|\mathrm{Y}_\alpha|v\rangle = \langle v|\mathrm{Y}|v\rangle + \sum_a I_{vava}(0)\,, \tag{4.39}$$

where Σ and Y operators differ from the corresponding operators with the subscript α just by setting in Eqs. (4.23) and (4.27) $E^F_\alpha = 0$. In other words, to extract the interelectronic interactions arising from the one-particle graphs in the redefined vacuum state Eq. (4.28), one has to subtract the identical graph in the standard vacuum state, as inferred from the above equations. Obviously, the two-particle contribution (4.36) is not affected by such manipulations. The resulting first-order energy correction in the standard vacuum state can be written as

$$\begin{aligned}\Delta E^{(1)}_{vh} = & \sum_a [I_{vava}(0) - I_{vaav}(\Delta_{va})] - \sum_a [I_{haha}(0) - I_{haah}(\Delta_{ha})] \\ & + F_{v_1h_1}F_{v_2h_2}\left[I_{v_1h_2h_1v_2}(\Delta_{hv}) - I_{v_1h_2v_2h_1}(0)\right] \\ & + \langle v|\Sigma(\epsilon_v)|v\rangle + \langle v|\mathrm{Y}|v\rangle - U_{vv} - \langle h|\Sigma(\epsilon_h)|h\rangle - \langle h|\mathrm{Y}|h\rangle + U_{hh}\,. \end{aligned} \tag{4.40}$$

Now, the interaction between valence and hole particles with core electrons appears in the first line of Eq. (4.40), respectively. Furthermore, the interelectronic interaction obtained [the three terms involving square brackets in Eq. (4.40)] is in perfect agreement, when the Breit approximation [Eqs. (A.14, A.15)] is applied in the Coulomb gauge, with the one found in Ref. [101], where RMBPT corrections to the valence-hole state up to second order were derived. The other contributions (line three) found are the SE and VP corrections to each particle, as expected.

Last, but not least, employing of a vacuum state redefinition allows us to identify GI subsets in the standard vacuum state. Following the logic and proofs presented in Sections 3.2.1 and 3.2.2, the contributions involving square brackets in Eq. (4.40) are independently gauge invariant. Moreover, each term in line three is also separately gauge invariant.

4.3. Discussion

The formalism and expressions presented in this chapter are ready to be applied to a closed-shell atom or ion, such as Be- and Ne-like ions. Be-like ions having the least number of electrons were already treated within the complete BSQED description. In particular, the ground-state and ionization energies were evaluated in Refs. [77, 78], respectively, while the transition energies between low-lying levels were just recently addressed in Ref. [79]. In last case [79], the formal expressions were derived with the TTGF method employing the redefined vacuum state prescription, where the $1s^2$ shell was considered to belong to the vacuum state and the other two electrons were treated as the valence electrons. For Ne-like ions such decomposition is rather complicated since one has to consider eight electrons to be the valence ones.

The energy levels in Ne-like ions have been investigated for a long time within the RMBPT approach [100, 101, 128, 129]. The discrepancies between theory and experiment for different transitions and ions, in absolute value, were less than 2 eV in the earliest work, which shrunk down to less than 1 eV in a more recent one [130]. In the case of Ne-like Ge a recent study [131] reports remarkable agreement up to 10^{-4} relative uncertainty between RMBPT calculations and measured values. The QED effects have been incorporated at the first order via the model Lamb-shift-operator approach [56, 132–134], and the interelectronic interaction has been captured with the Breit interaction treated in the vanishing frequency limit. Results have been compared with previous computations performed by Safronova *et al.* [130] for Ne-like Mo and showed a difference less than 0.25 eV, in absolute value, except for one case. Another recent measurement campaign on Ne-like Eu [135] showed agreement, in absolute value, of the order of 1 eV between RMBPT predictions and experimental values. Overall, these results show that RMBPT treatment reliably captures the essence of the energy difference in Ne-like ions. Nevertheless, a rigorous BSQED treatment of valence-hole excitation in closed-shell system has been lacking so far. BSQED contributions could fill the energy gap by rigorously including all first-order corrections in α. It could help to achieve outstanding agreement among theory and experiment, which could be especially interesting in view of possible applications as optical atomic clocks with valence-hole transitions in B^+, Al^+, In^+, and Tl^+ ions [136], or in Ni^{12+} [137]. An additional application might be seen in searching for an explanation of the disagreement in oscillator-strength ratio in Ne-like Fe [138, 139][4].

[4] At the time when this study was conducted, the Letter [139] was not yet published.

CHAPTER 5.

THREE-PHOTON-EXCHANGE CORRECTIONS FOR SINGLE-VALENCE ELECTRON OVER CLOSED SHELLS

This chapter treats (a partial) third-order interelectronic corrections to a single-valence state [$N = 1$, Eq. (3.14)] over closed-shells. The aim is to demonstrate that it is feasible to assess third-order interelectronic corrections even though such calculations are challenging and especially difficult. To overcome the high likelihood of mistakes occurrence, and as a cross-check of the derived expressions, two different methods are utilised to obtain the results. The first one is an effective one-particle approach, which relies on the redefinition of the vacuum state, and deals with one-particle three-loop diagrams. The idea is to provide a proof-of-principle that third-order interelectronic corrections can be tackled, in the redefined vacuum state framework, owing to the transcription of the one-particle GI subsets to many-electron diagrams. The second one considers a perturbation theory approach to a two-photon-exchange subset, involving a loop contribution, under the regard of a perturbative potential-like interaction. Then, the results are mapped to the three-photon-exchange corrections. In such a way, the formulas are derived independently and the possibly occurring mistakes are minimized as much as possible. The resulting expressions contain infrared divergences. They are inspected, regularized by the introduction of a photon mass term, and it is shown that they are cancelled by terms within the expected-to-be GI subsets.

5.1. Redefined vacuum state approach

The effective one-particle approach, based on a redefinition of the vacuum state, is applied to more involved Feynman diagrams, as a proof-of-principle that advanced calculation can be undertaken in this way. The investigation is carried out for the state given by Eq. (3.32). Its Green's function matrix element is provided in Eq. (3.33), which is inserted into the third-order correction to the energy shift given in Eq. (3.31).

Knowledge gathered from the two-photon-exchange corrections is exploited to select the possible subsets to inspect. Recall that the ladder- and crossed-loop arose from the SESE and S(VP)E subsets[1]. The S(VP)E subset, based on one diagram, generates the direct parts of the two-photon-exchange. Thus, the decision made to pick it out as a starting point. The one-particle three-loop Feynman diagrams, corresponding to all possible insertion of a VP loop[2] in the S(VP)E graph, are given in Figs. 5.1 [S[V(VP)P]E subset] and 5.2 [S(VP)EVP subset]. Note that the inclusion of an extra interelectronic operator, arising from the cut in the inserted VP loop, does not spoil gauge invariance [see Eq. (3.63)]. An important point to highlight is that the ω integration in the VP loop must be symmetrized in the final expressions in order to achieve gauge invariance. It was a crucial step when dealing with the S(VP)E subset [see the footnote in Section 3.2.2]. The equality stated there, and its third-order-pole version, were applied to the derived expressions in order to compare them with those based on the perturbation theory approach.

S[V(VP)P]E subset

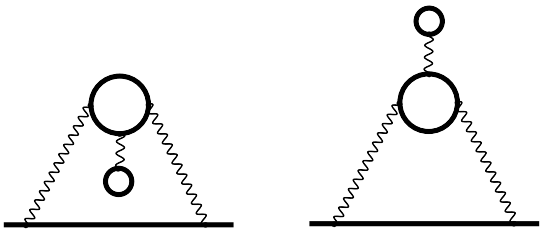

Figure 5.1.: One-particle three-loop Feynman diagrams of the S[V(VP)P]E subset participating to the third-order contribution to the energy shift of a single-particle (valence or hole) state. They are denoted by H_1 (left) and H_2 (right). Notations are similar to Fig. 2.3.

The Green's function corresponding to each diagram in the subset is given by

$$\begin{aligned}\Delta g^{(3)H_1}_{\alpha,vv}(E) = \frac{1}{(E-\epsilon_v)^2}\left(\frac{i}{2\pi}\right)^3 \sum_{i,j,k,l,p} \int d\omega dk_1 dk_2 \frac{I_{vpik}(\omega)}{[E-\omega-\epsilon_i+i\varepsilon(\epsilon_i-E^F_\alpha)]} \\ \times \frac{I_{kjlj}(0)}{[k_1-\epsilon_j+i\varepsilon(\epsilon_j-E^F_\alpha)][k_2-\epsilon_k+i\varepsilon(\epsilon_k-E^F_\alpha)][k_2-\epsilon_l+i\varepsilon(\epsilon_l-E^F_\alpha)]} \\ \times \frac{I_{lipv}(\omega)}{[k_2-\omega-\epsilon_p+i\varepsilon(\epsilon_p-E^F_\alpha)]}\,, \end{aligned} \tag{5.1}$$

[1] See below Eq. (3.69) and Eq. (3.79), respectively.

[2] The simplest extension towards a one-loop three-photon-exchange corrections.

for H_1 and by

$$\Delta g^{(3)H_2}_{\alpha,vv}(E) = \frac{1}{(E-\epsilon_v)^2}\left(\frac{i}{2\pi}\right)^3 \sum_{i,j,k,l,p} \int d\omega dk_1 dk_2 \frac{I_{vkij}(\omega)}{[E-\omega-\epsilon_i+i\varepsilon(\epsilon_i-E^F_\alpha)]} \times \frac{I_{lpkp}(0)}{[k_1-\epsilon_j+i\varepsilon(\epsilon_j-E^F_\alpha)][k_1-\omega-\epsilon_k+i\varepsilon(\epsilon_k-E^F_\alpha)][k_1-\omega-\epsilon_l+i\varepsilon(\epsilon_l-E^F_\alpha)]} \times \frac{I_{jilv}(\omega)}{[k_2-\epsilon_p+i\varepsilon(\epsilon_p-E^F_\alpha)]}\,. \tag{5.2}$$

for H_2. According to the line of reasoning presented in the treatment of the SESE subset (Chapter 3.2.2), starting from the previous Green's functions, the extraction of the different three-photon-exchange corrections is carried out with the subtraction of the corresponding expression in the standard vacuum state. As the diagrams are 1PI, one does not need to worry about the disconnected terms in Eq. (3.31). Note that double cuts are possible in both diagrams, leading to so called non-diagrammatic terms, that are important to consider in order to properly treat the reducible elements. The results are separated in three- and four-electron contributions. To keep things short, as the resulting expressions are already lengthy, only the final results are displayed. The term-by-term three-electron contribution (loop diagram) is given explicitly below. The four-electron terms are displayed in appendix A.6.1, for a comparison with the perturbation theory approach.

The presentation of the results starts with expressions arising from the H_1 Feynman diagram. One distinguishes between three different type of terms: irreducible (irr), reducible 1 (red1) and reducible 2 (red2). The different terms corresponding to crossed graphs are found to be

$$\Delta E^{(3\mathrm{I})3\mathrm{e,cross,irr}}_{v,H_1} = \frac{i}{2\pi}\int d\omega \sum_{i,j,k}^{k\neq b} \frac{I_{vjib}(\omega) I_{baka}(0) I_{kijv}(\omega)}{(\epsilon_v-\omega-\epsilon_i u)(\epsilon_b-\omega-\epsilon_j u)(\epsilon_b-\epsilon_k u)}\,, \tag{5.3}$$

$$\Delta E^{(3\mathrm{I})3\mathrm{e,cross,irr}}_{v,H_1} = \frac{i}{2\pi}\int d\omega \sum_{i,j,k}^{k\neq b} \frac{I_{vjik}(\omega) I_{kaba}(0) I_{bijv}(\omega)}{(\epsilon_v-\omega-\epsilon_i u)(\epsilon_b-\omega-\epsilon_j u)(\epsilon_b-\epsilon_k u)}\,. \tag{5.4}$$

The terms associated to ladder graphs are given as follows,

$$\Delta E^{(3I)3e,lad,irr}_{v,H_1} = \frac{i}{2\pi}\int d\omega \sum_{i,j,k}^{\{i,j\}\neq\{v,b\},\{i,k\}\neq\{v,b\}} \frac{I_{vbij}(\omega)I_{jaka}(0)I_{kibv}(\omega)}{(\epsilon_v-\omega-\epsilon_i u)(\epsilon_b+\omega-\epsilon_j u)(\epsilon_b+\omega-\epsilon_k u)}\,, \tag{5.5}$$

$$\Delta E^{(3I)3e,lad,red1}_{v,H_1} = -\frac{i}{2\pi}\int d\omega \sum_{i,j,k}^{\{i,j\}=\{v,b\},\{i,k\}\neq\{v,b\}} \frac{I_{vbij}(\omega)I_{jaka}(0)I_{kibv}(\omega)}{(\epsilon_v-\omega-\epsilon_i u)^2(\epsilon_b+\omega-\epsilon_k u)}\,, \tag{5.6}$$

$$\Delta E^{(3I)3e,lad,red1}_{v,H_1} = -\frac{i}{2\pi}\int d\omega \sum_{i,j,k}^{\{i,j\}\neq\{v,b\},\{i,k\}=\{v,b\}} \frac{I_{vbij}(\omega)I_{jaka}(0)I_{kibv}(\omega)}{(\epsilon_v-\omega-\epsilon_i u)^2(\epsilon_b+\omega-\epsilon_j u)}\,, \tag{5.7}$$

$$\Delta E^{(3I)3e,lad,red2}_{v,H_1} = \frac{i}{2\pi}\int d\omega \sum_{i,j,k}^{\{i,j\}=\{v,b\},\{i,k\}=\{v,b\}} \frac{I_{vbij}(\omega)I_{jaka}(0)I_{kibv}(\omega)}{(\epsilon_v-\omega-\epsilon_i u)^3}\,. \tag{5.8}$$

The non-diagrammatic part for H_1 reads

$$\Delta E^{(3I)3e,cross,red1}_{v,H_1} = -\frac{i}{2\pi}\int d\omega \sum_{i,j} \frac{I_{vjib}(\omega)I_{bab_1a}(0)I_{b_1ijv}(\omega)}{(\epsilon_v-\omega-\epsilon_i u)(\epsilon_b-\omega-\epsilon_j u)^2}\,. \tag{5.9}$$

The expressions extracted from the H_2 Feynman diagram are found as follows,

$$\Delta E^{(3I)3e,cross}_{v,H_2} = \frac{i}{2\pi}\int d\omega \sum_{i,j,k} \frac{I_{vjib}(\omega)I_{kaja}(0)I_{bikv}(\omega)}{(\epsilon_v-\omega-\epsilon_i u)(\epsilon_b-\omega-\epsilon_j u)(\epsilon_b-\omega-\epsilon_k u)}\,, \tag{5.10}$$

$$\Delta E^{(3I)3e,lad,irr}_{v,H_2} = \frac{i}{2\pi}\int d\omega \sum_{i,j,k}^{k\neq b,\{i,j\}\neq\{b,v\}} \frac{I_{vbij}(\omega)I_{kaba}(0)I_{jikv}(\omega)}{(\epsilon_v-\omega-\epsilon_i u)(\epsilon_b+\omega-\epsilon_j u)(\epsilon_b-\epsilon_k u)}\,, \tag{5.11}$$

$$\Delta E^{(3I)3e,lad,red1}_{v,H_2} = -\frac{i}{2\pi}\int d\omega \sum_{i,j,k}^{k\neq b,\{i,j\}=\{b,v\}} \frac{I_{vbij}(\omega)I_{kaba}(0)I_{jikv}(\omega)}{(\epsilon_v-\omega-\epsilon_i u)^2(\epsilon_b-\epsilon_k u)}\,, \tag{5.12}$$

$$\Delta E^{(3I)3e,lad,irr}_{v,H_2} = \frac{i}{2\pi}\int d\omega \sum_{i,j,k}^{k\neq b,\{i,j\}\neq\{b,v\}} \frac{I_{vkij}(\omega)I_{baka}(0)I_{jibv}(\omega)}{(\epsilon_v-\omega-\epsilon_i u)(\epsilon_b+\omega-\epsilon_j u)(\epsilon_b-\epsilon_k u)}\,, \tag{5.13}$$

$$\Delta E^{(3I)lad,red1}_{v,H_2} = -\frac{i}{2\pi}\int d\omega \sum_{i,j,k}^{k\neq b,\{i,j\}=\{b,v\}} \frac{I_{vkij}(\omega)I_{baka}(0)I_{jibv}(\omega)}{(\epsilon_v-\omega-\epsilon_i u)^2(\epsilon_b-\epsilon_k u)}\,. \tag{5.14}$$

The non-diagrammatic term for H_2 are found to be

$$\Delta E^{(3I)3e,lad,red1}_{v,H_2} = -\frac{i}{2\pi}\int d\omega \sum_{i,j}^{\{i,j\}\neq\{b,v\}} \frac{I_{vbij}(\omega)I_{b_1aba}(0)I_{jib_1v}(\omega)}{(\epsilon_v-\omega-\epsilon_i u)(\epsilon_b+\omega-\epsilon_j u)^2}\,, \tag{5.15}$$

$$\Delta E^{(3I)3e,lad,red2}_{v,H_2} = -\frac{i}{2\pi}\int d\omega \sum_{i,j}^{\{i,j\}=\{b,v\}} \frac{I_{vbij}(\omega)I_{b_1aba}(0)I_{jib_1v}(\omega)}{(\epsilon_v-\omega-\epsilon_i u)^3}\,. \tag{5.16}$$

The expressions presented above are the bare results after carrying out the difference of the vacuum states to extract the interelectronic interactions. The IR divergences are extracted and regularized later on, such as the symmetrization of the poles with regard to the real axis. The final expressions are found in Appendix A.6.2, when comparing with the results from the perturbation theory approach.

S(VP)EVP subset

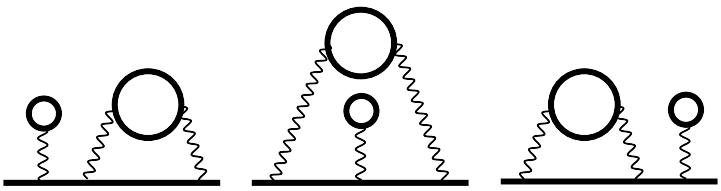

Figure 5.2.: One-particle three-loop Feynman diagrams of the S(VP)EVP subset participating to the third-order contribution to the energy shift of a single-particle (valence or hole) state. They are denoted by F_1 (left), F_2 (middle) and F_3 (right). Notations are similar to Fig. 2.3.

Within this subset, the Green's function associated to each diagram reads

$$\begin{aligned}\Delta g^{(3)F_1}_{\alpha,vv}(E) = &\frac{1}{(E-\epsilon_v)^2}\left(\frac{i}{2\pi}\right)^3 \sum_{i,j,k,l,p}\int d\omega dk_1 dk_2 \frac{I_{viji}(0)}{[k_1-\epsilon_i+i\varepsilon(\epsilon_i-E^F_\alpha)]}\\ &\times\frac{I_{jpkl}(\omega)}{[E-\epsilon_j+i\varepsilon(\epsilon_j-E^F_\alpha)][E-\omega-\epsilon_k+i\varepsilon(\epsilon_k-E^F_\alpha)][k_2-\epsilon_l+i\varepsilon(\epsilon_l-E^F_\alpha)]}\\ &\times\frac{I_{klvp}(\omega)}{[k_2-\omega-\epsilon_p+i\varepsilon(\epsilon_p-E^F_\alpha)]}\,,\end{aligned} \tag{5.17}$$

for F_1,

$$\begin{aligned}\Delta g^{(3)F_2}_{\alpha,vv}(E) = &\frac{1}{(E-\epsilon_v)^2}\left(\frac{i}{2\pi}\right)^3 \sum_{i,j,k,l,p}\int d\omega dk_1 dk_2 \frac{I_{vlil}(\omega)}{[E-\omega-\epsilon_i+i\varepsilon(\epsilon_p-E^F_\alpha)]}\\ &\times\frac{I_{ijkj}(0)}{[k_1-\epsilon_j+i\varepsilon(\epsilon_j-E^F_\alpha)][E-\omega-\epsilon_k+i\varepsilon(\epsilon_p-E^F_\alpha)][k_2-\epsilon_l+i\varepsilon(\epsilon_l-E^F_\alpha)]}\\ &\times\frac{I_{lkpv}(\omega)}{[k_2-\omega-\epsilon_p+i\varepsilon(\epsilon_p-E^F_\alpha)]}\,,\end{aligned} \tag{5.18}$$

for F_2, and

$$\begin{aligned}\Delta g^{(3)F_3}_{\alpha,vv}(E) = &\frac{1}{(E-\epsilon_v)^2}\left(\frac{i}{2\pi}\right)^3 \sum_{i,j,k,l,p}\int d\omega dk_1 dk_2 \frac{I_{vkij}(\omega)}{[E-\omega-\epsilon_i+i\varepsilon(\epsilon_i-E^F_\alpha)]}\\ &\times\frac{I_{ijlk}(\omega)}{[k_1-\epsilon_j+i\varepsilon(\epsilon_j-E^F_\alpha)][k_1-\omega-\epsilon_k+i\varepsilon(\epsilon_k-E^F_\alpha)][E-\epsilon_l+i\varepsilon(\epsilon_l-E^F_\alpha)]}\\ &\times\frac{I_{lpvp}(0)}{[k_2-\epsilon_p+i\varepsilon(\epsilon_p-E^F_\alpha)]}\,.\end{aligned} \tag{5.19}$$

for F_3. The identical procedure as stated above is applied to infer the three-photon-exchange corrections. The diagrams are not 1PI, with the exception of F_2. Therefore, one has to consider the second-order Green's function $\Delta g^{(2)\mathrm{S(VP)E}}_\alpha$ and the first-order one $\Delta g^{(1)\mathrm{VP}}_\alpha$ to evaluate the disconnected terms in Eq. (3.31). It turns out that only the first part of the fourth line survives. The disconnected terms take care to have a single exemplar of the reducible elements. To illustrate, F_1 and F_3 give redundant reducible terms, but the disconnected contributions remove the extra ones, coming from F_1 in this case. A small nuance is nevertheless needed if an extra pole is explicitly extracted. In such a case, this reducible term is kept, first because it can not be generated in the disconnected ones, second and more importantly to achieve the IR finiteness

of the expressions in the subset. Hence, for the S(VP)EVP subset, on the top of the peculiar extra-pole-term in F_1, only the F_2 and F_3 reducible IR divergent expressions are displayed in Table 5.1. Non-diagrammatic terms are only present in the F_2 diagram, and are of four-electron type. The results are separated in three- and four-electron contributions. As stated before, only the end formulas are provided. The term-by-term loop contribution, three-electron contribution, is given below. The four-electron terms are displayed, when comparing with the perturbation theory approach, in appendix A.6.1.

The extraction procedure is carried out for the F_1 Feynman diagram, which contributes as follow. The terms associated to the crossed graphs are

$$\Delta E^{(3\mathrm{I})3\mathrm{e,cross,irr}}_{v,F_1} = \frac{i}{2\pi}\int d\omega \sum_{i,j,k}^{i\neq v} \frac{I_{vaia}(0)I_{ikjb}(\omega)I_{bjkv}(\omega)}{(\epsilon_v-\epsilon_i)(\epsilon_v-\omega-\epsilon_j u)(\epsilon_b-\omega-\epsilon_k u)}\,, \tag{5.20}$$

$$\Delta E^{(3\mathrm{I})3\mathrm{e,cross,red1}}_{v,F_1} = -\frac{i}{2\pi}\int d\omega \sum_{i,j} \frac{I_{vav_1a}(0)I_{v_1kjb}(\omega)I_{bjkv}(\omega)}{(\epsilon_v-\omega-\epsilon_j u)^2(\epsilon_b-\omega-\epsilon_k u)}\,. \tag{5.21}$$

The expressions corresponding to the ladder-loop graph read

$$\Delta E^{(3\mathrm{I})3\mathrm{e,lad,irr}}_{v,F_1} = \frac{i}{2\pi}\int d\omega \sum_{i,j,k}^{i\neq v,\{j,k\}\neq\{v,b\}} \frac{I_{vaia}(0)I_{ibjk}(\omega)I_{jkvb}(\omega)}{(\epsilon_v-\epsilon_i u)(\epsilon_v-\omega-\epsilon_j u)(\epsilon_b+\omega-\epsilon_k u)}\,, \tag{5.22}$$

$$\Delta E^{(3\mathrm{I})3\mathrm{e,lad,red1}}_{v,F_1} = -\frac{i}{2\pi}\int d\omega \sum_{i,j,k}^{\{j,k\}\neq\{v,b\}} \frac{I_{vav_1a}(0)I_{v_1bjk}(\omega)I_{jkvb}(\omega)}{(\epsilon_v-\omega-\epsilon_j u)^2(\epsilon_b+\omega-\epsilon_k u)}\,, \tag{5.23}$$

$$\begin{aligned}\Delta E^{(3\mathrm{I})3\mathrm{e,lad,red1}}_{v,F_1} = &-\frac{i}{2\pi}\int d\omega \sum_{i,j,k}^{i\neq v,\{j,k\}=\{v,b\}} \left\{ \frac{I_{vaia}(0)I_{ibjk}(\omega)I_{jkvb}(\omega)}{(\epsilon_v-\epsilon_i u)^2}\left[\frac{1}{(\epsilon_v-\omega-\epsilon_j u)}\right.\right.\\ &\left.\left. + \frac{1}{(\epsilon_b+\omega-\epsilon_k u)}\right] + \frac{I_{vaia}(0)I_{ibjk}(\omega)I_{jkvb}(\omega)}{(\epsilon_v-\epsilon_i u)(\epsilon_v-\omega-\epsilon_j u)^2}\right\}\,,\end{aligned} \tag{5.24}$$

$$\Delta E^{(3\mathrm{I})3\mathrm{e,lad,red2}}_{v,F_1} = \frac{i}{2\pi}\int d\omega \sum_{j,k}^{\{j,k\}=\{v,b\}} \frac{I_{vav_1a}(0)I_{v_1bjk}(\omega)I_{jkvb}(\omega)}{(\epsilon_v-\omega-\epsilon_j u)^3}\,. \tag{5.25}$$

For the disconnected parts, the terms presented below cancel the reducible elements found in F_1, namely the term on the first line cancels (5.21), the term on the second line cancels (5.23) and the term on the third line cancels (5.25). It leaves only the irreducible expressions and the ladder reducible 1 term (5.24).

$$\begin{aligned}\Delta E^{(3I)3e,disc}_{v,F} = &\frac{i}{2\pi}\int d\omega \sum_{i,j}\frac{I_{vava}(0)I_{v_1jib}(\omega)I_{ibv_1j}(\omega)}{(\epsilon_v-\omega-\epsilon_i u)^2(\epsilon_b-\omega-\epsilon_j u)}\\ &+\frac{i}{2\pi}\int d\omega \sum_{i,j}^{\{i,j\}\neq\{b,v\}}\frac{I_{vava}(0)I_{v_1bij}(\omega)I_{ijv_1bj}(\omega)}{(\epsilon_v-\omega-\epsilon_i u)^2(\epsilon_b+\omega-\epsilon_j u)}\\ &-\frac{i}{2\pi}\int d\omega \sum_{i,j}^{\{i,j\}=\{b,v\}}\frac{I_{vava}(0)I_{v_1bij}(\omega)I_{ijv_1bj}(\omega)}{(\epsilon_v-\omega-\epsilon_i u)^3}\,. \end{aligned} \tag{5.26}$$

The Feynman diagram F_2 leads to the subsequent terms. Only a term associated to a crossed-loop graph is found

$$\Delta E^{(3I)3e,cross}_{v,F_2} = \frac{i}{2\pi}\int d\omega \sum_{i,j,k}\frac{I_{vkib}(\omega)I_{iaja}(0)I_{bjkv}(\omega)}{(\epsilon_v-\omega-\epsilon_i u)(\epsilon_v-\omega-\epsilon_j u)(\epsilon_b-\omega-\epsilon_k u)}\,, \tag{5.27}$$

so it is for the ladder-loop graph, but incorporating the different types stated above

$$\Delta E^{(3I)3e,lad,irr}_{v,F_2} = \frac{i}{2\pi}\int d\omega \sum_{i,j,k}^{\{i,k\}\neq\{v,b\},\{j,k\}\neq\{v,b\}}\frac{I_{vbik}(\omega)I_{iaja}(0)I_{kjbv}(\omega)}{(\epsilon_v-\omega-\epsilon_i u)(\epsilon_v-\omega-\epsilon_j u)(\epsilon_b+\omega-\epsilon_k u)}\,, \tag{5.28}$$

$$\begin{aligned}\Delta E^{(3I)3e,lad,red1}_{v,F_2} = &-\frac{i}{2\pi}\int d\omega \sum_{i,j,k}^{\{i,k\}=\{v,b\},\{j,k\}\neq\{v,b\}}\left\{\frac{I_{vbik}(\omega)I_{iaja}(0)I_{kjbv}(\omega)}{(\epsilon_v-\omega-\epsilon_j u)^2}\left[\frac{1}{(\epsilon_v-\omega-\epsilon_i u)}\right.\right.\\ &\left.\left.+\frac{1}{(\epsilon_b+\omega-\epsilon_k u)}\right]+\frac{I_{vbik}(\omega)I_{iaja}(0)I_{kjbv}(\omega)}{(\epsilon_v-\omega-\epsilon_i u)^2(\epsilon_v-\omega-\epsilon_j u)}\right\}, \end{aligned} \tag{5.29}$$

$$\begin{aligned}\Delta E^{(3I)3e,lad,red1}_{v,F_2} = &-\frac{i}{2\pi}\int d\omega \sum_{i,j,k}^{\{i,k\}\neq\{v,b\},\{j,k\}=\{v,b\}}\left\{\frac{I_{vbik}(\omega)I_{iaja}(0)I_{kjbv}(\omega)}{(\epsilon_v-\omega-\epsilon_i u)^2}\left[\frac{1}{(\epsilon_v-\omega-\epsilon_j u)}\right.\right.\\ &\left.\left.+\frac{1}{(\epsilon_b+\omega-\epsilon_k u)}\right]+\frac{I_{vbik}(\omega)I_{iaja}(0)I_{kjbv}(\omega)}{(\epsilon_v-\omega-\epsilon_i u)(\epsilon_v-\omega-\epsilon_j u)^2}\right\}, \end{aligned} \tag{5.30}$$

$$\Delta E^{(3I)3e,lad,red2}_{v,F_2} = \frac{i}{2\pi}\int d\omega \sum_{i,j,k}^{\{i,k\}=\{v,b\},\{j,k\}=\{v,b\}} \left\{ \frac{I_{vbik}(\omega) I_{iaja}(0) I_{kjbv}(\omega)}{(\epsilon_v - \omega - \epsilon_i u)^3} - \frac{I_{vbik}(\omega) I_{iaja}(0) I_{kjbv}(\omega)}{(\epsilon_v - \omega - \epsilon_i u)(\epsilon_v - \omega - \epsilon_j u)} \left[\frac{1}{(\epsilon_v - \omega - \epsilon_i u)} + \frac{1}{(\epsilon_v - \omega - \epsilon_j u)} \right] \right\} . \tag{5.31}$$

From the F_3 Feynman diagram arises the coming terms. Similarly to the F_1 graph, the terms corresponding to the crossed graph are

$$\Delta E^{(3I)3e,cross,irr}_{v,F_3} = \frac{i}{2\pi}\int d\omega \sum_{i,j,k}^{k\neq v} \frac{I_{vjib}(\omega) I_{ibkj}(\omega) I_{kava}(0)}{(\epsilon_v - \omega - \epsilon_i u)(\epsilon_b - \omega - \epsilon_j u)(\epsilon_v - \epsilon_k u)} , \tag{5.32}$$

$$\Delta E^{(3I)3e,cross,red}_{v,F_3} = \frac{-i}{2\pi}\int d\omega \sum_{i,j} \frac{I_{vjib}(\omega) I_{ibv_1 j}(\omega) I_{v_1 ava}(0)}{(\epsilon_v - \omega - \epsilon_i u)^2(\epsilon_b - \omega - \epsilon_j u)} . \tag{5.33}$$

The ones associated to the ladder graph read

$$\Delta E^{(3I)3e,lad,irr}_{v,F_3} = \frac{i}{2\pi}\int d\omega \sum_{i,j,k}^{\{i,j\}\neq\{b,v\},k\neq v} \frac{I_{vbij}(\omega) I_{ijkb}(\omega) I_{kava}(0)}{(\epsilon_v - \omega - \epsilon_i u)(\epsilon_b + \omega - \epsilon_j u)(\epsilon_v - \epsilon_k u)} , \tag{5.34}$$

$$\Delta E^{(3I)lad,red1}_{v,F_3} = \frac{-i}{2\pi}\int d\omega \sum_{i,j}^{\{i,j\}\neq\{b,v\}} \frac{I_{vbij}(\omega) I_{ijv_1 b}(\omega) I_{v_1 ava}(0)}{(\epsilon_v - \omega - \epsilon_i u)^2(\epsilon_b + \omega - \epsilon_j u)} , \tag{5.35}$$

$$\Delta E^{(3I)3e,lad,red1}_{v,F_3} = \frac{-i}{2\pi}\int d\omega \sum_{i,j,k}^{\{i,j\}=\{b,v\},k\neq v} \left\{ \frac{I_{vbij}(\omega) I_{ijkb}(\omega) I_{kava}(0)}{(\epsilon_v - \epsilon_k u)^2} \left[\frac{1}{(\epsilon_v - \omega - \epsilon_i u)} + \frac{1}{(\epsilon_b + \omega - \epsilon_j u)} \right] + \frac{I_{vbij}(\omega) I_{ijkb}(\omega) I_{kava}(0)}{(\epsilon_v - \omega - \epsilon_i u)^2(\epsilon_v - \epsilon_k u)} \right\} , \tag{5.36}$$

$$\Delta E^{(3I)3e,lad,red2}_{v,F_3} = \frac{i}{2\pi}\int d\omega \sum_{i,j}^{\{i,j\}=\{b,v\}} \frac{I_{vbij}(\omega) I_{ijv_1 b}(\omega) I_{v_1 ava}(0)}{(\epsilon_v - \omega - \epsilon_i u)^3} . \tag{5.37}$$

As in the case of the S[V(VP)P]E subset, the expressions displayed are the results obtained in the extraction procedure of the interelectronic interaction, as the difference of the vacuum states. Some more work is required to extract the IR divergences, to regularize them, as well as to symmetrize the poles with regard to the real axis. The final expressions are found in Appendix A.6.2, when comparing with the results from the perturbation theory approach.

5.2. Perturbation theory approach

The idea behind this approach is to perturb a two-photon-exchange correction by the presence of some potential-like interaction $\mathcal{V}$, to its first order. This method was applied in Ref. [140] to generate the two-photon-exchange corrections to the g-factor of Li-like ions. Specifically, the one-electron external wave function is perturbed as

$$|i\rangle \to |i\rangle + |\delta i\rangle, \quad |\delta i\rangle = \sum_{j\neq i} \frac{|j\rangle \mathcal{V}_{ji}}{\epsilon_i - \epsilon_j}\,, \tag{5.38}$$

the energy accordingly to

$$\epsilon_i \to \epsilon_i + \delta\epsilon_i, \quad \delta\epsilon_i = \mathcal{V}_{ii}\,, \tag{5.39}$$

leading to the perturbation in the argument of the interelectronic operator

$$I(\Delta_{va}) \to I(\Delta_{va} + \delta\Delta_{va}) \approx I(\Delta_{va}) + I'(\Delta_{va})(\delta\epsilon_v - \delta\epsilon_a)\,. \tag{5.40}$$

The electron propagator (2.53) involved in the loops has to be perturbed as well. One finds

$$\begin{aligned} S_{\delta\mathcal{V}}(\epsilon_k \pm \omega; \mathbf{x}, \mathbf{y}) &= \delta_{\mathcal{V}} \left(\sum_i \frac{|i\rangle\langle i|}{\epsilon_k \pm \omega - \epsilon_i u} \right) \\ &= \sum_{i,j} \frac{|i\rangle \mathcal{V}_{ij} \langle j|}{(\epsilon_k \pm \omega - \epsilon_i u)(\epsilon_k \pm \omega - \epsilon_j u)} - \sum_i \frac{|i\rangle \mathcal{V}_{kk} \langle i|}{(\epsilon_k \pm \omega - \epsilon_i u)^2}\,. \end{aligned} \tag{5.41}$$

It is a slight generalization of the propagator found in Ref. [141]. This expression is also valid in the case $\omega = 0$, namely for the four-electron subset. However, one should consider two cases: (i) if both parenthesis $(\epsilon_k \pm \omega - \epsilon_{i,j} u)$ are non-zero, then the first piece of the perturbed propagator is to be used, (ii) if one of the parenthesis $(\epsilon_k \pm \omega - \epsilon_{i,j} u)$ is zero, then the second piece of the perturbed propagator is to be used, with the appropriate index. In such a way, it reproduces the operator Ξ of Eq. (46) in Ref. [140].

In the end, one trades the potential-link interaction matrix element for a one-photon-exchange one,

$$\mathcal{V}_{ij} \to I_{iaja}(0)\,, \tag{5.42}$$

to match the three-photon-exchange formulas. Let us pause and comment the last step presented above. A link between the potential-like interaction and the one-photon-exchange interaction is drawn. The logic goes as follows; consider for example, the Wichmann-Kroll potential [142]. It accounts for an all-order treatment, in αZ, of the interaction of the free-electron vacuum-polarization loop (first order in α) with the Coulomb potential[3]. As a side comment, the Uehling potential [148], which takes into account the electric polarization of the vacuum (state), is the lowest order approximation (in αZ) of the vacuum-polarization loop within the Coulomb field of the nucleus. One usually considers that the Wichmann-Kroll potential does not take the Uehling potential into account. Albeit the Wichmann-Kroll potential is such a potential-like interaction, it deals with the full Green's function. Though, the potential-like interaction considered above incorporates only the core electrons. Therefore, going half a step back, one can imagine to have an all-order αZ Wichmann-Kroll potential-like mapped to the vacuum-polarization loop only for the core electrons. The inner structure of the "vacuum-polarization potential-like" interaction is then unravelled by a cut in the loop. Hence, one can think of the potential-like interaction as an effective one-electron operator, but hiding a corrected wave function or representing a screened correction.

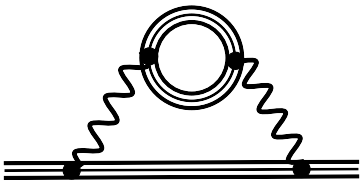

Figure 5.3.: One-particle two-loop Feynman diagram corresponding to the perturbed S(VP)P subset in the redefined vacuum state formalism in an external potential V. The triple line indicates the electron propagator perturbed by the potential-like interaction $\mathcal{V}$. Notation is similar to Fig. 2.3.

The reasons invoked in the previous section to select a GI subset are still relevant. Thus, one perturbs the S(VP)E equations (3.79)–(3.82) according to Eqs. (5.38–5.41) and finds the desired formulas under the replacement (5.42). The Feynman diagram corresponding to the $\mathcal{V}$-perturbed, represented by the triple line notation, S(VP)E subset is displayed in Fig. 5.3.

[3] A potential which accounts for a partial two-loop (second order in α) VP correction is the Källén-Sabry potential [143–147].

It was shown that the two-electron subset and the three-electron subset are gauge invariant separately[4]. It implies that the gauge invariance of the selected three-photon-exchange subsets, at the three- and four-electron level, independently, is expected since the perturbation is initially a potential-like interaction $\mathcal{V}$, turned into a one-photon-exchange operator[5]. The open question is whether the separation into S(VP)EVP and S[V(VP)P]E subsets holds also at the three- and four-electron level, as it is though to be the case. Hence, starting from the $\mathcal{V}$-perturbed S(VP)E GI expressions, one should be able to disentangle the various terms found via the redefinition of the vacuum state approach and assign them either to the three- or four-electron contribution. The results relying on this method are displayed in Appendix A.6.

5.3. Regularization of infrared divergences

Infrared divergences occur when the energy flowing through the loop (ω) leads to a vanishing denominator of the electron propagator at $\omega \to 0$. At the two-photon-exchange level, it was only met in ladder reducible terms[6], where the removal of terms in the crossed parts was carried out to cancel IR divergences in the ladder terms [72]. In the case of the three-photon-exchange corrections, it can also arise from crossed reducible terms. The analysis of IR divergences is conducted in the Feynman gauge, but the resulting pairing of the expressions is valid generally in virtue of gauge invariance. According to Shabaev [85], one introduces the following integral representation for the complex-exponential term of the photon propagator (2.34), including a photon mass term μ,

$$e^{i\sqrt{\omega^2-\mu^2+i\varepsilon}|\mathbf{x}-\mathbf{y}|} = \frac{-2}{\pi}\int_0^\infty dk \frac{k\sin(k|\mathbf{x}-\mathbf{y}|)}{(\omega^2-k^2-\mu^2+i\varepsilon)}\,. \tag{5.43}$$

The photon mass plays the role of a energy cutoff (IR regulator). Notice that the condition on the branch of the square root is changed to $\mathrm{Im}(\sqrt{\omega^2-\mu^2+i\varepsilon}) > 0$. In the rest of the chapter, the use of $r_{12} \equiv |\mathbf{x}-\mathbf{y}|$ is preferred. Such type of integrals are met when facing IR divergences

$$\mathcal{I}_{n,m_\pm,p} \equiv \frac{-i}{2\pi}\int d\omega \frac{I(\omega)I(\omega)I(0)}{(-\omega+i\varepsilon)^n(\Delta\pm\omega+i\varepsilon)^m\widetilde{\Delta}^p}\,, \tag{5.44}$$

[4]The proof for the former is given numerically in Tables 3.1 and A.1 at the corresponding lines, and analytically for the later in Eq. (3.83).

[5]The one-photon-exchange operator was shown to be gauge invariant in Eq. (3.63).

[6]See Eqs. (3.69, 3.79) and comments below them.

with $n = 1,2,3$, $m = 0,1$, $p = 0,1$ and the constraint $n+m+p = 3$. The $+$ sign stands for the IR divergent ladder reducible terms and the $-$ sign for the compensating crossed terms. Calculations are performed by the application of #3.773(3) [or #3.729(2)] in Gradshteyn and Ryzhik [149]. The first step is to show that for a first-order pole, $n = 1$, the result is IR finite. There is no necessity to introduce a photon mass nor to use the integral representation of the complex exponential. It is sufficient to Wick rotate the integration contour with the substitution $\omega = i\omega_E$. Afterward, the principal value of the integral, denoted by $\mathcal{P}$, is considered. One shall start with the simplest case,

$$\mathcal{I}_{1,0,2} = \frac{-i}{2\widetilde{\Delta}^2} I(0)I(0)I(0) + \frac{I(0)}{2\pi\widetilde{\Delta}^2}\mathcal{P}\int_0^{i\infty} d\omega_E \frac{I(-i\omega_E)I(-i\omega_E) - I(i\omega_E)I(i\omega_E)}{i\omega_E}\,. \tag{5.45}$$

The integral term reads explicitly

$$\frac{\alpha^2}{r_{12}r_{34}}\alpha_{1\mu}\alpha_2^{\mu}\alpha_{3\nu}\alpha_4^{\nu}\,\mathcal{P}\int_0^{i\infty} d\omega_E \frac{e^{-\omega_E R} - e^{\omega_E R}}{i\omega_E}\,, \tag{5.46}$$

giving a finite contribution in the limit $\omega \to 0$. R stands for $R = r_{12} + r_{34}$. One sees that the real part is IR finite, the imaginary one as well in this simple example. The second case, $\mathcal{I}_{1,2_,0}$, requires one more step, a partial fraction decomposition, so that the Cauchy principal value can be applied. Recall that the principal value picks only the residues, hence no contribution from second or higher order poles.

$$\begin{aligned}\mathcal{I}_{1,2_,0} =& \frac{-i}{\Delta^2}\left[I(0)I(0) - I(\Delta)I(\Delta)\right] I(0) \\ &+ \frac{I(0)}{2\pi\Delta^2}\mathcal{P}\int_0^{i\infty} d\omega_E \left\{\frac{I(-i\omega_E)I(-i\omega_E) - I(i\omega_E)I(i\omega_E)}{i\omega_E}\right. \\ &\left. - \frac{I(-i\omega_E)I(-i\omega_E)}{\Delta + i\omega_E} - \frac{I(i\omega_E)I(i\omega_E)}{\Delta - i\omega_E}\right\}.\end{aligned} \tag{5.47}$$

The first integrand was shown to IR finite just above. For the remaining two integrands, it is clear that Δ plays the role of an IR cutoff, preventing the expression to diverge in the limit $\omega \to 0$. The case $\mathcal{I}_{1,1_,1}$ is not met in the diagrams under consideration and is therefore not assessed. Let us discuss the IR divergences arising from second-order poles. The first case considers the insertion of the interelectronic operator on the external leg of a one-loop diagram.

One has,

$$\begin{aligned}\mathcal{I}_{2,0,1} &= \frac{-\alpha^3 R}{\pi r_{12} r_{34} r_{56} \widetilde{\Delta}} \alpha_{1\mu} \alpha_2^{\mu} \alpha_{3\nu} \alpha_4^{\nu} \alpha_{5\rho} \alpha_6^{\rho} K_0(\mu R) \\ &\approx \frac{-\alpha^3 R}{\pi r_{12} r_{34} r_{56} \widetilde{\Delta}} \alpha_{1\mu} \alpha_2^{\mu} \alpha_{3\nu} \alpha_4^{\nu} \alpha_{5\rho} \alpha_6^{\rho} \left(\ln \frac{\mu}{2} + \gamma + \ln R \right) , \end{aligned} \tag{5.48}$$

in the limit $\mu \to 0$. $K_n(x)$ are imaginary Bessel functions of the second kind. The identical IR logarithmic divergent behaviour as in the two-photon-exchange ladder reducible case is recovered [85]. The corresponding crossed diagram cancels the IR divergent term, leaving a well-behaved expression. The second case is when the interelectronic operator is inserted within the loop. One faces

$$\begin{aligned}\mathcal{I}_{2,1_+,0} &= \frac{\alpha^3}{\pi r_{12} r_{34} r_{56}} \alpha_{1\mu} \alpha_2^{\mu} \alpha_{3\nu} \alpha_4^{\nu} \alpha_{5\rho} \alpha_6^{\rho} \\ &\times \int_0^{\infty} dk k \sin(kR) \left[\frac{1}{(k^2+\mu^2)^{3/2} (\Delta - \sqrt{k^2+\mu^2})} - \frac{2}{(k^2+\mu^2)\Delta^2} \right] . \end{aligned} \tag{5.49}$$

The IR divergence is compensated by a similar crossed graph, where the interelectronic operator is also inserted within the loop

$$\begin{aligned}\mathcal{I}_{2,1_-,0} &= \frac{-\alpha^3}{\pi r_{12} r_{34} r_{56}} \alpha_{1\mu} \alpha_2^{\mu} \alpha_{3\nu} \alpha_4^{\nu} \alpha_{5\rho} \alpha_6^{\rho} \int_0^{\infty} dk k \sin(kR) \\ &\times \left[\frac{-1}{(k^2+\mu^2)^{3/2} (\Delta + \sqrt{k^2+\mu^2})} + \frac{2}{(k^2+\mu^2-\Delta^2)\Delta^2} - \frac{2}{(k^2+\mu^2)\Delta^2} \right] . \end{aligned} \tag{5.50}$$

However, the cancellation is not obvious at this step. A partial fraction decomposition allows to greatly simplify the previous expressions, when they are added together.

$$\begin{aligned}\mathcal{I}_{2,1_-,0} + \mathcal{I}_{2,1_+,0} &= \frac{-2\alpha^3}{\pi r_{12} r_{34} r_{56} \Delta^2} \alpha_{1\mu} \alpha_2^{\mu} \alpha_{3\nu} \alpha_4^{\nu} \alpha_{5\rho} \alpha_6^{\rho} \int_0^{\infty} dk \frac{k \sin(kR)}{k^2+\mu^2} \\ &= \frac{-2\alpha^3}{\pi r_{12} r_{34} r_{56} \Delta^2} \alpha_{1\mu} \alpha_2^{\mu} \alpha_{3\nu} \alpha_4^{\nu} \alpha_{5\rho} \alpha_6^{\rho} \sqrt{\frac{\pi \mu R}{2}} K_{1/2}(\mu R) \\ &\approx \frac{\alpha^3}{r_{12} r_{34} r_{56} \Delta^2} \alpha_{1\mu} \alpha_2^{\mu} \alpha_{3\nu} \alpha_4^{\nu} \alpha_{5\rho} \alpha_6^{\rho} \left(\mu R - 1 \right) . \end{aligned} \tag{5.51}$$

Thus, it turned out to be a spurious divergence; the IR divergence is ruled out and a finite part remains in the limit $\mu \to 0$. Last, but not least, the IR divergence arising from the third-order pole is treated. The corresponding integral to evaluate is

$$\begin{aligned}\mathcal{I}_{3,0,0} &= \frac{-\alpha^3}{\pi r_{12} r_{34} r_{56}} \alpha_{1\mu} \alpha_2^{\mu} \alpha_{3\nu} \alpha_4^{\nu} \alpha_{5\rho} \alpha_6^{\rho} \sqrt{\frac{\pi R}{2\mu}} \frac{R}{2} K_{1/2}(\mu R) \\ &\approx \frac{-\alpha^3 R}{4 r_{12} r_{34} r_{56}} \alpha_{1\mu} \alpha_2^{\mu} \alpha_{3\nu} \alpha_4^{\nu} \alpha_{5\rho} \alpha_6^{\rho} \left(\frac{1}{\mu} - R \right) , \end{aligned} \tag{5.52}$$

leading to a singular behaviour when the limit $\mu \to 0$ is taken. The behaviour of the IR divergence arising from the third-order pole is in agreement with the one presented in Ref. [141], where a similar analysis was performed for the self-energy screening effects in g-factor calculations. Similarly to the IR divergence arising from the second-order pole, one looks for the compensating crossed diagram to ensure that the total expression is finite. A different treatment for the regularization of IR divergence for these terms, based on a symmetry argument, is proposed in Appendix A.7.

The explicit cancellation of IR divergences, at the individual Feynman diagram level by the appropriate crossed term, is demonstrated in Table 5.1. An exception is met for the ladder reducible 2 terms, which compensate themselves. A swapping of the indices in the expressions presented in Chapter 5.1 might be sometimes necessary in order to make the compensation apparent. Moreover, it was shown that IR divergences are absorbed by expressions belonging to the same subset. This is a very engaging indication towards the gauge invariance of the selected subsets.

$\Delta E_v^{(3I)3e} \in$ S[V(VP)P]E	type of IR divergence	Crossed	IR compensation
H_1: ladder red 1 (5.6)	$\mathcal{I}_{2,1_+,0}$	H_2: crossed (5.10)	$\mathcal{I}_{2,1_-,0}$
H_1: ladder red 1(5.7)	$\mathcal{I}_{2,1_+,0}$	H_2: crossed (5.10)	$\mathcal{I}_{2,1_-,0}$
H_1: ladder red 2 (5.8)	$\mathcal{I}_{3,0,0}$	H_2: ladder red 2 (5.16)	$\mathcal{I}_{3,0,0}$
H_1: crossed red (5.9)	$\mathcal{I}_{2,1_-,0}$, $\mathcal{I}_{3,0,0}$	H_2: crossed (5.10)	$\mathcal{I}_{2,1_-,0}$, $\mathcal{I}_{3,0,0}$
H_2: ladder red 1 (5.12)	$\mathcal{I}_{2,0,1}$	H_1: crossed irr (5.4)	$\mathcal{I}_{2,0,1}$
H_2: ladder red 1 (5.14)	$\mathcal{I}_{2,0,1}$	H_1: crossed irr (5.3)	$\mathcal{I}_{2,0,1}$
H_2: ladder red 2 (5.16)	$\mathcal{I}_{3,0,0}$	H_1: ladder red 2 (5.8)	$\mathcal{I}_{3,0,0}$
$\Delta E_v^{(3I)3e} \in$ S(VP)EVP	type of IR divergence	Crossed	IR compensation
F_1: ladder red 1 (5.24)	$\mathcal{I}_{2,0,1}$	F_1 : crossed (5.20)	$\mathcal{I}_{2,0,1}$
F_2: ladder red 1(5.29)	$\mathcal{I}_{2,1_+,0}$	F_2: crossed (5.27)	$\mathcal{I}_{2,1_-,0}$
F_2: ladder red 1 (5.30)	$\mathcal{I}_{2,1_+,0}$	F_2 : crossed (5.27)	$\mathcal{I}_{2,1_-,0}$
F_2: ladder red 2 (5.31)	$\mathcal{I}_{3,0,0}$	F_2: crossed (5.27)	$\mathcal{I}_{3,0,0}$
F_3: ladder red 1 (5.36)	$\mathcal{I}_{2,0,1}$	F_3: crossed irr (5.32)	$\mathcal{I}_{2,0,1}$
F_3: ladder red 2 (5.37)	$\mathcal{I}_{3,0,0}$	F_3: crossed red (5.33)	$\mathcal{I}_{3,0,0}$
F_3: crossed red (5.33)	$\mathcal{I}_{2,1_-,0}$	F_2 : crossed (5.27)	$\mathcal{I}_{2,1_-,0}$

Table 5.1.: IR divergences regularization at the individual Feynman diagram level. IR divergences are found in the reducible expressions, both for ladder- and crossed-loops. Crossed stands for the crossed compensating term. $\mathcal{I}_{n,m_\pm,p}$ describes the type of divergent integral met in the graph. Each term can be found in Chapter. 5.1, following the referenced equation. The labels are simplified in comparison to the ones presented there, only the difference among them is highlighted.

5.4. Comparison

Two different approaches were utilized to infer a partial third-order interelectronic correction to the energy shift. A comparison between the results of each of these two approaches is undertaken in this section.

The discussion begins with the four-electron contribution, which involves three types of terms: the irreducible [$\Delta E_v^{(3I)4e,irr}$ (A.28, A.29)], the reducible 1 [$\Delta E_v^{(3I)4e,red1}$ (A.30, A.31)] and the reducible 2 [$\Delta E_v^{(3I)4e,red2}$ (A.32, A.33)]. For every type previously stated, agreement

between the perturbative treatment of the $\mathcal{V}$-perturbed S(VP)E three-electron subset and the effective one-particle approach is met. Hence, the separation of the different terms, according to the two one-particle three-loop sets, provided when presenting the results in the appendix A.6.1.

For the three-electron contribution, an identical separation as above is conducted. The irreducible type is composed of three parts, two of which correspond to crossed diagrams, [$\Delta E_v^{(3I)3e,cross}$ (A.37,A.38), $\Delta E_v^{(3I)3e,cross,irr}$ (A.35, A.36)] and one corresponding to ladder diagrams [$\Delta E_v^{(3I)3e,lad,irr}$ (A.39, A.40)]. The outcomes of the two methods are in full concordance for these terms. Regarding the reducible 1 type, the cross reducible [$\Delta E_v^{(3I)3e,cross,red}$ (A.41, A.42)] and the ladder reducible 1 IR free ω [$\Delta E_{v,\,\text{IR free}\,\omega}^{(3I)lad,red1}$ (A.47, A.48)] terms extracted from the two treatments are in good agreement.
However, for the remaining reducible 1 terms [$\Delta E_{v,\,\text{IR div}}^{(3I)3e,lad,red1}$ (A.43, A.44), $\Delta E_{v,\,\text{IR free}}^{(3I)3e,lad,red1}$ (A.45, A.46)] a discrepancy is encountered. Yerokhin, in Ref. [140], already pointed out that the perturbation theory approach runs into troubles to deal with reducible terms[7]. He is invoking gauge invariance to fix the problem. If proceeding as explained at the end of the section dedicated to perturbation theory approach, an identical problem to the one highlighted by Yerokhin is met, namely that the poles differ by the sign of the $i\varepsilon$ prescription[8],

$$\frac{1}{(\omega+i\varepsilon)(-\omega+i\varepsilon)} \quad \text{versus} \quad \frac{1}{(\omega+i\varepsilon)^2} \;\text{ or }\; \frac{1}{(-\omega+i\varepsilon)^2}\,, \tag{5.53}$$

when facing ladder reducible 1 terms, $\Delta E_{v,\,\text{IR div}}^{(3I)3e,lad,red1}$ and $\Delta E_{v,\,\text{IR free}}^{(3I)3e,lad,red1}$. The difference in the topology of the poles arises from unaccounted restrictions in the summations. Surprisingly, and possibly related to the topology problem associated with the poles, the two approaches differ regarding the extra terms

$$\Delta E_{v,\,\text{S[V(VP)P]E}}^{(3I)3e,red1} = \sum_{a,b,b_1,v_1,i}^{i\neq v} \frac{I_{vbb_1v_1}(\Delta_{vb})I_{v_1aia}(0)I_{ib_1bv}(\Delta_{vb})}{(\epsilon_v-\epsilon_i)^2}\,, \tag{5.54}$$

$$\Delta E_{v,\,\text{S(VP)EVP}}^{(3I)3e,red1} = -\sum_{a,b,b_1,v_1,i}^{i\neq b} \frac{I_{vbb_1v_1}(\Delta_{vb})I_{b_1aia}(0)I_{iv_1vb}(\Delta_{vb})}{(\epsilon_b-\epsilon_i)^2}\,. \tag{5.55}$$

These are not found via the perturbative analysis but are present in the redefined vacuum state approach. They are obtained as the interplay among terms generated from the ladder reducible 1 terms, upon the symmetrisation of the energy flow in the loop, and four-electron reducible

[7] See remarks below Eqs. (32, 35, 37) in Ref. [140].

[8] The same problem was met when comparing the two-photon-exchange expressions with the ones derived by Sapirstein and Cheng, see below Eq. (3.95).

1 terms. The former originates from H_1 while the latter originates from F_2. They look like four-electron reducible 1 contribution, due to the absence of the ω integration. According to the gauge invariance of the three-electron S(VP)E subset of the two-photon-exchange corrections, they should be incorporated in the three-electron contribution of the three-photon-exchange corrections. The structure of these terms suggests them to be included in the reducible 1 contribution. The last point to be made concerning these two terms is that they are obviously IR finite.

The reducible 2 type contains only ladder reducible 2 terms, the IR free one [$\Delta E^{(3\mathrm{I})3\mathrm{e,lad,red2}}_{v,\,\mathrm{IR\ free}}$ (A.51, A.52)] , and the IR divergent one [$\Delta E^{(3\mathrm{I})3\mathrm{e,lad,red2}}_{v,\,\mathrm{IR\ div}}$ (A.49, A.50)]. The expressions obtained from the two different methods are identical.

Overall, a reasonable agreement is met and the comparison made strongly suggests the absence of mistakes in the derived expressions. Stated differently, if errors occurred in the different three-electron types, one would expect to see repercussions in the four-electron contribution. The four-electron contribution would suffer from discrepancies between the two methods, which is not the case. Thereby, it hints towards a decent agreement between both approaches, and is moreover a good sanity check of the obtained formulas. The perturbation theory approach also helped to sort out the three- and four-electron contributions, especially for the extra terms given in Eqs. (5.54, 5.55). Last, but not least, a successful verification was also carried out for the three-electron contribution with the g-factor formulas derived in Ref. [105], under the replacement (5.42). Note that the extra terms are also present in those formulas; they manifest themselves when one proceeds towards numerical evaluations[9]. In summary, the gathered cluster of clues points towards the consistency and the absence of mistakes of the derived formulas.
Concerning the separation into the proposed GI subsets, S[V(VP)P]E and S(VP)EVP, the cancellation of IR divergences by elements from the same subset is very assuring. A numerical evaluation of the derived expressions is the sole way to either infirm this statement, based on analytical considerations, or confirm it and turn it into a claim.

[9]Private communication with A. Volotka.

CHAPTER 6.

CONCLUSION AND OUTLOOKS

In recent years, the accuracy of large-scale correlation calculations of transition energies in many-electron atoms and ions drastically improved [30, 54, 60, 150–152]. Various highly efficient computer codes have been developed for this purpose [56, 133, 134, 153–158]. In view of this rapid progress, it becomes increasingly important to include QED effects in these calculations as well. At present, such an account is mainly based on the approximate treatment via QED model potentials [159, 160]. Even though effective methods provide access to higher-order contributions, it is usually not clear how one can reliably estimate the accuracy of the results. In contrast, *ab initio* calculations are more accurate up to the corresponding order and allow for a good control over uncertainties. However, *ab initio* QED calculations for many-electron atoms constitute a rather difficult problem. The first step towards these challenging calculations is to develop the framework that simplifies the derivation of the BSQED formulas. In this thesis, an efficient method was presented in details, based on the vacuum state redefinition and the TTGF approach, to derive calculationally tractable expressions within the rigorous BSQED framework. A redefined vacuum state allows to drastically reduce the complexity of the many-electron *ab initio* QED formulation, keeping only valence electrons or vacancies under consideration. Contributions to the binding energy are expressed in terms of Green's function matrix elements involving active particles (electrons or holes) only. The interaction of these active particles with core electrons is included via the consideration of radiative corrections.

The spectral representation of the two-time Green's function, in a redefined vacuum state, showed a odd-parity symmetry between the energy shift of an N-valence state and the one of an N-hole state, with respect to the redefined Fermi level (separating the dynamics into "core" and "valence" electrons). This odd-parity claim was stated within the RMBPT realm [101] but was so far not established in a field theoretical framework. It is manifest for the single-particle case, and can furthermore be extended to any N-particle state. The single-electron state over closed shells served as an illustrative example to introduce the techniques of the formalism. It was shown that the one-particle GI subsets, in the effective one-particle approach, are transcribed to the many-electron frame. This explained the numerically observed gauge invariance [72] among the direct and exchange parts in the loop contribution to the two-photon-exchange corrections. Building on this ability to transcript GI subsets from one framework to the other,

the complete second-order corrections in the fine-structure constant were investigated and the GI subsets were identified in the many-electron description. The two-photon-exchange-corrections extraction and analysis was carried out for a single-valence electron state, whereas the screened-radiative corrections were tackled for the single-hole state. In both cases, the derivation was performed in the extended Furry picture, thus, the presence of a counterpotential, its associated diagrams and GI subsets. The decomposition in GI subsets was demonstrated, for the two-photon-exchange corrections, both analytically and numerically. Moreover, a different initial equal-time choice for the TTGF enables to consider systems with neutrally charged states, which was not possible in Shabaev's framework. The proper two-time Green's function suited for a valence-hole excitation in closed-shell systems, within the rigorous BSQED framework, was derived in the redefined vacuum state formalism. Its spectral representation confirms the poles at valence-hole excitation energies. A contour integral formula, which connects the energy shift and the Green's function was derived. The complete first-order corrections were considered and the explicit formulas were derived. The resulting expressions were mapped to the standard vacuum state case and the GI subsets were identified. These results can readily be applied for the rigorous BSQED calculations of the transition energies in a closed-shell system. The one-photon-exchange formula, upon Breit approximation, matches with the RMBPT expression derived in Ref. [101]. This constitutes a sound validation of the framework devised.

The method based on a vacuum state redefinition in QED has been shown, in this thesis, to be a well-suited tool to tackle atoms with a complicated electronic structure. In contrast to other methods, it permits the identification of GI subsets and, thus, checks the consistency of the obtained results. Developing on this intrinsic characteristic, and to highlight the possibility to apply the formalism for advanced calculations, an investigation on third-order interelectronic corrections was carried out. The three-photon-exchange formulas were derived for two expected-to-be GI subsets arising from two classes of one-particle three-loop Feynman diagrams. An independent derivation was conducted with the help of perturbation theory. It helped to resolve the different reducible types (red1 and red2) and to sort out the distribution of different terms (three-electron and four-electron) in each contribution of the subsets (S[V(VP)P]E and S(VP)EVP). A reasonable agreement among the two results was met. The explicit cancellation of IR divergences, within each subset, is very assuring.

The presented redefined vacuum state approach can be further employed for atoms with a (more) sophisticated electronic structure, as it allows to focus only on the particles that differentiate between the configurations. Moreover, the identification of GI expressions within this approach paves the way for calculating higher-order corrections, which can be split into GI subsets and tackled one after the other. This asset can be very useful in future derivations of higher-order contributions since it provides a robust verification.

APPENDIX A.

APPENDICES

"Le savant n'étudie pas la nature parce que cela est utile;
il l'étudie parce qu'il y prend plaisir,
et il y prend plaisir parce qu'elle est belle."
— Henri Poincaré, 1854–1912

A.1. Renormalization of the free-electron self-energy and vertex operators

The renormalization procedure was developed, in the Feynman gauge, in Refs. [161–163] for the one-loop radiative corrections; the self-energy operator and the vertex operator [1]. The two-loop case was addressed in Ref. [165]. In the Coulomb gauge, the renormalization procedure was presented by Adkins, in Ref. [166] for the electron self-energy loop, in Ref. [167] for the vertex function, and summarized in Ref. [168]. Ref. [169] deals with the two-loop case.

The results presented in this appendix are those found in Ref. [163]. The free-electron self-energy operator in the Feynman gauge reads

$$\Sigma^{(0)}(p) = -4\pi i\alpha \int \frac{d^4k}{(2\pi)^4}\frac{1}{k^2}\gamma_\sigma \frac{\not{p} - \not{k} + \mathrm{m}_e}{(p-k)^2 - \mathrm{m}_e^2}\gamma^\sigma \,. \tag{A.1}$$

This expression is ultraviolet divergent (high k regime) but remains finite in the infrared (low k regime). In a covariant regularization scheme, such as the dimensional regularization one, with $d = 4 - 2\epsilon$, it can be shown to be logarithmically divergent. The ultraviolet divergence part of Z_2, the electron field-strength renormalization constant, is separated as follow

$$\Sigma^{(0)}(p) = \delta\mathrm{m}_e - \frac{\alpha}{4\pi}\left(\not{p} - \mathrm{m}_e\right)\frac{1}{\tilde{\epsilon}} + \Sigma_R^{(0)}(p)\,, \tag{A.2}$$

[1] Tadpole, or vacuum-polarization diagram vanishes in free QED due to Furry's theorem [164].

with

$$\delta \mathrm{m}_e = \frac{3\alpha}{4\pi}\mathrm{m}_e\left(\frac{1}{\tilde{\epsilon}}+\frac{4}{3}\right) \tag{A.3}$$

and

$$\frac{1}{\tilde{\epsilon}} = \frac{1}{\epsilon} - \gamma_E + \ln\left(\frac{4\pi}{\mathrm{m}_e^2}\right). \tag{A.4}$$

γ_E is the Euler-Mascheroni constant. The renormalized self-energy operator is given by

$$\Sigma_R^{(0)}(p) = \frac{\alpha}{4\pi}\left[a(\rho) + b(\rho)\not{p}\right], \tag{A.5}$$

with

$$a(\rho) = 2\left(1+\frac{2\rho}{1-\rho}\ln\rho\right), \tag{A.6}$$

$$b(\rho) = -\frac{2-\rho}{1-\rho}\left(1+\frac{\rho}{1-\rho}\ln\rho\right), \tag{A.7}$$

where $\rho = (\mathrm{m}_e^2 - p^2)/\mathrm{m}_e^2$.

The free-electron vertex operator in the Feynman gauge is

$$\Gamma^\mu(p',p) = -4\pi i\alpha\int\frac{d^4k}{(2\pi)^4}\frac{1}{k^2}\gamma_\sigma\frac{\not{p}'-\not{k}+\mathrm{m}_e}{(p'-k)^2-\mathrm{m}_e^2}\gamma^\mu\frac{\not{p}-\not{k}+\mathrm{m}_e}{(p-k)^2-\mathrm{m}_e^2}\gamma^\sigma. \tag{A.8}$$

This expression is ultraviolet divergent (high k regime) but remains finite in the infrared (low k regime). As in the previous case, dimensional regularization handles the logarithmic divergence. Only the ultraviolet divergent part of Z_1, the vertex renormalization constant, is separated

$$\Gamma^\mu(p',p) = \frac{\alpha}{4\pi}\gamma^\mu\frac{1}{\tilde{\epsilon}} + \Gamma_R^\mu(p',p). \tag{A.9}$$

For the sake of brevity, and because the renormalization condition is given for zero momentum transfer, $q = p - p' = 0$, [see Eq. (2.17)], the renormalized expression for identical argument is displayed

$$\Gamma_R^\mu(p,p) = \frac{\alpha}{4\pi}\left[b_1(\rho)\gamma^\mu + b_2(\rho)\not{p}p^\mu + b_3(\rho)p^\mu\right], \tag{A.10}$$

where

$$b_1(\rho) = \frac{2-\rho}{1-\rho}\left(1+\frac{\rho}{1-\rho}\ln\rho\right), \tag{A.11}$$

$$b_2(\rho) = -\frac{2}{(1-\rho)^2}\left(3-\rho+\frac{2}{1-\rho}\ln\rho\right), \tag{A.12}$$

$$b_3(\rho) = \frac{8}{1-\rho}\left(1+\frac{1}{1-\rho}\ln\rho\right). \tag{A.13}$$

A.2. Convergence plots for the principal values contributions in the truncated κ expansion

Sparse details were provided in section 3.2.2, especially concerning the convergence of the computed values. This is a important concern in achieving numerical results, see for example Mohr's original papers on the evaluation of the self-energy correction to $1s_{1/2}$ state in hydrogen-like system [161, 170]. Hence, the following figures are presented to show the convergence for the principal values contributions in the truncated κ expansion, the most time-consuming numerical step (ranging from a day to a week of calculation's time).

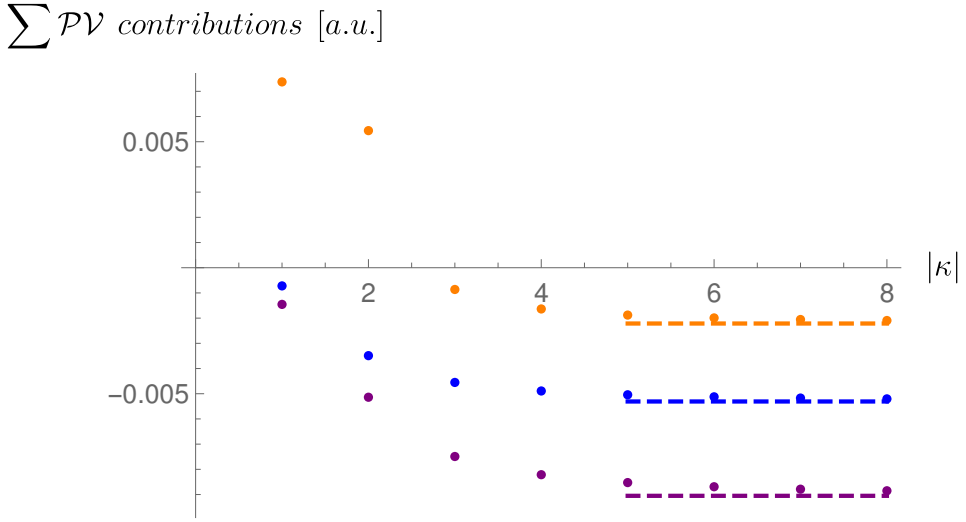

Figure A.1.: Sum of the principal value ($\mathcal{PV}$) contributions for each κ ranging from 0 to 8, in absolute value. The dashed line represents the value obtained after fitting the values. Computations are carried out for the $2s$ (blue), $2p_{1/2}$ (purple) and $2p_{3/2}$ (orange) state in the Coulomb gauge, using $N_{basis} = 80$ basis functions for Lithium-like Uranium ($Z = 92$). Kohn-Sham potential is used as the starting screening potential (extended Furry picture).

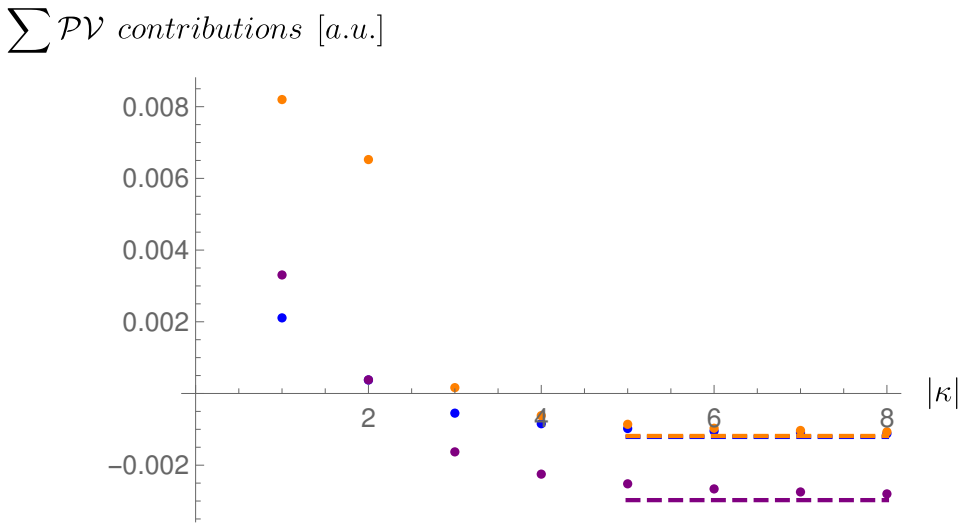

Figure A.2.: Sum of the principal value ($\mathcal{PV}$) contributions for each κ ranging from 0 to 8, in absolute value. The dashed line represents the value obtained after fitting the values. Computations are carried out for the the $2s$ (blue), $2p_{1/2}$ (purple) and $2p_{3/2}$ (orange) state in the Feynman gauge, using $N_{basis} = 80$ basis functions for Lithium-like Bismuth ($Z = 83$). Kohn-Sham potential is used as the starting starting screening potential (extended Furry picture).

Note that only the values computed for $N_{\text{basis}} = 80$ are presented, since the difference in the values obtained with $N_{\text{basis}} = 40$ and $N_{\text{basis}} = 60$ are tiny, and therefore difficult to observe on a figure, see below.

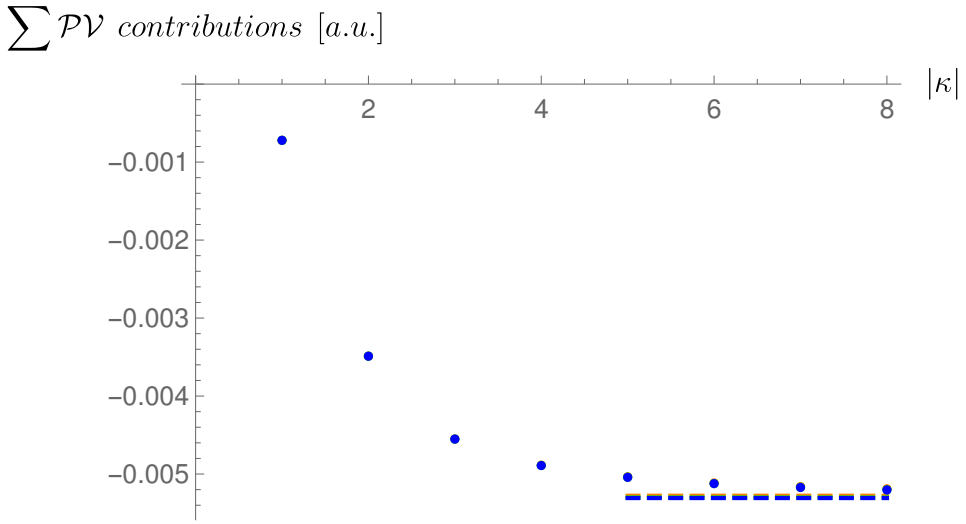

Figure A.3.: Sum of the principal value ($\mathcal{PV}$) contributions for each κ ranging from 0 to 8, in absolute value. The dashed line represents the value obtained after fitting the values. Computations are carried out for the $2s$ state for $N_{basis} = 40$ (orange), $N_{basis} = 60$ (green) and$N_{basis} = 80$ (blue), in the Coulomb gauge, for Lithium-like Uranium ($Z = 92$). Kohn-Sham potential is used as the starting screening potential (extended Furry picture).

The least-squares inverse polynomial fitting provides a fitted value starting from $|\kappa| = 5$, since a fourth-order polynomial is used. The summation over κ is truncated once the error/uncertainty of the fitted value is below the error of the sum, which includes the last contribution in the κ-expansion. The uncertainty of the fitted values is usually of the order of $1,..\times 10^{-6}$ a.u.. The fitted values are added to the pole contributions arising from both the direct and exchange part. This final value is then extrapolated, applying a linear regression in $1/N_{\text{basis}}$, to infer $N_{\text{basis}} \to \infty$ limit. This extrapolated value is the one displayed in the two tables.

A.3. Two-photon-exchange gauge-invariant subsets in extended Furry picture

	$2s$		$2p_{1/2}$		$2p_{3/2}$	
	Feynman	Coulomb	Feynman	Coulomb	Feynman	Coulomb
SESE,2e,irr	0.027109	0.030293	0.023004	0.026182	0.027727	0.031227
SESE,2e,red	0.002958	-0.000226	0.002785	-0.000394	0.003631	0.000130
SESE,2e	0.030067	0.030066	0.025789	0.025789	0.031358	0.031357
S(VP)E,2e,irr	-0.189003	-0.188689	-0.324700	-0.324633	-0.214022	-0.213855
S(VP)E,2e,red	0.000316	0.000001	0.000048	-0.000019	0.000164	-0.000002
S(VP)E,2e	-0.188687	-0.188688	-0.324652	-0.324652	-0.213857	-0.213857
SESE,3e,irr	-0.026394	-0.027326	-0.016618	-0.018611	-0.022634	-0.024685
SESE,3e,red	-0.000886	0.000048	-0.002033	-0.000040	-0.002437	-0.000386
SESE,3e	-0.027280	-0.027280	-0.018651	-0.018651	-0.025071	-0.025071
SEVP,3e,irr	0.035830	0.037949	0.019778	0.024279	0.038359	0.042952
SEVP,3e,red	0.002009	-0.000110	0.004585	0.000085	0.005452	0.000859
SEVP,3e	0.037839	0.037839	0.024364	0.024364	0.043811	0.043811
S(VP)E,3e,irr	0.177970	0.177851	0.308182	0.308145	0.200231	0.200128
S(VP)E,3e,red	-0.000119	0.000000	-0.000037	0.000001	-0.000122	-0.000018
S(VP)E,3e	0.177851	0.177851	0.308145	0.308146	0.200109	0.200110
VPVP,3e	-0.306234	-0.306234	-0.488841	-0.488841	-0.436894	-0.436894
V(VP)P,3e	-0.049365	-0.049365	-0.036796	-0.036796	-0.028280	-0.028280
V(SE)P,3e,irr	0.021462	0.021462	0.016290	0.016290	0.012550	0.012550
SECP,irr	-0.035830	-0.037949	-0.019778	-0.024279	-0.038359	-0.042952
SECP,red	-0.002009	0.000110	-0.004585	-0.000085	-0.005452	-0.000859
SECP	-0.037839	-0.037839	-0.024364	-0.024364	-0.043811	-0.043811
VPCP	0.661834	0.661834	1.014480	1.014480	0.902069	0.902069
CPCP	-0.306235		-0.488842		-0.436895	
Total	0.013412	0.013410	0.006921	0.006921	0.005089	0.005088

Table A.1.: Contributions of the identified gauge-invariant subsets to the two-photon exchange corrections for the $2s$, $2p_{1/2}$, and $2p_{3/2}$ states of the Li-like Sn ($Z = 50$) ion, in atomic units. The values are obtained within the extended Furry picture (core-Hartree potential). The results of the Feynman and Coulomb gauges are given. The Fermi model of the nuclear charge distribution is employed.

A.4. Two-photon-exchange corrections: matching between QED and RMBPT

The expressions in Eq. (3.99) are derived for the first time and require a critical view. Therefore, the Breit approximation is applied to the expressions presented in Eqs. (3.94)–(3.97), under a sign flip and the exchange $v \to h$ of the labels. The outcome is compared with the RMBPT expressions of Ref. [101]. To this end, let us first introduce the interelectronic-interaction operator in the Breit approximation:

$$I^B = I_{\rm C}(0)\,, \tag{A.14}$$

where "C" means the Coulomb gauge. Since I^B is ω-independent, the reducible contributions, which contain derivatives of I, vanish within this approximation. The second implication of the Breit approximation is to consider only the positive-energy states in summations, i.e.,

$$\sum_i = \sum_m + \sum_a, \tag{A.15}$$

where now i (and later j) means only positive-energy state, m (and later n) is an excited state, $\epsilon_m > E^F_\alpha > 0$, and a (and b) denotes one of the core states, $0 < \epsilon_a < E^F_\alpha$. One first applies the Breit approximation to the three-electron contribution, composed of Eqs. (3.96) and (3.97) , which is rewritten as follows,

$$\begin{aligned}\Delta E_h^{(2{\rm I})3{\rm e,B}} = &-\sum_{a,b,m} \frac{2\left[I^B_{mbab} - I^B_{mbba}\right]\left[I^B_{hahm} - I^B_{hamh}\right]}{\epsilon_a - \epsilon_m} - \sum_{a,b,i}^{i\neq h} \frac{\left[I^B_{haai} - I^B_{haia}\right]\left[I^B_{ibbh} - I^B_{ibhb}\right]}{\epsilon_h - \epsilon_i} \\ &- \sum_{a,b,m} \frac{\left[I^B_{abmh} - I^B_{abhm}\right] I^B_{hmab}}{\epsilon_a + \epsilon_b - \epsilon_h - \epsilon_m} - \sum_{a,b,m} \frac{\left[I^B_{habm} - I^B_{hamb}\right]\left[I^B_{bmah} - I^B_{bmha}\right]}{\epsilon_h + \epsilon_a - \epsilon_b - \epsilon_m}\,,\end{aligned} \tag{A.16}$$

and

$$\Delta E_h^{(2{\rm I}){\rm CP,B}} = -\sum_{a,i}^{i\neq h} \frac{2U_{hi}\left[I^B_{iaah} - I^B_{iaha}\right]}{\epsilon_h - \epsilon_i} - \sum_{a,m} \frac{2U_{am}\left[I^B_{hmah} - I^B_{hmha}\right]}{\epsilon_a - \epsilon_m} - \sum_{i}^{i\neq h} \frac{U_{hi}U_{ih}}{\epsilon_h - \epsilon_i}\,. \tag{A.17}$$

The summations were rewritten using Eq. (A.15). Notice that the core-electron contribution vanishes altogether upon relabeling of the indices and applying the symmetry propertie (2.38).

Furthermore, sums involving ϵ_h in the denominators are kept intact since the energy of the hole state lies in the positive-energy spectrum. The replacement also allows one to remove the restrictions in all the other sums.

It is left to evaluate the two-electron contribution. Recall that the integration path closes in the upper-half of the complex plane ,to consider only positive intermediate energy states, and that no reducible contributions are present. Let us divide the expressions in Eq. (3.94) into ladder and crossed parts, namely, the first and third terms are the direct- and exchange-ladder parts respectively and the second and the fourth are the direct- and exchange-crossed ones respectively. One starts by showing that both crossed parts vanish due to their pole structure. The crossed-exchange poles are $\omega = \epsilon_h - \epsilon_{i,j} + i\varepsilon$ and the crossed-direct poles are $\omega = \epsilon_h - \epsilon_i + i\varepsilon$ and $\omega = \epsilon_a - \epsilon_j + i\varepsilon$, for $\epsilon_i, \epsilon_j > E_\alpha^F$. It leads to the corresponding residue integration

$$\Delta E_h^{(2\mathrm{I})\mathrm{cr,B}} = \frac{i}{2\pi}\int d\omega \sum_{a,i,j}\left[\frac{I^B_{hjih}I^B_{iaaj}}{(\epsilon_h-\omega-\epsilon_i u)(\epsilon_h-\omega-\epsilon_j u)} - \frac{I^B_{hjia}I^B_{iahj}}{(\epsilon_h-\omega-\epsilon_i u)(\epsilon_a-\omega-\epsilon_j u)}\right] = 0\,. \tag{A.18}$$

Next, one inspects the ladder poles, which are found to be in $\omega = \epsilon_h - \epsilon_i + i\varepsilon$ and $\omega = \epsilon_j - \epsilon_a - i\varepsilon$, same for both direct and exchange parts. Performing the Cauchy integration, one finds

$$\begin{aligned}\Delta E_h^{(2\mathrm{I})\mathrm{lad,B}} &= \frac{i}{2\pi}\int d\omega \sum_{a,i,j}^{(i,j)\neq(a,h)}\left[\frac{I^B_{haij}I^B_{ijah} - I^B_{haij}I^B_{ijha}}{(\epsilon_h-\omega-\epsilon_i u)(\epsilon_a+\omega-\epsilon_j u)}\right] \\ &= \sum_{a,i,j}^{(i,j)\neq(a,h)}\frac{I^B_{haij}I^B_{ijah} - I^B_{haij}I^B_{ijha}}{\epsilon_h+\epsilon_a-\epsilon_i-\epsilon_j} \\ &= \sum_{a,m,n}\frac{I^B_{hamn}\left[I^B_{mnah} - I^B_{mnha}\right]}{\epsilon_h+\epsilon_a-\epsilon_m-\epsilon_n} - \sum_{a,b,m}\frac{\left[I^B_{hamb} - I^B_{habm}\right]\left[I^B_{mbha} - I^B_{mbah}\right]}{\epsilon_h+\epsilon_a-\epsilon_b-\epsilon_m}\,,\end{aligned} \tag{A.19}$$

where the first term in the last line is the one sought, while the second one compensates the fourth sum in Eq. (A.16). Thus, the final expression for the two-photon-exchange corrections

within the Breit approximation yields

$$\begin{aligned}\Delta E_h^{(2\mathrm{I})\mathrm{B}} = &-\sum_{a,b,m}\frac{2\left[I^B_{mbab}-I^B_{mbba}\right]\left[I^B_{hahm}-I^B_{hamh}\right]}{\epsilon_a-\epsilon_m}-\sum_{a,b,i}^{i\neq h}\frac{\left[I^B_{haai}-I^B_{haia}\right]\left[I^B_{ibbh}-I^B_{ibhb}\right]}{\epsilon_h-\epsilon_i}\\ &-\sum_{a,b,m}\frac{\left[I^B_{abmh}-I^B_{abhm}\right]I^B_{hmab}}{\epsilon_a+\epsilon_b-\epsilon_h-\epsilon_m}-\sum_{a,m,n}\frac{I^B_{hamn}\left[I^B_{mnha}-I^B_{mnah}\right]}{\epsilon_h+\epsilon_a-\epsilon_m-\epsilon_n}\\ &-\sum_{a,i}^{i\neq h}\frac{2U_{hi}\left[I^B_{iaah}-I^B_{iaha}\right]}{\epsilon_h-\epsilon_i}-\sum_{a,m}\frac{2U_{am}\left[I^B_{hmah}-I^B_{hmha}\right]}{\epsilon_a-\epsilon_m}-\sum_{i}^{i\neq h}\frac{U_{hi}U_{ih}}{\epsilon_h-\epsilon_i}\,,\end{aligned}\tag{A.20}$$

which is in full agreement with the RMBPT result of Ref. [101].

A.5. Valence-hole zeroth-order Green function

Here, the zeroth-order Green's function in Eq. (4.16) is calculated explicitly. The reason for the previously added terms and the role of prefactors will become clearer. Let us start by expressing the matrix element of the zero-order Green's function as

$$\begin{aligned}&\langle(vh)_{JM}|g^{(0)}_\alpha(E)|(vh)_{JM}\rangle\\ &\qquad=F_{vh}F_{vh}\langle\alpha|b_h a_v\left[\frac{1}{2!}\int d^3x_1d^3x_2d^3y_1d^3y_2\tilde{\mathcal{S}}(E;\mathbf{x}_1,\mathbf{x}_2;\mathbf{y}_1,\mathbf{y}_2)\right]a_v^\dagger b_h^\dagger|\alpha\rangle\,,\end{aligned}\tag{A.21}$$

where

$$\begin{aligned}&\tilde{\mathcal{S}}(E;\mathbf{x}_1,\mathbf{x}_2;\mathbf{y}_1,\mathbf{y}_2)\\ &\quad=\sum_{\epsilon_i,\epsilon_l>E^F_\alpha,\epsilon_j,\epsilon_k<E^F_\alpha}a_i^\dagger a_l b_k^\dagger b_j\left[\phi_i^\dagger(\mathbf{x}_1)\phi_j^\dagger(\mathbf{x}_2)\mathcal{G}^{(0)}_\alpha(E;\mathbf{x}_1,\mathbf{x}_2;\mathbf{y}_1,\mathbf{y}_2)\gamma_1^0\gamma_2^0\phi_k(\mathbf{y}_1)\phi_l(\mathbf{y}_2)\right]\\ &\quad+\sum_{\epsilon_j,\epsilon_k>E^F_\alpha,\epsilon_i,\epsilon_l<E^F_\alpha}a_j^\dagger a_k b_l^\dagger b_i\left[\phi_i^\dagger(\mathbf{x}_1)\phi_j^\dagger(\mathbf{x}_2)\mathcal{G}^{(0)}_\alpha(E;\mathbf{x}_1,\mathbf{x}_2;\mathbf{y}_1,\mathbf{y}_2)\gamma_1^0\gamma_2^0\phi_k(\mathbf{y}_1)\phi_l(\mathbf{y}_2)\right]\\ &\quad-\sum_{\epsilon_i,\epsilon_k>E^F_\alpha,\epsilon_j,\epsilon_l<E^F_\alpha}a_i^\dagger a_k b_l^\dagger b_j\left[\phi_i^\dagger(\mathbf{x}_1)\phi_j^\dagger(\mathbf{x}_2)\mathcal{G}^{(0)}_\alpha(E;\mathbf{x}_1,\mathbf{x}_2;\mathbf{y}_1,\mathbf{y}_2)\gamma_1^0\gamma_2^0\phi_k(\mathbf{y}_1)\phi_l(\mathbf{y}_2)\right]\\ &\quad-\sum_{\epsilon_j,\epsilon_l>E^F_\alpha,\epsilon_i,\epsilon_k<E^F_\alpha}a_j^\dagger a_l b_k^\dagger b_i\left[\phi_i^\dagger(\mathbf{x}_1)\phi_j^\dagger(\mathbf{x}_2)\mathcal{G}^{(0)}_\alpha(E;\mathbf{x}_1,\mathbf{x}_2;\mathbf{y}_1,\mathbf{y}_2)\gamma_1^0\gamma_2^0\phi_k(\mathbf{y}_1)\phi_l(\mathbf{y}_2)\right]\,.\end{aligned}\tag{A.22}$$

The zeroth-order spectral representation of the Green's function is given by

$$\mathcal{G}_{\alpha}^{(0)}(E;\mathbf{x}_1,\mathbf{x}_2;\mathbf{y}_1,\mathbf{y}_2) = \frac{1}{2!}\frac{\mathcal{A}_{vh}^{(0)}(\mathbf{x}_1,\mathbf{x}_2;\mathbf{y}_1,\mathbf{y}_2)}{E - E_{vh}^{(0)} + i\varepsilon}\,, \tag{A.23}$$

with

$$\begin{aligned}\mathcal{A}_{vh}^{(0)}(\mathbf{x}_1,\mathbf{x}_2;\mathbf{y}_1,\mathbf{y}_2) = \langle\alpha|\,\Big[&\psi_{\alpha}^{(0)}(0,\mathbf{x}_1)\bar{\psi}_{\alpha}^{(0)}(0,\mathbf{y}_1)|(vh)_{JM}\rangle\langle(vh)_{JM}|\psi_{\alpha}^{(0)}(0,\mathbf{x}_2)\bar{\psi}_{\alpha}^{(0)}(0,\mathbf{y}_2)\\ &- \psi_{\alpha}^{(0)}(0,\mathbf{x}_2)\bar{\psi}_{\alpha}^{(0)}(0,\mathbf{y}_1)|(vh)_{JM}\rangle\langle(vh)_{JM}|\psi_{\alpha}^{(0)}(0,\mathbf{x}_1)\bar{\psi}_{\alpha}^{(0)}(0,\mathbf{y}_2)\\ &- \psi_{\alpha}^{(0)}(0,\mathbf{x}_1)\bar{\psi}_{\alpha}^{(0)}(0,\mathbf{y}_2)|(vh)_{JM}\rangle\langle(vh)_{JM}|\psi_{\alpha}^{(0)}(0,\mathbf{x}_2)\bar{\psi}_{\alpha}^{(0)}(0,\mathbf{y}_1)\\ &+ \psi_{\alpha}^{(0)}(0,\mathbf{x}_2)\bar{\psi}_{\alpha}^{(0)}(0,\mathbf{y}_2)|(vh)_{JM}\rangle\langle(vh)_{JM}|\psi_{\alpha}^{(0)}(0,\mathbf{x}_1)\bar{\psi}_{\alpha}^{(0)}(0,\mathbf{y}_1)\Big]\,|\alpha\rangle\,.\end{aligned} \tag{A.24}$$

As a first step the previous expression, $\mathcal{A}_{vh}^{(0)}(\mathbf{x}_1,\mathbf{x}_2;\mathbf{y}_1,\mathbf{y}_2)$, can be further evaluated. Recalling that $a_i|\alpha\rangle = 0$, $b_j|\alpha\rangle = 0$, $\bar{\psi} = \psi^{\dagger}\gamma^0$, and $F_{vh}F_{vh} = 1$, one easily gets

$$\mathcal{A}_{vh}^{(0)}(\mathbf{x}_1,\mathbf{x}_2;\mathbf{y}_1,\mathbf{y}_2) = \left[\phi_v(\mathbf{x}_1)\phi_h(\mathbf{x}_2) - \phi_h(\mathbf{x}_1)\phi_v(\mathbf{x}_2)\right]\left[\bar{\phi}_h(\mathbf{y}_1)\bar{\phi}_v(\mathbf{y}_2) - \bar{\phi}_v(\mathbf{y}_1)\bar{\phi}_h(\mathbf{y}_2)\right]\,. \tag{A.25}$$

Two comments should be made at this point. If one were to consider Eq. (4.3), only the first term from the above expanded expression would be found. Furthermore, in Eq. (4.9), a factor $\frac{1}{2!}$ was introduced. The reason is to get a proper normalized two-body wave-function in the non-interacting case, as will be seen in the following. Using Eq. (4.11), one contracts the operators to obtain

$$\begin{aligned}&\langle(vh)_{JM}|g_{\alpha}^{(0)}(E)|(vh)_{JM}\rangle \\ &\quad= \frac{1}{2!}\left[g_{\alpha,v_1h_2h_1v_2}^{(0)}(E) - g_{\alpha,v_1h_2v_2h_1}^{(0)}(E) + g_{\alpha,h_2v_1v_2h_1}^{(0)}(E) - g_{\alpha,h_2v_1h_1v_2}^{(0)}(E)\right]\,,\end{aligned} \tag{A.26}$$

which can be rewritten according to Eq. (4.12) as

$$\begin{aligned}\langle (vh)_{JM}|g_{\alpha}^{(0)}(E)|(vh)_{JM}\rangle &= \frac{1}{E-E_{vh}^{(0)}+i\varepsilon} \\ &\times \int d^3x_1 d^3x_2 \frac{1}{2!}\left[\phi_v^\dagger(\mathbf{x}_1)\phi_h^\dagger(\mathbf{x}_2)-\phi_h^\dagger(\mathbf{x}_1)\phi_v^\dagger(\mathbf{x}_2)\right]\left[\phi_v(\mathbf{x}_1)\phi_h(\mathbf{x}_2)-\phi_h(\mathbf{x}_1)\phi_v(\mathbf{x}_2)\right] \\ &\times \int d^3y_1 d^3y_2 \frac{1}{2!}\left[\phi_h^\dagger(\mathbf{y}_1)\phi_v^\dagger(\mathbf{y}_2)-\phi_v^\dagger(\mathbf{y}_1)\phi_h^\dagger(\mathbf{y}_2)\right]\left[\phi_h(\mathbf{y}_1)\phi_v(\mathbf{y}_2)-\phi_v(\mathbf{y}_1)\phi_h(\mathbf{y}_2)\right] \\ &= \frac{1}{E-E_{vh}^{0}+i\varepsilon}\,. \end{aligned} \tag{A.27}$$

A.6. Third-order interelectronic corrections derived by a perturbative treatment

A.6.1. Four-electron subset

One perturbs the S(VP)E three-electron expressions (3.81, 3.82) according to Eqs. (5.38–5.41) and finds, under the replacement (5.42), three different types of four-electron contribution: irreducible (irr), reducible 1 (red1) and reducible 2 (red2). They are displayed below, and furthermore separated into S(V(VP)P)E and S(VP)VP subsets. This separation relies on the redefined vacuum state analysis and its comparison with the perturbative one.

Irreducible terms

The four-electron irreducible contribution is found to be

$$\begin{aligned}
\Delta E^{(3\mathrm{I})4\mathrm{e,irr}}_{v,\,\mathrm{S(VP)EVP}} = &- \sum_{a,b,c,i,j}^{j\neq v,(i,c)\neq(v,b)} \left\{ \frac{I_{avaj}(0)\left[I_{jbci}(\Delta_{vc})I_{civb}(\Delta_{vc}) + I_{jbic}(\Delta_{cb})I_{icvb}(\Delta_{cb})\right]}{(\epsilon_v+\epsilon_b-\epsilon_c-\epsilon_i)(\epsilon_v-\epsilon_j)} \right. \\
&\left. + \frac{\left[I_{cijb}(\Delta_{vc})I_{vbci}(\Delta_{vc}) + I_{vbic}(\Delta_{cb})I_{icjb}(\Delta_{cb})\right] I_{java}(0)}{(\epsilon_v+\epsilon_b-\epsilon_c-\epsilon_i)(\epsilon_v-\epsilon_j)} \right\} \\
&- \sum_{a,b,c,i,j}^{j\neq v} \frac{I_{avaj}(0)I_{jicb}(\Delta_{vc})I_{cbvi}(\Delta_{vc}) + I_{vicb}(\Delta_{vc})I_{cbji}(\Delta_{vc})I_{java}(0)}{(\epsilon_b+\epsilon_c-\epsilon_v-\epsilon_i)(\epsilon_v-\epsilon_j)} \\
&- \sum_{a,b,c,i,j}^{j\neq c} \frac{I_{vijb}(\Delta_{vc})I_{jaca}(0)I_{cbvi}(\Delta_{vc}) + I_{vicb}(\Delta_{vc})I_{acaj}(0)I_{jbvi}(\Delta_{vc})}{(\epsilon_b+\epsilon_c-\epsilon_v-\epsilon_i)(\epsilon_c-\epsilon_j)} \\
&- \sum_{a,b,c,i,j}^{j\neq c,(i,c)\neq(v,b)} \frac{I_{acaj}(0)I_{vbci}(\Delta_{vc})I_{jivb}(\Delta_{vc}) + I_{vbji}(\Delta_{vc})I_{civb}(\Delta_{vc})I_{jaca}(0)}{(\epsilon_v+\epsilon_b-\epsilon_c-\epsilon_i)(\epsilon_c-\epsilon_j)} \\
&- \sum_{i,j} \frac{I_{vicb}(\Delta_{vc})I_{iaja}(0)I_{cbvj}(\Delta_{vc})}{(\epsilon_b+\epsilon_c-\epsilon_v-\epsilon_i)(\epsilon_b+\epsilon_c-\epsilon_v-\epsilon_j)}\,,
\end{aligned} \tag{A.28}$$

for the S(VP)EVP subset and,

$$\begin{aligned}
\Delta E^{(3\mathrm{I})4\mathrm{e,irr}}_{v,\,\mathrm{S[V(VP)P]E}} = &- \sum_{a,b,c,i,j}^{j\neq b,(i,c)\neq(v,b)} \left\{ \frac{I_{abaj}(0)\left[I_{vjci}(\Delta_{vc})I_{civb}(\Delta_{vc}) + I_{vjic}(\Delta_{cb})I_{icvb}(\Delta_{cb})\right]}{(\epsilon_v+\epsilon_b-\epsilon_c-\epsilon_i)(\epsilon_b-\epsilon_j)} \right. \\
&\left. + \frac{\left[I_{civj}(\Delta_{vc})I_{vbci}(\Delta_{vc}) + I_{vbic}(\Delta_{cb})I_{icvj}(\Delta_{cb})\right] I_{jaba}(0)}{(\epsilon_v+\epsilon_b-\epsilon_c-\epsilon_i)(\epsilon_b-\epsilon_j)} \right\} \\
&- \sum_{a,b,c,i,j}^{j\neq b} \frac{I_{vicj}(\Delta_{vc})I_{jaba}(0)I_{cbvi}(\Delta_{vc}) + I_{vicb}(\Delta_{vc})I_{abaj}(0)I_{cjvi}(\Delta_{vc})}{(\epsilon_b+\epsilon_c-\epsilon_v-\epsilon_i)(\epsilon_b-\epsilon_j)} \\
&- \sum_{a,b,c,i,j}^{(i,c)\neq(v,b),(j,c)\neq(v,b)} \frac{I_{vbci}(\Delta_{vc})I_{iaja}(0)I_{cjvb}(\Delta_{vc}) + I_{vbic}(\Delta_{cb})I_{iaja}(0)I_{jcvb}(\Delta_{cb})}{(\epsilon_v+\epsilon_b-\epsilon_c-\epsilon_i)(\epsilon_v+\epsilon_b-\epsilon_c-\epsilon_j)} \\
&- \sum_{a,b,c,i,j}^{j\neq c,(i,c)\neq(v,b)} \frac{I_{vbij}(\Delta_{cb})I_{icvb}(\Delta_{cb})I_{jaca}(0) + +I_{acaj}(0)I_{vbic}(\Delta_{cb})I_{ijvb}(\Delta_{cb})}{(\epsilon_v+\epsilon_b-\epsilon_c-\epsilon_i)(\epsilon_c-\epsilon_j)}\,,
\end{aligned} \tag{A.29}$$

for the S[V(VP)P]E one.

Reducible 1 terms

The reducible 1 contribution is also split into S(VP)EVP and S[V(VP)P]E subsets, respectively, and can be cast in the form

$$
\begin{aligned}
\Delta E^{(3\mathrm{I})4\mathrm{e,red1}}_{v,\,\mathrm{S(VP)EVP}} = &- \sum_{a,b,b_1,v_1,i}^{i\neq b} \frac{I_{vbb_1v_1}(\Delta_{vb})I_{ab_1ai}(0)I'_{iv_1vb}(\Delta_{vb}) + I_{abai}(0)I_{vib_1v_1}(\Delta_{vb})I'_{b_1v_1vb}(\Delta_{vb})}{(\epsilon_b-\epsilon_i)} \\
&- \sum_{a,b,b_1,v_1,i}^{i\neq v} \frac{I_{vbb_1i}(\Delta_{vb})I_{iav_1a}(0)I'_{b_1v_1vb}(\Delta_{vb}) + I_{vbb_1v_1}(\Delta_{vb})I'_{b_1v_1ib}(\Delta_{vb})I_{iava}(0)}{(\epsilon_v-\epsilon_i)} \\
&- \sum_{a,b,c,v_1,i}^{(i,c)\neq(v,b)} \frac{\left[I_{vbci}(\Delta_{vc})I'_{civb}(\Delta_{vc}) + I'_{vbci}(\Delta_{vc})I_{civb}(\Delta_{vc})\right] I_{v_1av_1a}(0)}{(\epsilon_v+\epsilon_b-\epsilon_c-\epsilon_i)} \\
&+ \sum_{a,b,c,c_1,i}^{(i,c)\neq(v,b)} \frac{\left[I_{vbci}(\Delta_{vc})I'_{civb}(\Delta_{vc}) + I'_{vbci}(\Delta_{vc})I_{civb}(\Delta_{vc})\right] I_{c_1ac_1a}(0)}{(\epsilon_v+\epsilon_b-\epsilon_c-\epsilon_i)} \\
&- \sum_{a,b,c,v_1,i} \frac{\left[I_{vicb}(\Delta_{vc})I'_{cbvi}(\Delta_{vc}) + I'_{vicb}(\Delta_{vc})I_{cbvi}(\Delta_{vc})\right] I_{v_1av_1a}(0)}{(\epsilon_b+\epsilon_c-\epsilon_v-\epsilon_i)} \\
&+ \sum_{a,b,c,c_1,i} \frac{\left[I_{vicb}(\Delta_{vc})I'_{cbvi}(\Delta_{vc}) + I'_{vicb}(\Delta_{vc})I_{cbvi}(\Delta_{vc})\right] I_{c_1ac_1a}(0)}{(\epsilon_b+\epsilon_c-\epsilon_v-\epsilon_i)} \\
&+ \sum_{a,b,c,v_1,i}^{(i,c)\neq(v,b)} \frac{I_{v_1av_1a}(0)\left[I_{vbci}(\Delta_{vc})I_{civb}(\Delta_{vc}) + I_{vbic}(\Delta_{cb})I_{icvb}(\Delta_{cb})\right]}{(\epsilon_v+\epsilon_b-\epsilon_c-\epsilon_i)^2} \\
&- \sum_{a,b,c,v_1,i} \frac{I_{v_1av_1a}(0)I_{vicb}(\Delta_{vc})I_{cbvi}(\Delta_{vc})}{(\epsilon_b+\epsilon_c-\epsilon_v-\epsilon_i)^2} \\
&+ \sum_{a,b,c,c_1,i} \frac{I_{c_1ac_1a}(0)I_{vicb}(\Delta_{vc})I_{cbvi}(\Delta_{vc})}{(\epsilon_b+\epsilon_c-\epsilon_v-\epsilon_i)^2} \\
&- \sum_{a,b,c,c_1,i}^{(i,c)\neq(v,b)} \frac{I_{c_1ac_1a}(0)I_{vbci}(\Delta_{vc})I_{civb}(\Delta_{vc})}{(\epsilon_v+\epsilon_b-\epsilon_c-\epsilon_i)^2},
\end{aligned}
\tag{A.30}
$$

and

$$\begin{aligned}
\Delta E^{(3\mathrm{I})4\mathrm{e,red1}}_{v,\,\mathrm{S[V(VP)P]E}} = &- \sum_{a,b,b_1,v_1,i}^{i\neq v} \frac{I_{avai}(0)\, I_{ibb_1v_1}(\Delta_{vb})\, I'_{b_1v_1vb}(\Delta_{vb}) + I_{vbb_1v_1}(\Delta_{vb})\, I_{av_1ai}(0)\, I'_{b_1ivb}(\Delta_{vb})}{(\epsilon_v - \epsilon_i)} \\
&- \sum_{a,b,b_1,v_1,i}^{i\neq b} \frac{I_{vbb_1v_1}(\Delta_{vb})\, I'_{b_1v_1vi}(\Delta_{vb})\, I_{iaba}(0) + I_{vbiv_1}(\Delta_{vb})\, I_{iab_1a}(0)\, I'_{b_1v_1vb}(\Delta_{vb})}{(\epsilon_b - \epsilon_i)} \\
&- \sum_{a,b,c,c_1,i}^{(i,c)\neq(v,b)} \frac{\left[I_{vbic}(\Delta_{cb})\, I'_{icvb}(\Delta_{cb}) + I'_{vbic}(\Delta_{cb})\, I_{icvb}(\Delta_{cb})\right] I_{c_1ac_1}(0)}{(\epsilon_v + \epsilon_b - \epsilon_c - \epsilon_i)} \\
&+ \sum_{a,b,c,b_1,i}^{(i,c)\neq(v,b)} \frac{\left[I_{vbic}(\Delta_{cb})\, I'_{icvb}(\Delta_{cb}) + I'_{vbic}(\Delta_{cb})\, I_{icvb}(\Delta_{cb})\right] I_{b_1ab_1a}(0)}{(\epsilon_v + \epsilon_b - \epsilon_c - \epsilon_i)} \\
&+ \sum_{a,b,c,b_1,i}^{(i,c)\neq(v,b)} \frac{I_{b_1ab_1a}(0)\left[I_{vbci}(\Delta_{vc})\, I_{civb}(\Delta_{vc}) + I_{vbic}(\Delta_{cb})\, I_{icvb}(\Delta_{cb})\right]}{(\epsilon_v + \epsilon_b - \epsilon_c - \epsilon_i)^2} \\
&+ \sum_{a,b,c,b_1,i} \frac{I_{b_1ab_1a}(0)\, I_{vicb}(\Delta_{vc})\, I_{cbvi}(\Delta_{vc})}{(\epsilon_b + \epsilon_c - \epsilon_v - \epsilon_i)^2} \\
&- \sum_{a,b,c,c_1,i}^{(i,c)\neq(v,b)} \frac{I_{c_1ac_1a}(0)\, I_{vbic}(\Delta_{cb})\, I_{icvb}(\Delta_{cb})}{(\epsilon_v + \epsilon_b - \epsilon_c - \epsilon_i)^2}\,. \qquad \text{(A.31)}
\end{aligned}$$

Reducible 2 terms

Each of the inspected subset participates equally to the reducible 2 contribution. One finds

$$\begin{aligned}
\Delta E^{(3\mathrm{I})4\mathrm{e,red2}}_{v,\,\mathrm{S(VP)EVP}} = &- \frac{1}{2} \sum_{a,b,b_1,v_1,v_2} \left[I_{vbb_1v_1}(\Delta_{vb})\, I''_{b_1v_1vb}(\Delta_{vb}) + I'_{vbb_1v_1}(\Delta_{vb})\, I'_{b_1v_1vb}\right] I_{v_2av_2a}(0) \\
&+ \frac{1}{2} \sum_{a,b,b_1,b_2,v_1} \left[I_{vbb_1v_1}(\Delta_{vb})\, I''_{b_1v_1vb}(\Delta_{vb}) + I'_{vbb_1v_1}(\Delta_{vb})\, I'_{b_1v_1vb}\right] I_{b_2ab_2a}(0)\,, \qquad \text{(A.32)}
\end{aligned}$$

originated from the H diagrams, as well as

$$\begin{aligned}
\Delta E^{(3\mathrm{I})4\mathrm{e,red2}}_{v,\,\mathrm{S[V(VP)P]E}} = &- \frac{1}{2} \sum_{a,b,b_1,v_1,v_2} \left[I_{vbb_1v_1}(\Delta_{vb})\, I''_{b_1v_1vb}(\Delta_{vb}) + I'_{vbb_1v_1}(\Delta_{vb})\, I'_{b_1v_1vb}\right] I_{v_2av_2a}(0) \\
&+ \frac{1}{2} \sum_{a,b,b_1,b_2,v_1} \left[I_{vbb_1v_1}(\Delta_{vb})\, I''_{b_1v_1vb}(\Delta_{vb}) + I'_{vbb_1v_1}(\Delta_{vb})\, I'_{b_1v_1vb}\right] I_{b_2ab_2a}(0)\,, \qquad \text{(A.33)}
\end{aligned}$$

for the F diagrams.

A.6.2. Three-electron subset

The idea would be to proceed similarly as in the four-electron subset; one perturbs the S(VP)E two-electron expressions (3.79, 3.80) according to Eqs. (5.38–5.41) and finds the desired formulas under the replacement (5.42). However, the issue is, as already pointed out by Yerokhin in Ref. [140], that this approach suffers from troubles to deal with reducible terms[2]. He is invoking gauge invariance to fix the problem. If proceeding as explained just above, an identical problem to the one highlighted by Yerokhin is met, namely that the poles differ by the sign of the $i\varepsilon$ prescription[3],

$$\frac{1}{(\omega+i\varepsilon)(-\omega+i\varepsilon)} \quad \text{versus} \quad \frac{1}{(\omega+i\varepsilon)^2} \text{ or } \frac{1}{(-\omega+i\varepsilon)^2}\,, \tag{A.34}$$

when facing ladder reducible 1 contributions, $\Delta E^{(3\mathrm{I})3\mathrm{e,lad,red1}}_{v,\,\mathrm{IR\ div}}$ and $\Delta E^{(3\mathrm{I})3\mathrm{e,lad,red1}}_{v,\,\mathrm{IR\ free}}$. The difference in the topology of the poles arises from unaccounted restrictions in the summations. Nevertheless, for the sake of the verification, it is worth tackling this perturbative analysis and see how far one can get. However, due to this previous discrepancy, the different three-electron terms presented below are those derived within the redefinition of the vacuum state formalism. They are separated into irreducible (irr), reducible 1 (red1) and reducible 2 (red2) types, and moreover into S[V(VP)P]E and S(VP)EVP according to their originated diagrams.

Irreducible terms

The crossed irreducible expression, a new feature showing up at this order, is presented first. A separation according to the belonging to each subset is conducted,

$$\Delta E^{(3\mathrm{I})3\mathrm{e,cross,irr}}_{v,\,\mathrm{S[V(VP)P]E}} = \frac{i}{2\pi}\int d\omega \sum_{a,b,i,j,k}^{k\neq b} \frac{I_{vjib}(\omega)I_{baka}(0)I_{ikvj}(\omega)+I_{vjik}(\omega)I_{kaba}(0)I_{ibvj}(\omega)}{(\epsilon_v-\omega-\epsilon_i u)(\epsilon_b-\omega-\epsilon_j u)\Delta_{bk}}\,, \tag{A.35}$$

[2] See remarks below Eqs. (32, 35, 37) in Ref. [140].

[3] The same problem was met when comparing the two-photon-exchange expressions with the ones derived by Sapirstein and Cheng, see below Eq. (3.95).

$$\Delta E^{(3I)3e,cross,irr}_{v,\,S(VP)EVP} = \frac{i}{2\pi}\int d\omega \sum_{a,b,i,j,k}^{i\neq v} \frac{I_{vaia}(0)I_{ikjb}(\omega)I_{bjkv}(\omega) + I_{vkjb}(\omega)I_{jbik}(\omega)I_{aiav}(0)}{\Delta_{vi}(\epsilon_v - \omega - \epsilon_j u)(\epsilon_b - \omega - \epsilon_k u)}\,. \tag{A.36}$$

Then, the crossed expression, also separated according to their origin diagrams, is displayed,

$$\Delta E^{(3I)3e,cross}_{v,\,S[V(VP)P]E} = \frac{i}{2\pi}\int d\omega \sum_{a,b,i,j,k} \frac{I_{vjib}(\omega)I_{akaj}(0)I_{ibvk}(\omega)}{(\epsilon_v - \omega - \epsilon_i u)(\epsilon_b - \omega - \epsilon_j u)(\epsilon_b - \omega - \epsilon_k u)} \tag{A.37}$$

$$\Delta E^{(3I)3e,cross}_{v,\,S(VP)EVP} = \frac{i}{2\pi}\int d\omega \sum_{a,b,i,j,k} \frac{I_{vkib}(\omega)I_{iaja}(0)I_{bjkv}(\omega)}{(\epsilon_v - \omega - \epsilon_i u)(\epsilon_v - \omega - \epsilon_j u)(\epsilon_b - \omega - \epsilon_k u)}\,. \tag{A.38}$$

Finally, the ladder irreducible expression is found as

$$\begin{aligned}\Delta E^{(3I)3e,lad,irr}_{v,\,S[V(VP)P]E} = \frac{i}{2\pi}\int d\omega \Bigg[&\sum_{a,b,i,j,k}^{k\neq b,\{i,j\}\neq\{v,b\}} \frac{I_{vbij}(\omega)I_{akab}(0)I_{ijvk}(\omega) + I_{vkij}(\omega)I_{abak}(0)I_{ijvb}(\omega)}{(\epsilon_v - \omega - \epsilon_i u)(\epsilon_b + \omega - \epsilon_j u)\Delta_{bk}} \\ &+ \sum_{a,b,i,j,k}^{\{i,j\}\neq\{v,b\},\{i,k\}\neq\{v,b\}} \frac{I_{vbij}(\omega)I_{jaka}(0)I_{ikvb}(\omega)}{(\epsilon_v - \omega - \epsilon_i u)(\epsilon_b + \omega - \epsilon_j u)(\epsilon_b + \omega - \epsilon_k u)}\Bigg]\,,\end{aligned} \tag{A.39}$$

$$\begin{aligned}\Delta E^{(3I)3e,lad,irr}_{v,\,S(VP)EVP} = \frac{i}{2\pi}\int d\omega \Bigg[&\sum_{a,b,i,j,k}^{i\neq v,\{j,k\}\neq\{v,b\}} \frac{I_{vaia}(0)I_{ibjk}(\omega)I_{kjbv}(\omega) + I_{vbjk}(\omega)I_{jkib}(\omega)I_{aiav}(0)}{\Delta_{vi}(\epsilon_v - \omega - \epsilon_j u)(\epsilon_b + \omega - \epsilon_k u)} \\ &+ \sum_{a,b,i,j,k}^{\{i,k\}\neq\{v,b\},\{j,k\}\neq\{v,b\}} \frac{I_{vbik}(\omega)I_{iaja}(0)I_{kjbv}(\omega)}{(\epsilon_v - \omega - \epsilon_i u)(\epsilon_v - \omega - \epsilon_j u)(\epsilon_b + \omega - \epsilon_k u)}\Bigg]\,.\end{aligned} \tag{A.40}$$

Reducible 1 terms

Since a crossed irreducible expression exist, the associated crossed reducible terms are found and worked out. The result is separated as well according to the originated subset, and reads

$$\Delta E^{(3I)3e,cross,red}_{v,\,S[V(VP)P]E} = -\frac{i}{2\pi}\int d\omega \sum_{a,b,b_1,i,j} \frac{I_{vjib}(\omega)I_{bab_1a}(0)I_{ib_1vj}(\omega)}{(\epsilon_v - \omega - \epsilon_i u)(\epsilon_b - \omega - \epsilon_j u)^2}\,, \tag{A.41}$$

$$\Delta E^{(3\mathrm{I})3\mathrm{e,cross,red}}_{v,\,\mathrm{S(VP)EVP}} = -\frac{i}{2\pi}\int d\omega \sum_{a,b,v_1,i,j} \frac{I_{vjib}(\omega) I_{bijv_1}(\omega) I_{av_1av}(0)}{(\epsilon_v - \omega - \epsilon_i u)^2(\epsilon_b - \omega - \epsilon_j u)}\,. \tag{A.42}$$

Each ladder reducible 1 term is separated into an IR free and an IR divergent part, and displayed according to its provenance. Beginning with the latter, one has

$$\begin{aligned}\Delta E^{(3\mathrm{I})3\mathrm{e,lad,red1}}_{v,\,\mathrm{S[V(VP)P]E,\,IR\,div}} = &-\frac{i}{2\pi}\int \frac{d\omega}{(-\omega+i\varepsilon)^2} \sum_{a,b,b_1,v_1,i}^{i\neq b} \\ &\left[\frac{I_{vbv_1b_1}(\omega) I_{aiab}(0) I_{v_1b_1vi}(\omega) + I_{viv_1b_1}(\omega) I_{abai}(0) I_{v_1b_1vb}(\omega)}{\Delta_{bi}}\right. \\ &\left.+\frac{I_{vbv_1b_1}(\omega) I_{b_1aia}(0) I_{v_1ivb}(\omega) + I_{vbv_1i}(\omega) I_{iab_1a}(0) I_{v_1b_1vb}(\omega)}{(\Delta_{bi}+\omega+i\varepsilon)}\right],\end{aligned} \tag{A.43}$$

$$\begin{aligned}\Delta E^{(3\mathrm{I})3\mathrm{e,lad,red1}}_{v,\,\mathrm{S(VP)EVP,\,IR\,div}} = &-\frac{i}{2\pi}\int \frac{d\omega}{(-\omega+i\varepsilon)^2} \sum_{a,b,b_1,v_1,i}^{i\neq v} \\ &\left[\frac{I_{vaia}(0) I_{ibv_1b_1}(\omega) I_{b_1v_1bv}(\omega) + I_{vbv_1b_1}(\omega) I_{v_1b_1ib}(\omega) I_{aiav}(0)}{\Delta_{vi}}\right. \\ &\left.+\frac{I_{vbib_1}(\omega) I_{iav_1a}(0) I_{b_1v_1bv}(\omega) + I_{vbv_1b_1}(\omega) I_{v_1aia}(0) I_{b_1ibv}(\omega)}{(\Delta_{vi}-\omega+i\varepsilon)}\right],\end{aligned} \tag{A.44}$$

for the IR divergent part. The IR finite part is further separated, because its first part is the counterpart of the previously introduced IR divergent terms,

$$\begin{aligned}\Delta E^{(3\mathrm{I})3\mathrm{e,lad,red1}}_{v,\,\mathrm{S[V(VP)P]E,\,IR\,free}} = &-\frac{i}{4\pi}\int d\omega \left[\frac{1}{(\Delta_{vb}-\omega+i\varepsilon)^2}+\frac{1}{(\Delta_{vb}-\omega-i\varepsilon)^2}\right] \\ &\times\left[\sum_{a,b,b_1,v_1,i}^{i\neq v} \frac{I_{vbb_1v_1}(\omega) I_{v_1aia}(0) I_{b_1ivb}(\omega) + I_{vbb_1i}(\omega) I_{iav_1a}(0) I_{b_1v_1vb}(\omega)}{(\Delta_{bi}+\omega+i\varepsilon)}\right. \\ &\left.+\sum_{a,b,b_1,v_1,i}^{i\neq b} \frac{I_{vbb_1v_1}(\omega) I_{aiab}(0) I_{b_1v_1vi}(\omega) + I_{vib_1v_1}(\omega) I_{abai}(0) I_{b_1v_1vb}(\omega)}{\Delta_{bi}}\right],\end{aligned} \tag{A.45}$$

$$\Delta E^{(3I)3e,lad,red1}_{v,\,S(VP)EVP,\,IR\ free} = -\frac{i}{4\pi}\int d\omega \left[\frac{1}{(\Delta_{vb}-\omega+i\varepsilon)^2}+\frac{1}{(\Delta_{vb}-\omega-i\varepsilon)^2}\right] \times \left[\sum_{a,b,b_1,v_1,i}^{i\neq v}\frac{I_{vaia}(0)I_{ibb_1v_1}(\omega)I_{v_1b_1bv}(\omega)+I_{vbb_1v_1}(\omega)I_{b_1v_1ib}(\omega)I_{aiav}(0)}{\Delta_{vi}} + \sum_{a,b,b_1,v_1,i}^{i\neq b}\frac{I_{vbb_1v}(\omega)I_{b_1aia}(0)I_{v_1ibv}(\omega)+I_{vbiv_1}(\omega)I_{iab_1a}(0)I_{v_1b_1bv}(\omega)}{(\Delta_{vi}-\omega+i\varepsilon)}\right], \tag{A.46}$$

while its second part is simply the terms excluded in sums of certain diagrams,

$$\Delta E^{(3I)3e,lad,red1}_{v,\,S[V(VP)P]E,\,IR\ free\ \omega} = -\frac{i}{2\pi}\int d\omega \sum_{a,b,b_1,i,j}^{\{i,j\}\neq\{v,b\}}\frac{I_{vbij}(\omega)I_{ab_1ab}(0)I_{ijvb_1}(\omega)}{(\epsilon_v-\omega-\epsilon_iu)(\epsilon_b+\omega-\epsilon_ju)^2}, \tag{A.47}$$

$$\Delta E^{(3I)3e,lad,red1}_{v,\,S(VP)EVP,\,IR\ free\ \omega} = -\frac{i}{2\pi}\int d\omega \sum_{a,b,v_1,i,j}^{\{i,j\}\neq\{v,b\}}\frac{I_{vbij}(\omega)I_{ijv_1b}(\omega)I_{av_1av}(0)}{(\epsilon_v-\omega-\epsilon_iu)^2(\epsilon_b+\omega-\epsilon_ju)}. \tag{A.48}$$

Reducible 2 terms

Facing now the reducible 2 contribution, the identical separation into IR divergent and IR free terms is conducted, on the top of the distinction among the two different subsets. The IR divergent terms are

$$\Delta E^{(3I)3e,lad,red2}_{v,\,S[V(VP)P]E,\,IR\ div} = \frac{i}{2\pi}\int\frac{d\omega}{(-\omega+i\varepsilon)^3}\sum_{a,b,b_1,b_2,v_1}\left[I_{vbv_1b_1}(\omega)I_{b_1ab_2a}(0)I_{v_1b_2vb}(\omega)-I_{vbv_1b_2}(\omega)I_{ab_1ab}(0)I_{v_1b_2vb_1}(\omega)\right], \tag{A.49}$$

$$\Delta E^{(3I)3e,lad,red2}_{v,\,S(VP)EVP,\,IR\ div} = \frac{i}{2\pi}\int\frac{d\omega}{(-\omega+i\varepsilon)^3}\sum_{a,b,b_1,v_1,v_2}\left[I_{vbv_1b_1}(\omega)I_{v_1b_1v_2b}(\omega)I_{av_2av}(0)-I_{vbv_1b_1}(\omega)I_{v_1av_2a}(0)I_{b_1v_2bv}(\omega)\right], \tag{A.50}$$

and the IR free ones are

$$\Delta E^{(3I)3e,lad,red2}_{v,\,S[V(VP)P]E,\,IR\ free} = \frac{i}{4\pi}\int d\omega \left[\frac{1}{(\Delta_{vb}-\omega+i\varepsilon)^3}+\frac{1}{(\Delta_{vb}-\omega-i\varepsilon)^3}\right] \times \left[\sum_{a,b,b_1,v_1,v_2} I_{vbb_1v_1}(\omega) I_{v_1av_2a}(0) I_{b_1v_2vb}(\omega) - \sum_{a,b,b_1,,b_2,v_1} I_{vbb_2v_1}(\omega) I_{ab_1ab}(0) I_{b_2v_1vb_1}(\omega)\right], \tag{A.51}$$

$$\Delta E^{(3I)3e,lad,red2}_{v,\,S(VP)EVP,\,IR\ free} = \frac{i}{4\pi}\int d\omega \left[\frac{1}{(\Delta_{vb}-\omega+i\varepsilon)^3}+\frac{1}{(\Delta_{vb}-\omega-i\varepsilon)^3}\right] \times \left[\sum_{a,b,b_1,v_1,v_2} I_{vbb_1v_1}(\omega) I_{b_1v_1v_2b}(\omega) I_{av_2av}(0) - \sum_{a,b,b_1,b_2,v_1} I_{vbb_1v_1}(\omega) I_{b_2v_1vb}(\omega) I_{b_1ab_2a}(0)\right]. \tag{A.52}$$

Extra terms

The remaining terms

$$\Delta E^{(3I)3e,red1}_{v,\,S[V(VP)P]E} = \sum_{a,b,b_1,v_1,i}^{i\neq v} \frac{I_{vbb_1v_1}(\Delta_{vb}) I_{v_1aia}(0) I_{ib_1bv}(\Delta_{vb})}{(\epsilon_v-\epsilon_i)^2}, \tag{A.53}$$

$$\Delta E^{(3I)3e,red1}_{v,\,S(VP)EVP} = -\sum_{a,b,b_1,v_1,i}^{i\neq b} \frac{I_{vbb_1v_1}(\Delta_{vb}) I_{b_1aia}(0) I_{iv_1vb}(\Delta_{vb})}{(\epsilon_b-\epsilon_i)^2}, \tag{A.54}$$

are not found via the perturbative analysis but are present in the redefined vacuum state approach. They are obtained as the interplay among terms generated from the ladder reducible 1 terms, upon the symmetrization of the energy flow in the loop, and four-electron reducible 1 terms. The former originates from H_1 while the latter originates from F_2. They look like four-electron reducible 1 contribution, due to the absence of the ω integration. According to the gauge invariance of the three-electron S(VP)E subset of the two-photon-exchange corrections, they should be incorporated in the three-electron contribution of the three-photon-exchange corrections. The structure of these terms suggests then to be included in the reducible 1 contribution.

A.7. Symmetry argument for vanishing ladder reducible 2 terms

The cancellation of the $1/\mu$ IR divergence in ladder reducible 2 terms was shown in Table 5.1. This was achieved by searching for a compensating term within the subset of the investigated term. A symmetry argument might also rule out this issue at the individual Feynman diagram level, without the need of a term to absorb its divergence. The naive way to argue would be as follows. Recall that in Feynman gauge, $I(\omega)$ is a symmetric operator. Therefore, when the IR divergence is met in the ladder reducible 2 term, one faces a symmetric numerator divided by an anti-symmetric denominator integrated over a symmetric interval. It vanishes due to parity consideration. However, the problem is that the $i\varepsilon$ prescription spoils the anti-symmetric behaviour of the denominator. Hence, a Wick rotation is applied and the expression looks as

$$\begin{aligned}
\frac{i}{2\pi}\int_{-\infty}^{\infty} d\omega \frac{I(\omega)I(\omega)I(0)}{(-\omega+i\varepsilon)^3} &= \frac{-I(0)}{2\pi}\int_0^{i\infty} d\omega_E \left[\frac{I(-i\omega_E)I(-i\omega_E)}{(i\omega_E+i\varepsilon)^3} + \frac{I(i\omega_E)I(i\omega_E)}{(-i\omega_E+i\varepsilon)^3}\right] \\
&= \frac{-I(0)}{2\pi}\mathcal{P}\int_0^{i\infty} d\omega_E \frac{I(-i\omega_E)I(-i\omega_E) - I(i\omega_E)I(i\omega_E)}{(i\omega_E)^3} \\
&\propto \frac{-i}{2\pi} I(0)\mathcal{P}\int_0^{i\infty} d\omega_E \frac{2\sinh\omega_E R}{\omega_E^3} \\
&\overset{\text{B.H}}{=} \frac{-iR}{3\pi} I(0)\mathcal{P}\int_0^{i\infty} d\omega_E \frac{\cosh\omega_E R}{\omega_E^2} \\
&\overset{\text{Taylor}}{\approx} \frac{-iR}{3\pi} I(0)\mathcal{P}\int_0^{i\infty} d\omega_E \left[\frac{1}{\omega_E^2} + \frac{1}{2!}R^2\right]
\end{aligned} \tag{A.55}$$

Only the principal value is considered since the third order pole does not contribution to the pole term. One can take the exponential terms of the interelectronic operators out and rephrase them as a hyperbolic sine. Then, Bernoulli-L'Hospital rule is applied once and the hyperbolic cosine is Taylor expanded. Here R stands for $R = r_{12} + r_{34}$. An interesting feature is seen at this point, it leads to a pure imaginary end result. Furthermore, one retrieves the $1/\mu$ divergent behavior encountered previously. The imaginary contribution to the energy, the decay rate, accounts for the possible instability of the excited states. One can neglect it since, in Chapter 3.1, it was said that this pure imaginary part is not considered. For completeness, if the ground state is under consideration, it features obviously no instabilities.

BIBLIOGRAPHY

[1] W. Heisenberg, Zeitschrift für Physik A Hadrons and Nuclei **33**, 879 (1925).

[2] E. Schrödinger, Physical Review **28**, 1049 (1926).

[3] M. Born, Zeitschrift für physik **38**, 803 (1926).

[4] M. Born, W. Heisenberg, and P. Jordan, Zeitschrift für Physik **35**, 557 (1926).

[5] P. A. M. Dirac and R. H. Fowler, Proceedings of the Royal Society of London. Series A, Containing Papers of a Mathematical and Physical Character **117**, 610 (1928).

[6] P. A. M. Dirac and R. H. Fowler, Proceedings of the Royal Society of London. Series A, Containing Papers of a Mathematical and Physical Character **118**, 351 (1928).

[7] W. E. Lamb and R. C. Retherford, Phys. Rev. **72**, 241 (1947).

[8] P. Kusch and H. M. Foley, Phys. Rev. **74**, 250 (1948).

[9] H. A. Bethe, Phys. Rev. **72**, 339 (1947).

[10] R. P. Feynman, Phys. Rev. **76**, 749 (1949).

[11] R. P. Feynman, Phys. Rev. **76**, 769 (1949).

[12] J. Schwinger, Phys. Rev. **73**, 416 (1948).

[13] J. Schwinger, Phys. Rev. **74**, 1439 (1948).

[14] J. Schwinger, Phys. Rev. **75**, 651 (1949).

[15] J. Schwinger, Phys. Rev. **76**, 790 (1949).

[16] Y. Nambu, Progress of Theoretical Physics **5**, 614 (1950).

[17] J. Schwinger, Proceedings of the National Academy of Sciences **37**, 455 (1951).

[18] M. Gell-Mann and F. Low, Physical Review **84**, 350 (1951).

[19] E. E. Salpeter and H. A. Bethe, Phys. Rev. **84**, 1232 (1951).

[20] E. E. Salpeter, Phys. Rev. **87**, 328 (1952).

[21] J. Sucher, Physical Review **107**, 1448 (1957).

[22] J. Sucher, *Energy levels of the two-electron atom, to order (alpha-cube) Rydberg* (Columbia University, 1958).

[23] A. A. Logunov and A. N. Tavkhelidze, Nuovo Cim. **29**, 380 (1963).

[24] R. N. Faustov, Theor. Math. Phys. **3**, 478 (1970).

[25] A. Gumberidze and on behalf of the SPARC collaboration, Phys. Scr. **T156**, 014084 (2013).

[26] P. Indelicato, J. Phys. B **52**, 232001 (2019).

[27] V. A. Yerokhin, P. Indelicato, and V. M. Shabaev, Phys. Rev. A **77**, 062510 (2008).

[28] V. A. Yerokhin, Eur. Phys. J. D **58**, 57 (2010).

[29] W. H. Furry, Phys. Rev. **81**, 115 (1951).

[30] M. G. Kozlov, M. S. Safronova, J. R. Crespo López-Urrutia, and P. O. Schmidt, Rev. Mod. Phys. **90**, 045005 (2018).

[31] S. G. Karshenboim, Phys. Rep. **422**, 1 (2005).

[32] V. A. Yerokhin and V. M. Shabaev, J. Phys. Chem. Ref. Data **44**, 033103 (2015).

[33] A. Gumberidze *et al.*, Phys. Rev. Lett. **94**, 223001 (2005).

[34] V. A. Yerokhin, P. Indelicato, and V. M. Shabaev, Phys. Rev. Lett. **91**, 073001 (2003).

[35] T. Gassner *et al.*, New J. Phys. **20**, 073033 (2018).

[36] J. Sucher, Phys. Rev. A **22**, 348 (1980).

[37] D. B. Thorn *et al.*, Phys. Rev. Lett. **103**, 163001 (2009).

[38] A. Gumberidze *et al.*, Phys. Rev. Lett. **92**, 203004 (2004).

[39] H. Bruhns, J. Braun, K. Kubiček, J. R. Crespo López-Urrutia, and J. Ullrich, Phys. Rev. Lett. **99**, 113001 (2007).

[40] M. Trassinelli *et al.*, EPL (Europhysics Letters) **87**, 63001 (2009).

[41] P. Amaro *et al.*, Phys. Rev. Lett. **109**, 043005 (2012).

[42] C. T. Chantler *et al.*, Phys. Rev. Lett. **109**, 153001 (2012).

[43] C. Brandau *et al.*, Phys. Rev. Lett. **91**, 073202 (2003).

[44] P. Beiersdorfer, H. Chen, D. B. Thorn, and E. Träbert, Phys. Rev. Lett. **95**, 233003 (2005).

[45] D. Feili *et al.*, Phys. Scr. **71**, 48 (2005).

[46] D. Bernhardt *et al.*, J. Phys. B: At., Mol. Opt. Phys. **48**, 144008 (2015).

[47] P. Beiersdorfer, A. L. Osterheld, and S. R. Elliott, Phys. Rev. A **58**, 1944 (1998).

[48] I. Draganić *et al.*, Phys. Rev. Lett. **91**, 183001 (2003).

[49] V. Mäckel, R. Klawitter, G. Brenner, J. R. Crespo López-Urrutia, and J. Ullrich, Phys. Rev. Lett. **107**, 143002 (2011).

[50] X. Liu *et al.*, Phys. Rev. A **104**, 062804 (2021).

[51] G. O'Neil *et al.*, Phys. Rev. A **102**, 032803 (2020).

[52] Q. Lu *et al.*, Phys. Rev. A **102**, 042817 (2020).

[53] S. X. Wang *et al.*, Phys. Rev. A **106**, 042808 (2022).

[54] M. C. Li, R. Si, T. Brage, R. Hutton, and Y. M. Zou, Phys. Rev. A **98**, 020502(R) (2018).

[55] A. V. Volotka *et al.*, Phys. Rev. A **100**, 010502 (2019).

[56] V. Shabaev *et al.*, Physical Review A **101**, 052502 (2020).

[57] W. R. Johnson, S. A. Blundell, and J. Sapirstein, Phys. Rev. A **38**, 2699 (1988).

[58] M. H. Chen and K. T. Cheng, Phys. Rev. A **55**, 3440 (1997).

[59] U. I. Safronova, C. Namba, J. R. Albritton, W. R. Johnson, and M. S. Safronova, Phys. Rev. A **65**, 022507 (2002).

[60] R. Si *et al.*, Phys. Rev. A **98**, 012504 (2018).

[61] S. A. Blundell, P. J. Mohr, W. R. Johnson, and J. Sapirstein, Phys. Rev. A **48**, 2615 (1993).

[62] I. Lindgren, H. Persson, S. Salomonson, and L. Labzowsky, Phys. Rev. A **51**, 1167 (1995).

[63] H. Persson, S. Salomonson, P. Sunnergren, and I. Lindgren, Phys. Rev. Lett. **76**, 204

(1996).

[64] P. J. Mohr and J. Sapirstein, Phys. Rev. A **62**, 052501 (2000).

[65] O. Y. Andreev, L. N. Labzowsky, G. Plunien, and G. Soff, Phys. Rev. A **64**, 042513 (2001).

[66] O. Y. Andreev, L. N. Labzowsky, G. Plunien, and G. Soff, Phys. Rev. A **67**, 012503 (2003).

[67] A. N. Artemyev, V. M. Shabaev, V. A. Yerokhin, G. Plunien, and G. Soff, Phys. Rev. A **71**, 062104 (2005).

[68] A. V. Malyshev, Y. S. Kozhedub, D. A. Glazov, I. I. Tupitsyn, and V. M. Shabaev, Phys. Rev. A **99**, 010501(R) (2019).

[69] Y. S. Kozhedub, A. V. Malyshev, D. A. Glazov, V. M. Shabaev, and I. I. Tupitsyn, Phys. Rev. A **100**, 062506 (2019).

[70] A. V. Malyshev, Y. S. Kozhedub, D. A. Glazov, I. I. Tupitsyn, and V. M. Shabaev, Phys. Rev. A **9**9, 010501 (2019).

[71] J. Sapirstein and K. T. Cheng, Phys. Rev. A **64**, 022502 (2001).

[72] V. A. Yerokhin *et al.*, Phys. Rev. A **64**, 032109 (2001).

[73] A. N. Artemyev *et al.*, Phys. Rev. A **67**, 062506 (2003).

[74] V. A. Yerokhin, A. N. Artemyev, and V. M. Shabaev, Phys. Rev. A **75**, 062501 (2007).

[75] Y. S. Kozhedub *et al.*, Phys. Rev. A **81**, 042513 (2010).

[76] J. Sapirstein and K. T. Cheng, Phys. Rev. A **83**, 012504 (2011).

[77] A. V. Malyshev *et al.*, Phys. Rev. A **90**, 062517 (2014).

[78] A. V. Malyshev *et al.*, Phys. Rev. A **92**, 012514 (2015).

[79] A. V. Malyshev *et al.*, Phys. Rev. Lett. **126**, 183001 (2021).

[80] A. N. Artemyev, V. M. Shabaev, I. I. Tupitsyn, G. Plunien, and V. A. Yerokhin, Phys. Rev. Lett. **98**, 173004 (2007).

[81] A. N. Artemyev *et al.*, Phys. Rev. A **88**, 032518 (2013).

[82] A. V. Malyshev *et al.*, Phys. Rev. A **96**, 022512 (2017).

[83] J. Sapirstein and K. T. Cheng, Phys. Rev. A **91**, 062508 (2015).

[84] V. M. Shabaev and I. G. Fokeeva, Phys. Rev. A **49**, 4489 (1994).

[85] V. M. Shabaev, Phys. Rep. **356**, 119 (2002).

[86] S. Weinberg*The Quantum Theory of Fields* Vol. 1 (Cambridge University Press, 1995).

[87] T.-P. Cheng and L.-F. Li, *Gauge theory of elementary particle physics* (Oxford university press, 1994).

[88] M. E. Peskin and D. V. Schroeder, *An Introduction to Quantum Field Theory* (Westview Press, 1995).

[89] H. M. Fried and D. Yennie, Physical Review **112**, 1391 (1958).

[90] P. J. Mohr, G. Plunien, and G. Soff, Phys. Rep. **293**, 227 (1998).

[91] In fact, for hydrogen and deuterium it is not justified, because of the slow convergence and large cancellations due to the renormalization. That obliged to do all-order self-energy calculations to account for the 15 digits accuracy of the measurement and required very advanced convergence techniques [171–173]. Thanks to P. Indelicato for this remark.

[92] W. E. Lamb Jr., Phys. Rev. **85**, 259 (1952).

[93] D. R. Hartree, The wave mechanics of an atom with a non-coulomb central field. part i. theory and methods, in *Mathematical Proceedings of the Cambridge Philosophical Society* Vol. 24, pp. 89–110, Cambridge university press, 1928.

[94] D. R. Hartree, The wave mechanics of an atom with a non-coulomb central field. part ii. some results and discussion, in *Mathematical Proceedings of the Cambridge Philosophical Society* Vol. 24, pp. 111–132, Cambridge University Press, 1928.

[95] D. Hartree, The wave mechanics of an atom with a non-coulomb central field. part iii. term values and intensities in series in optical spectra, in *Mathematical Proceedings of the Cambridge Philosophical Society* Vol. 24, pp. 426–437, Cambridge University Press, 1928.

[96] D. Hartree, The wave mechanics of an atom with a non-coulomb central field. part iv. further results relating to terms of the optical spectrum, in *Mathematical Proceedings of the Cambridge Philosophical Society* Vol. 25, pp. 310–314, Cambridge University Press, 1929.

[97] W. Kohn and L. J. Sham, Phys. Rev. **140**, A1133 (1965).

[98] I. Lindgren and J. Morrison, *Atomic Many-Body Theory* (Springer-Verlag, Berlin, 1985).

[99] W. R. Johnson, *Atomic Structure Theory. Lectures on Atomic Physics* (Springer-Verlag, Berlin, Heidelberg, 2007).

[100] E. Avgoustoglou *et al.*, Phys. Rev. A **46**, 5478 (1992).

[101] W. R. Johnson, J. Sapirstein, and K. T. Cheng, Phys. Rev. A **51**, 297 (1995).

[102] A. V. Volotka, D. A. Glazov, V. M. Shabaev, I. I. Tupitsyn, and G. Plunien, Phys. Rev. Lett. **103**, 033005 (2009).

[103] D. A. Glazov, A. V. Volotka, V. M. Shabaev, I. I. Tupitsyn, and G. Plunien, Phys. Rev. A **81**, 062112 (2010).

[104] A. V. Volotka *et al.*, Phys. Rev. Lett. **108**, 073001 (2012).

[105] A. V. Volotka, D. A. Glazov, V. M. Shabaev, I. I. Tupitsyn, and G. Plunien, Phys. Rev. Lett. **112**, 253004 (2014).

[106] V. M. Shabaev, Izv. Vuz. Fiz. **33**, 43 [Sov. Phys. J. **33**, 660] (1990).

[107] I. Lindgren, S. Salomonson, and B. Åsén, Phys. Rep. **389**, 161 (2004).

[108] I. Lindgren, S. Salomonson, and D. Hedendahl, Phys. Rev. A **7**3, 062502 (2006).

[109] I. Lindgren, P. Indelicato, and W. Liu, Handbook of Relativistic Quantum Chemistry , 313 (2017).

[110] O. Yu. Andreev, L. N. Labzowsky, G. Plunien, and D. A. Solovyev, Phys. Rep. **455**, 135 (2008).

[111] V. Balakrishnan, *Mathematical physics: applications and problems* (Springer Nature, 2020).

[112] R. N. Soguel *et al.*, Phys. Rev. A **103**, 042818 (2021).

[113] R. N. Soguel, A. V. Volotka, D. A. Glazov, and S. Fritzsche, Symmetry **13** (2021).

[114] B. d. S. Nagy, Commentarii Mathematici Helvetici **19**, 347 (1946).

[115] T. Kato, Progress of Theoretical Physics **4**, 514 (1949).

[116] T. Kato *et al.*, Perturbation theory for linear operators (1966).

[117] V. A. Yerokhin, P. Indelicato, and V. M. Shabaev, Phys. Rev. Lett. **97**, 253004 (2006).

[118] I. Angeli and K. P. Marinova, At. Data Nucl. Data Tables **99**, 69 (2013).

[119] V. M. Shabaev, I. I. Tupitsyn, V. A. Yerokhin, G. Plunien, and G. Soff, Phys. Rev. Lett. **93**, 130405 (2004).

[120] J. Sapirstein and W. R. Johnson, J. Phys. B **29**, 5213 (1996).

[121] P. Beiersdorfer, A. L. Osterheld, J. H. Scofield, J. R. Crespo López-Urrutia, and K. Widmann, Phys. Rev. Lett. **80**, 3022 (1998).

[122] D. Layzer and J. Bahcall, Ann. Phys. (NY) **17**, 177 (1962).

[123] R. N. Soguel, A. V. Volotka, and S. Fritzsche, Phys. Rev. A **106**, 012802 (2022).

[124] A. L. Fetter and J. D. Walecka, *Quantum Theory of Many-Particle Systems* (McGraw-Hill, New York, 1971).

[125] J. Oddershede and P. Jörgensen, J. Chem. Phys. **66**, 1541 (1977).

[126] C.-M. Liegener, Mol. Phys. **43**, 1 (1981).

[127] I. Lindgren, *Relativistic Many-Body Theory: A New Field-Theoretical Approach* (Springer-Verlag, New York, 2011).

[128] E. Avgoustoglou, W. R. Johnson, Z. W. Liu, and J. Sapirstein, Phys. Rev. A **51**, 1196 (1995).

[129] E. Avgoustoglou and Z. W. Liu, Phys. Rev. A **54**, 1351 (1996).

[130] U. I. Safronova, C. Namba, I. Murakami, W. R. Johnson, and M. S. Safronova, Phys. Rev. A **64**, 012507 (2001).

[131] P. Beiersdorfer *et al.*, Phys. Rev. A **100**, 032516 (2019).

[132] V. M. Shabaev, I. I. Tupitsyn, and V. A. Yerokhin, Phys. Rev. A **88**, 012513 (2013).

[133] V. M. Shabaev, I. I. Tupitsyn, and V. A. Yerokhin, Comp. Phys. Comm. **189**, 175 (2015).

[134] I. S. Anisimova *et al.*, Phys. Rev. A **106**, 062823 (2022).

[135] P. Beiersdorfer *et al.*, Can. J. Phys. **98**, 239 (2020).

[136] A. D. Ludlow, M. M. Boyd, J. Ye, E. Peik, and P. O. Schmidt, Rev. Mod. Phys. **87**, 637 (2015).

[137] S. Chen *et al.*, arXiv preprint arXiv:2303.04552 (2023).

[138] S. Kühn *et al.*, Phys. Rev. Lett. **124**, 225001 (2020).

[139] S. Kühn *et al.*, Phys. Rev. Lett. **129**, 245001 (2022).

[140] V. A. Yerokhin, C. H. Keitel, and Z. Harman, Phys. Rev. A **104**, 022814 (2021).

[141] V. A. Yerokhin, K. Pachucki, M. Puchalski, C. H. Keitel, and Z. Harman, Phys. Rev. A **102**, 022815 (2020).

[142] E. H. Wichmann and N. M. Kroll, Phys. Rev. **101**, 843 (1956).

[143] G. Kallen and A. Sabry, Selsk. Mat.—Fys. Medd **29**, 17 (1955).

[144] R. Barbieri, J. Mignaco, and E. Remiddi, Lettere al Nuovo Cimento (1969-1970) **3**, 588 (1970).

[145] R. Barbieri, J. Mignaco, and E. Remiddi, Nuovo Cimento. A **11**, 824 (1972).

[146] R. Barbieri, J. Mignaco, and E. Remiddi, Nuovo Cimento A Serie **11**, 865 (1972).

[147] R. Barbieri and E. Remiddi, Nuovo Cimento. A **13**, 99 (1973).

[148] E. A. Uehling, Phys. Rev. **48**, 55 (1935).

[149] I. S. Gradshteyn, I. M. Ryzhik, A. Jeffrey, and D. Zwillinger, *Table of Integrals, Series, and Products* (, 2007).

[150] V. A. Dzuba, V. V. Flambaum, and S. Schiller, Phys. Rev. A **98**, 022501 (2018).

[151] R. T. Imanbaeva and M. G. Kozlov, Annalen der Physik **531**, 1800253.

[152] C. Cheung *et al.*, Phys. Rev. Lett. **124**, 163001 (2020).

[153] J. Desclaux, J. Dolbeault, M. Esteban, P. Indelicato, and E. Séré, Computational approaches of relativistic models in quantum chemistry, in *Special Volume, Computational Chemistry*, , Handbook of Numerical Analysis Vol. 10, pp. 453–483, Elsevier, 2003.

[154] P. Jönsson, G. Gaigalas, J. Bieroń, C. Froese Fischer, and I. P. Grant, Comput. Phys. Commun. **184**, 2197 (2013).

[155] M. Kozlov, S. Porsev, M. Safronova, and I. Tupitsyn, Computer Physics Communications **195**, 199 (2015).

[156] C. Cheung, M. Safronova, and S. Porsev, Symmetry **13** (2021).

[157] V. Dzuba, Symmetry **12** (2020).

[158] E. Kahl and J. Berengut, Computer Physics Communications **238**, 232 (2019).

[159] J. S. M. Ginges and J. C. Berengut, Phys. Rev. A **9**3, 052509 (2016).

[160] I. I. Tupitsyn, M. G. Kozlov, M. S. Safronova, V. M. Shabaev, and V. A. Dzuba, Phys. Rev. Lett. **117**, 253001 (2016).

[161] P. J. Mohr, Annals of Physics **88**, 52 (1974).

[162] N. J. Snyderman, Ann. Phys. (NY) **2**11, 43 (1991).

[163] V. A. Yerokhin and V. M. Shabaev, Phys. Rev. A **60**, 800 (1999).

[164] W. H. Furry, Phys. Rev. **51**, 125 (1937).

[165] G. S. Adkins, R. N. Fell, and J. Sapirstein, Physical Review D **63**, 125009 (2001).

[166] G. S. Adkins, Physical Review D **27**, 1814 (1983).

[167] G. S. Adkins, Physical Review D **34**, 2489 (1986).

[168] G. S. Adkins, Physical Review D **36**, 1929 (1987).

[169] G. S. Adkins, P. M. Mitrikov, and R. N. Fell, Physical review letters **78**, 9 (1997).

[170] P. J. Mohr, Annals of Physics **88**, 26 (1974).

[171] U. D. Jentschura, P. J. Mohr, and G. Soff, Phys. Rev. Lett. **82**, 53 (1999).

[172] U. D. Jentschura, P. J. Mohr, G. Soff, and E. J. Weniger, Computer Physics Communications **116**, 28 (1999).

[173] U. D. Jentschura, P. J. Mohr, and G. Soff, Phys. Rev. A **63**, 042512 (2001).

Ehrenwörtliche Erklärung

Ich erkläre hiermit ehrenwörtlich, dass ich die vorliegende Arbeit selbstständing, ohne unzuässige Hilfe Dritter und ohne Benutzung anderer als der angegebenen Hilfsmittel und Literatur angefertigt habe. Die aus anderen Quellen direkt oder indirekt übernommenen Daten und Konzepte sind unter Angabe der Quelle gekennzeichnet. Bei der Anfertigung dieser Arbeit haben mir meine Betreuer und die Koautoren oben genannter Publikationen geholfen.

Weitere Personen waren an der inhaltlich-materiellen Erstellung der vorliegenden Arbeit nicht beteiligt. Insbesondere habe ich hierfür nicht die entgeltliche Hilfe von Vermittlungs- bzw. Beratungsdiensten (Promotionsberater oder andere Personen) in Anspruch genommen.

Niemand hat von mir unmittelbar oder mittelbar geldwerte Leistungen für Arbeiten erhalten, die im Zusammenhang mit dem Inhalt der vorgelegten Dissertation stehen. Die Arbeit wurde bisher weder im In- noch im Ausland in gleicher oder ähnlicher Form einer anderen Prüfungsbehörde vorgelegt. Die geltende Promotionsordnung der Physikalisch-Astronomischen Fakultät ist mir bekannt. Ich versichere ehrenwörtlich, dass ich nach bestem Wissen die reine Wahrheit gesagt und nichts verschwiegen habe.

Jena,

Romain Soguel